UNIVERSITY OF ALBERTA

TOPICS IN TWO-BODY HADRONIC DECAYS OF D MESONS

By

EL HASSAN EL AAOUD ©

A thesis submitted to the Faculty of Graduate Studies and Research
in partial fulfillment of the requirements for the degree of
Doctor of Philosophy

Department of Physics

Edmonton, Alberta
Fall 2000

National Library of Canada
Acquisitions and Bibliographic Services
395 Wellington Street
Ottawa ON K1A 0N4
Canada

Bibliothèque nationale du Canada
Acquisitions et services bibliographiques
395, rue Wellington
Ottawa ON K1A 0N4
Canada

Your file Votre référence

Our file Notre référence

The author has granted a non-exclusive licence allowing the National Library of Canada to reproduce, loan, distribute or sell copies of this thesis in microform, paper or electronic formats.

The author retains ownership of the copyright in this thesis. Neither the thesis nor substantial extracts from it may be printed or otherwise reproduced without the author's permission.

L'auteur a accordé une licence non exclusive permettant à la Bibliothèque nationale du Canada de reproduire, prêter, distribuer ou vendre des copies de cette thèse sous la forme de microfiche/film, de reproduction sur papier ou sur format électronique.

L'auteur conserve la propriété du droit d'auteur qui protège cette thèse. Ni la thèse ni des extraits substantiels de celle-ci ne doivent être imprimés ou autrement reproduits sans son autorisation.

0-612-59582-X

Canada

UNIVERSITY OF ALBERTA

LIBRARY RELEASE FORM

NAME OF AUTHOR:	EL HASSAN EL AAOUD
TITLE OF THESIS:	Topics in two-body hadronic decays of D mesons
DEGREE:	Doctor of Philosophy
YEAR THE DEGREE GRANTED:	2000

Permission is hereby granted to the University of Alberta Library to reproduce single copies of this thesis and to lend or sell such copies for private, scholarly or scientific research purposes only.

The author reserves all other publication and other rights in association with the copyright in the thesis, and except as hereinbefore provided, neither the thesis nor any substantial portion thereof may be printed or otherwise reproduced in any material form whatever without the author's prior written permission.

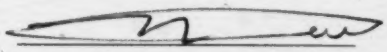

EL HASSAN EL AAOUD

Department of Physics

University of Alberta

Edmonton, Alberta T6G 2J1

Date: Aug. 30/2000

UNIVERSITY OF ALBERTA

FACULTY OF GRADUATE STUDIES AND RESEARCH

The undersigned certify that they have read, and recommend to the Faculty of Graduate Studies and Research for acceptance, a thesis entitled "topics in two-body hadronic decays of D mesons" submitted by EL HASSAN EL AAOUD in partial fulfilment of the requirements for the degree of Doctor of Philosophy.

Dr. H. Sherif (*Supervisor*)

Dr. M. Razavy (*Committee Chair*)

Dr. G. Ludwig

Dr. D. Gingrich

Dr. A. Czarnecki

Dr. P. O'Donnell (*External Examiner*)
U of T, Toronto, Canada

Date: Aug. 22/2000

Abstract

We have carried out an analysis of helicity and partial-wave amplitudes for the decay of D mesons to two vector mesons V_1V_2, $D \to V_1V_2$. In particular we have studied the Cabibbo-favored decays $D_s^+ \to \rho\phi$ and $D \to K^*\rho$ in the factorization approximation using several models for the form factors. All the models, with the exception of one, generate partial-wave amplitudes with the hierarchy $\mid S \mid > \mid P \mid > \mid D \mid$. Even though in most models the D-wave amplitude is an order of magnitude smaller than the S-wave amplitude, its effect on the longitudinal polarization could be as large as 30%. Due to a misidentification of the partial-wave amplitudes in terms of the Lorentz structures in the relevant literature, we cast doubt on the veracity of the listed data for the decay $D \to K^*\rho$, particularly the partial-wave branching ratios.

We have also investigated the effect of the isospin $\frac{1}{2}$, $J^P = 0^+$ resonant state $\bar{K}_0^*(1950)$ on the decays $D^0 \to \bar{K}^0\eta$ and $D^0 \to \bar{K}^0\eta'$ as a function of the branching ratio sum $r = Br(\bar{K}_0^*(1950) \to \bar{K}^0\eta) + Br(\bar{K}_0^*(1950) \to \bar{K}^0\eta')$ and the coupling constants $g_{\bar{K}_0^*\bar{K}^0\eta}$, and $g_{\bar{K}_0^*\bar{K}^0\eta'}$. We have used a factorized input for the $D^0 \to \bar{K}_0^*(1950)$ weak transition through a πK loop. We estimated both on- and off-shell contributions from the loop. Our calculation shows that the off-shell effects are significant. For $r \geq 30\%$ a fit to the decay amplitude $\mid A(D^0 \to \bar{K}^0\eta') \mid$ was possible, but the amplitude $A(D^0 \to \bar{K}^0\eta)$ remained at its factorized value and hence a branching ratio too low compared to data. For small values of r, $r \leq 18\%$, we were able to fit $\mid A(D^0 \to \bar{K}^0\eta) \mid$, and despite the fact that $\mid A(D^0 \to \bar{K}^0\eta') \mid$ could be raised by almost 100% over its factorized value, it still falls short of its experimental value. A simultaneous fit to both amplitudes $\mid A(D^0 \to \bar{K}^0\eta') \mid$ and $\mid A(D^0 \to \bar{K}^0\eta) \mid$ was not possible. We have also determined the strong phase of the resonant amplitudes for both decays.

To the Future Generation, ...

Preface

The research presented in this thesis was carried out in the Department of Physics at the University of Alberta under the supervision of A. N. Kamal.

Unless otherwise stated, the material presented is based on the following papers:

1. El hassan El aaoud, $D_s^+ \to \phi\rho^+$ decay, Phys. Rev. D 58, 037502 (1998).

2. El hassan El aaoud and A. N. Kamal, Helicity and partial wave amplitude analysis of $D \to K^*\rho$ decays, Phys. Rev. D 59, 114013 (1999).

3. El hassan El aaoud and A. N. Kamal, Resonant final-state interactions in $D^0 \to \bar{K}^0\eta, \bar{K}^0\eta'$ decays, (accepted for publication in Int. J. Mod. Phys. A XX, XXXX (2000)), hep-ph/9910327.

ACKNOWLEDGEMENT

I wish to express my deep appreciation to my supervisors Professors A. N. Kamal and H. Sherif for their great support and guidance. The work presented in this thesis was undertaken under the supervision of Dr. Kamal, however because of his health, the completion of thesis writing was done under the supervision of Dr. H. Sherif. I also wish to thank the other members of my thesis committee for their cooperation and constructive comments.

Thanks to the physics department and all its members, specially Lynn Chandler, for their assistance and support. I wish to thank my colleague Dr. F. Al-Shamali for his countless help with computational issues, and for the many fruitful discussions we had together. I also wish to thank Dr. H. Darhmaoui for his help during my first days at U of A.

Contents

1 Introduction **1**

2 Effective weak hamiltonian for hadronic D decays **9**

2.1 Weak Hamiltonian 9

2.2 Strong Interaction Effects 15

2.2.1 Quark mass effects 23

2.3 Effective weak Hamiltonian 24

2.4 Numerical results for Wilson coefficients C_1 and C_2 27

2.4.1 B decays 27

2.4.2 D decays 28

3 Hadronic matrix elements **36**

3.1 Introduction 36

3.2 Diagrammatic Approach 37

3.3 Factorization 41

3.3.1 General Idea 41

3.3.2 Classification of two-body hadronic decays in the factorization approximation 44

3.4 Decay Amplitude in factorization scheme 47

3.4.1 $F \longrightarrow P_1 P_2$ 52

3.4.2 $F \longrightarrow PV$ 53

3.4.3 $P(K) \longrightarrow V_1(k_1)V_2(k_2)$ 54
3.4.4 Calculation of the Helicity Amplitudes A_{00} and $A_{\pm\pm}$ 55

4 $D_s^+ \to \phi\rho^+$ Decay **63**
4.1 Introduction 63
4.2 Details of the Calculations 65
4.3 Results and Discussion 71

5 Helicity and partial wave amplitude analysis of $D \to K^*\rho$ decay **78**
5.1 Introduction 78
5.2 Method 82
5.2.1 $D^0 \longrightarrow K^{*-}\rho^+$ 84
5.2.2 $D^0 \longrightarrow \bar{K}^{*0}\rho^0$ 87
5.2.3 $D^+ \longrightarrow \bar{K}^{*0}\rho^+$ 89
5.3 Results 90
5.3.1 Parameters 90
5.3.2 $D^0 \to K^{*-}\rho^+$ 91
5.3.3 $D^+ \to \bar{K}^{*0}\rho^+$ 93
5.3.4 $D^0 \to \bar{K}^{*0}\rho^0$ 94
5.4 S-wave and $A_1(q^2)$ dominance 94
5.5 Conclusion 96

6 Resonant final-state interactions in $D^0 \to \bar{K}^0\eta, \bar{K}^0\eta'$ Decays **103**
6.1 Introduction 103
6.2 Method of calculation 105
6.2.1 Calculation without final-state interactions 105
6.2.2 Calculation with resonant final-state interactions 107
6.3 Results 118
6.3.1 Factorized Amplitude 118
6.3.2 Resonant Amplitude 119

6.3.3 On-shell contribution 120
6.3.4 Off-shell contribution 120
6.3.5 Strong phases 121
6.4 Discussion 122

7 Conclusions **129**

A $SU(3)$ Symmetry **133**

B Helicity Formalism **136**
B.1 Single Particle State 136
B.1.1 Spin 1 particle 137
B.2 Two Particles State 138
B.2.1 Two Spin One Particles 138

C η and η' particles **142**

List of Tables

2.1 The QCD scale $\Lambda^{(5)}$ and the Wilson coefficients C_+, C_-, C_1 and C_2 for B decays at the scale $\mu = 4.4\ GeV$ in the leading order approximation. These values were obtained from Eqns. (2.24) and (2.42) with $f = 5$ and the running coupling constant normalized to $\alpha_s(M_Z) = 0.119 \pm 0.002$ as explained in the text. 30

2.2 The QCD scale $\Lambda^{(5)}$ and the Wilson coefficients C_+, C_-, C_1 and C_2 for B decays at scale $\mu = 4.4\ GeV$, in the next-to-leading order approximation. These values were obtained from Eqns. (2.26) and (2.44) with $f = 5$ and the running coupling constant normalized to $\alpha_s(M_Z) = 0.119 \pm 0.002$. 30

2.3 The QCD scale $\Lambda^{(4)}$ and the Wilson coefficients C_+, C_-, C_1 and C_2 for D decays at the scale $\mu = 1.4\ GeV$, in the leading order approximation. These values were obtained using Eqns. (2.24) and (2.48) with an effective number of flavors $f = 4$ and the running coupling constant normalized to $\alpha_s(M_Z) = 0.119 \pm 0.002$. 31

2.4 The QCD scale $\Lambda^{(4)}$ and the Wilson coefficients C_+, C_-, C_1 and C_2 for D decays at the scale $\mu = 1.4\ GeV$, in the next-to-leading order approximation. These values were obtained using Eqns. (2.26) and (2.49) with an effective number $f = 4$ and the running coupling constant normalized to $\alpha_s(M_Z) = 0.119 \pm 0.002$. 31

2.5 The QCD scale $\Lambda^{(5)}$ and the Wilson coefficients C_+, C_-, C_1 and C_2 for B decays at scale $\mu = 4.4\ GeV$ in the leading order approximation. These values were obtained from Eqns. (2.26) and (2.42) with $f = 5$ and the running coupling constant normalized to $\alpha_s(M_Z) = 0.119 \pm 0.002$ as explained in the text. 32

2.6 The QCD scale $\Lambda^{(4)}$ and the Wilson coefficients C_+, C_-, C_1 and C_2 for D decays at the scale $\mu = 1.4\ GeV$, in the leading order approximation. These values were obtained using Eqns. (2.26) and (2.48) with an effective number $f = 4$ and the running coupling constant normalized to $\alpha_s(M_Z) = 0.119 \pm 0.002$. 32

2.7 The QCD scales and Wilson coefficients C_+, C_-, C_1 and C_2 for D decays at the scale $\mu = 1.4\ GeV$, in the leading order approximation. These values are obtained using Eq. (2.42), instead of the correct Eq. (2.48), with QCD scale $\Lambda^{(5)}$ replaced by $\Lambda^{(4)}$ and an effective number of active flavors $f = 4.15$. 33

2.8 The QCD scales and Wilson coefficients C_+, C_-, C_1 and C_2 for D decays at the scale $\mu = 1.4\ GeV$, in the next-to-leading order approximation. These values were obtained using Eq. (2.44), instead of the correct Eq. (2.49), with $\Lambda^{(5)}$ replaced by $\Lambda^{(4)}$ and an effective number of active flavors $f = 4.15$. 33

4.1 Model predictions of $A_1^{D_s\phi}(0)$, $A_2^{D_s\phi}(0)$, $V^{D_s\phi}(0)$, $A_1^{D_s\phi}(m_\rho^2)$, $A_2^{D_s\phi}(m_\rho^2)$, and $V^{D_s\phi}(m_\rho^2)$ form factors and the ratios $x^{D_s\phi}(0)$, $y^{D_s\phi}(0)$, $x^{D_s\phi}(m_\rho^2)$, $y^{D_s\phi}(m_\rho^2)$ for the processes $D_s^+ \longrightarrow \rho^+\phi$. In the last column we use the experimentally measured form factors from the semi leptonic decays $D_s^+ \longrightarrow \phi l^+\nu_l$. 74

4.2 Decay rate, Γ, phase difference $\delta_{SD} = \delta_S - \delta_D$ and the ratios $r_{SP} = \frac{|S|}{|P|}$, $r_{SD} = \frac{|S|}{|D|}$ for $D_s^+ \longrightarrow \rho^+\phi$ decay. The values of Γ must be multiplied by $10^{12}s^{-1}$. δ_{SD} is the value needed to get agreement with the experimental values, to one standard deviation, of the longitudinal polarization $P_L = 0.370 \pm 0.052$. The last column uses experimentally measured form factors (see Table 4.1). 'Expt.FF' stands for 'Experimental form factors'. 75

5.1 Model and experimental predictions for the form factors: $A_1^{DK^*}(q^2)$, $A_2^{DK^*}(q^2), V^{DK^*}(q^2), A_1^{D\rho}(q^2), A_2^{D\rho}(q^2), V^{D\rho}(q^2)$ and the ratios $x^{DK^*}(q^2)$, $y^{DK^*}(q^2)$, $x^{D\rho}(q^2)$, $y^{D\rho}(q^2)$ at $q^2 = m_{K^*}^2, m_\rho^2, 0$ for the process $D \longrightarrow K^*\rho$ 92

5.2 Decay rates for $D^0 \longrightarrow \bar{K}^{*-}\rho^+$. The values of Γ must be multiplied by $10^{11}s^{-1}$. The experimental values of P_L are listed only if measurements of longitudinal or transverse branching ratios are available [5]. 98

5.3 Decay rates for $D^+ \longrightarrow \bar{K}^{*0}\rho^+$. The values of Γ must be multiplied by $10^{11}s^{-1}$. The experimental values of P_L are listed only if measurements of longitudinal or transverse branching ratios are available [5]. 98

5.4 Decay rates for $D^0 \longrightarrow \bar{K}^{*0}\rho^0$. The values of Γ must be multiplied by $10^{11}s^{-1}$. The experimental values of P_L are listed only if measurements of longitudinal or transverse branching ratios are available [5]. 99

6.1 Model predictions for the form factors : $F_0^{D\eta(\eta')}(m_K^2)$, $F_0^{DK(\pi)}(0)$ and the ratio $\frac{F_0^{D\pi}(0)}{F_0^{DK}(0)}$ for the processes $D^0 \longrightarrow \bar{K}^0\eta, \bar{K}^0\eta', K\pi$. 119

6.2 Model predictions for the factorized amplitude A^f for the process $D^0 \longrightarrow \bar{K}^0\eta$ and $D^0 \longrightarrow \bar{K}^0\eta'$ These values must be multiplied by a factor of $10^{-7}GeV$. 119

6.3 Phases of the total resonant and on-shell amplitudes defined in Eqs. (6.58) and (6.62), respectively, as functions of r for the processes $D^0 \longrightarrow \bar{K}^0\eta(\eta')$. δ_r is the phase of A^r (Eq. (6.58)) and $\delta_{on\text{-}shell}$ is the phase of $A^r(on\text{-}shell)$ (Eq. (6.62)). 121

A.1 The non-vanishing symmetric and antisymmetric structure constants d_{ijk} and f_{ijk} for SU(3) group. 135

List of Figures

2.1 Lowest order charged current weak decay of quarks. The vertices describe the coupling of quarks to W-boson with strength $V_{qq'}$. 11

2.2 a) Tree-level Feynman diagram for the process $q_1 \to q_2 q_3 \bar{q}_4$, through exchange of intermediate W-boson. b) For $q^2 << M_W^2$ the exchange diagram reduces to a local four point interaction where W-boson is integrated out. 11

2.3 Classification of non leptonic charm decays: a) Cabibbo-favored decay, amplitude $\propto \cos^2\theta_c$, b) and c) Cabibbo-suppressed decay, amplitude $\propto \sin\theta_c \cos\theta_c$, d) Double Cabibbo-suppressed decay amplitude $\propto \sin^2\theta_c$. 14

2.4 Quark diagrams for the decay of a charm-meson generated by the effective weak Hamiltonian in Eq. (2.12), $\bar{q}_s$ is a spectator quark: a) External W-emission, b) Internal W-emission. 16

2.5 A more realistic picture of two-body hadronic decay of a heavy flavor. The solid straight lines represent quarks, wavy and curly lines represents W-boson and gluons, respectively (compare with Fig. 2.4). 17

2.6 First order ($O(\alpha_s)$) QCD corrections to the 4-quark nonleptonic weak Hamiltonian. The solid straight lines represent quarks, wavy and curly lines represent W-boson and gluons, respectively. Diagrams differing by left-right and up-down reflection are not shown. 19

3.1 The six quark-diagrams contributing to heavy flavor decays (Q is a heavy quark c or b and $\bar{q}_s$ is a light antiquark $\bar{u}$, $\bar{d}$ or $\bar{s}$: a) color-favored tree diagram, b) color-suppressed tree diagram, c) annihilation, d) W-exchange diagram , e) penguin annihilation diagram, f) penguin diagram. 39

3.2 Hair-pin diagram contributing to final state with SU(3) singlet $\bar{q}q$ in the final state 39

3.3 Classification of nonleptonic two-body hadronic decays of charm meson, a) class I or color favored tree diagram determined by a_1, b) class II or color suppressed tree diagram determined by a_2, c) class III decay determined by $a_1 + xa_2$. 45

3.4 Helicities of the the particles V_1V_2 in the parent rest frame 55

4.1 External W-emission diagram contributing to the Cabibbo favored $D_s^+ \longrightarrow \rho^+\phi$ decay 65

4.2 Hair-pin quark diagram for $D_s^+ \longrightarrow \rho^+\phi$ decay. The singlet meson ϕ is created from the vacuum. 66

5.1 Quark diagrams contributing to $D \to K^*\rho$: a) class I or color favored tree diagram contributing to $D^0 \longrightarrow K^{-*}\rho^+$, b) class II or color suppressed tree diagram contributing to $D^0 \to \bar{K}^{0*}\rho^0$, c) class III diagram contributing to $D^+ \to \bar{K}^{0*}\rho^+$. 83

6.1 Quark diagram contributing to the factorized amplitude A^f for $D^0 \to \bar{K}^0\eta$ and $D^0 \to \bar{K}^0\eta'$. 106

6.2 Resonant contribution to $D^0 \to \bar{K}^0\eta$ and $D^0 \to \bar{K}^0\eta'$. The vertical dashed line represents the cut when the particles, $K\pi$, in the loop are on-shell. The thick line represents the resonance $K_0^*(1950)$, and the shaded circle represents the weak vertex $\mathcal{V}(k^2)$. 107

6.3 Plot for the two sets of solutions, $g^i_\eta(r), i = 1, 2$, as a function of the branching ratio sum $r = Br(K^*_0(1950) \to K^0\eta) + Br(K^*_0(1950) \to \bar{K}^0\eta')$. The thick and light parts of the curve correspond to $g^1_\eta(r)$ and $g^2_\eta(r)$, respectively. 113

6.4 Plot for the two sets of solutions, $g^i_{\eta'}(r), i = 1, 2$, as a function of the branching ratio sum $r = Br(K^*_0(1950) \to K^0\eta) + Br(K^*_0(1950) \to \bar{K}^0\eta')$. The thick and light parts of the curve correspond to $g^1_{\eta'}(r)$ and $g^2_{\eta'}(r)$, respectively. 114

6.5 Plot of the magnitude of the total amplitude $|A| = |A^f + A^r|$ in Eq. (6.65) for $D^0 \to \bar{K}^0\eta$ as a function of the branching ratio sum $r = Br(\bar{K}^*_0(1950) \to \bar{K}^0\eta) + Br(\bar{K}^*_0(1950) \to \bar{K}^0\eta')$. The thick and light parts of the curve correspond to the solution g^1_η and g^2_η, respectively. The shaded region represents the experimental value of the amplitude, the horizontal line represents the factorized amplitude A^f. The values on the y-axis must be multiplied by a factor of 10^{-7} GeV to get the absolute magnitude of the decay amplitude. 124

6.6 Plot of the magnitude of the total amplitude $|A| = |A^f + A^r|$ in Eq. (6.65) for $D^0 \to \bar{K}^0\eta'$ as a function of the branching ratio sum $r = Br(\bar{K}^*_0(1950) \to \bar{K}^0\eta) + Br(\bar{K}^*_0(1950) \to \bar{K}^0\eta')$. The thick and light parts of the curve correspond to the solution $g^1_{\eta'}$ and $g^2_{\eta'}$, respectively. The shaded region represents the experimental value of the amplitude, the horizontal line represents the factorized amplitude A^f. The values on the y-axis must be multiplied by a factor of 10^{-7} GeV to get the absolute magnitude of the decay amplitude. 125

Chapter 1

Introduction

Hadronic weak decays of the charm D meson to two mesons M_1, M_2 have been extensively studied both theoretically [1]–[3] and experimentally [4, 5]. At the theoretical level the effective weak Hamiltonian for the nonleptonic decay of the D meson is expressed in terms of local four-quark operators, $O_i(\mu)$, with Wilson coefficients $C_i(\mu)$ to be computed in perturbation theory at the appropriate scale μ,

$$\mathcal{H} = \frac{G_F}{\sqrt{2}} \sum_i \lambda_i^{CKM} C_i(\mu) O_i(\mu), \tag{1.1}$$

where λ_i^{CKM} are products of CKM matrix elements. The estimation of the hadronic matrix element,

$$A(D \to M_1 M_2) = \frac{G_F}{\sqrt{2}} \sum_i \lambda_i^{CKM} C_i(\mu) \langle M_1 M_2 \mid O_i(\mu) \mid D \rangle, \tag{1.2}$$

is of fundamental importance in any phenomenological analysis of the process $D \to M_1 M_2$. However, a systematic calculation of the matrix elements $A(D \to M_1 M_2)$ from first principles is not yet possible.

In most of the previous analyses, the evaluation of $A(D \to M_1 M_2)$ was based on the factorization assumption of Bauer, Stech, and M. Wirbel (BSW) [1] which utilizes model form factors. In this approximation the operators O_i are replaced by a product of hadronic currents J_μ, $O_i \equiv J^\mu J_\mu$, which mimic the quark current of weak

interactions. This leads to an effective weak Hamiltonian for hadronic D decay of the form

$$\mathcal{H} \equiv a_1 O_1 + a_2 O_2, \tag{1.3}$$

where the phenomenological parameters a_i are related to the Wilson coefficients C_i by $a_{1(2)} = C_{1(2)} + \frac{C_{2(1)}}{N}$ with N the number of colors. In this approach the decay amplitude can be approximated by the product of two current matrix elements

$$\langle M_1 M_2 \mid J^\mu J_\mu \mid D\rangle \simeq \langle M_1 \mid J^\mu \mid 0\rangle \langle M_2 \mid J_\mu \mid D\rangle. \tag{1.4}$$

Then, each of the matrix elements is expressed in terms of meson decay constants and generally model dependent form factors.

Since the final state in nonleptonic decay involves hadrons, there are strong final state interaction (FSI) effects which cannot be overlooked. Being non-perturbative such effects are difficult to treat. FSI are neglected in the factorization prescription of hadronic decays. The importance of FSI in the hadronic decays of D mesons has been known for a long time[6]. The weak decay amplitude picks up a phase factor $\exp(i\delta_X)$, where δ_X is the strong phase shift in the appropriate amplitude (partial wave, isospin, ...)[7]. The most dramatic effect of FSI is induced by the interference between different amplitudes which depends on their respective phase differences [1, 6, 8].

Of particular interest is the decay of D mesons into two vector mesons $V_1 V_2$; they are much richer than the decay to two pseudoscalars or a pseudoscalar and a vector meson. The hadronic matrix element

$$A(D \to V_1 V_2) = \langle V_1 V_2 \mid \mathcal{H} \mid D\rangle\,, \tag{1.5}$$

involves three invariant amplitudes which can be expressed in terms of three different, but equivalent, bases;

- the helicity basis $|++\rangle, |--\rangle, |00\rangle$,
- the partial-wave basis (or the LS-basis) $|S\rangle, |P\rangle, |D\rangle$

- the transversity basis $|0\rangle, |\,\|\rangle, |\,\perp\rangle$.

The amplitude $A(D \to V_1V_2)$ can be analyzed in any of these three bases. In the BSW model [1, 9], $A(D \to V_1V_2)$ depends on three invariant form factors $A_1(q^2)$, $A_2(q^2)$, and $V(q^2)$. What is not known at this stage is the behavior of these invariant form factors. Usually one appeals to theoretical models to evaluate these form factors and obtain numerical results to be compared with experimental data.

At the experimental level, while the branching ratio and the longitudinal polarization in $D_s^+ \to \rho^+\phi$ have been measured recently [4, 5], the data on $D \to K^*\rho$ were available for almost a decade [4]. Although the data for the latter decay are quoted either in terms of the helicity branching ratios or the partial-wave branching ratios, much of the effort in the past was devoted to understanding mainly the decay rate $\Gamma(D \to V_1V_2)$ [1, 2]. Studies based on the factorization model were carried out by Bauer *el al.* [1] and Kamal *et al.* [2]. Approaches based on flavor $SU(3)$ symmetry and broken $SU(3)$ symmetry were pursued also by Kamal *et al.* [2] and by Hinchliffe and Kaeding [2]. Bedaque *et al.* [2] have carried out a pole-dominance model calculation. In particular the decays, $D_s^+ \to \phi\rho^+$ and $D \to K^*\rho$, has been studied within the context of factorization by Kamal *et al.* [2] . The decay $D_s^+ \to \phi\rho^+$ has been studied also by Gourdin *et al.* [10]. Subsequently, nonfactorization contributions were included in the decay $D \to K^*\rho$ by the authors of [11] and in the decay $D_s^+ \to \phi\rho^+$ by the authors of [12].

No study of the helicity and partial wave amplitudes of the process $D \to V_1V_2$ has been undertaken in the past. It is evident that the completeness of helicity partial wave bases requires that the total branching ratio B for $D \to V_1V_2$ should be equal to the sum of the helicity branching ratios or the sum of partial wave branching ratios. However, the data, specially on $D^0 \to K^{*0}\rho^0$, does not meet this requirement.

The two-body hadronic weak decays of D^0 involving η and η' in the final state are not well understood theoretically. For example calculations in the factorization approximation not only underestimate the decay rates for $D^0 \to \bar{K}^0\eta$ and $D^0 \to \bar{K}^0\eta'$,

but it also generates $\Gamma(D^0 \to \bar{K}^0\eta) > \Gamma(D^0 \to \bar{K}^0\eta')$ in contradiction with the experiment [4]. Verma, *et al.* [13] had studied these decays in the factorization approximation but included the annihilation term. They found that unlikely large annihilation form factors for $K \to \eta$ and $K \to \eta'$ transitions were required in order to bridge the gap between theory and experiment. Reference [14] on the other hand introduced nonfactorized contributions and used a flavor-$SU(3)$ parameterization for the nonfactorized matrix elements to fit the data.

The decays $D^0 \to \bar{K}^0\eta$ and $D^0 \to \bar{K}^0\eta'$ have a single isospin final state. Consequently, isospin interference effects are absent. However, the D meson lies in a resonance region and resonant FSI could lead to a change in the magnitude of the decay amplitude.

Motivated by the measurement of the rate Γ, the longitudinal polarization P_L in $D_s^+ \to \rho^+\phi$ and the internal inconsistency of the data on $D \to K^*\rho$ and the fact that the factorization approximation gives decay rates $\Gamma(D^0 \to \bar{K}^0\eta)$ and $\Gamma(D^0 \to \bar{K}^0\eta')$ below experimental values, we have undertaken a theoretical analysis of the helicity and partial wave amplitudes for the decay, $D \to V_1V_2$, assuming factorization and using several models for the form factors. In particular we have studied the following decays $D_s^+ \to \rho^+\phi$, $D^0 \to K^{*-}\rho^+$, $D^+ \to \bar{K}^{*0}\rho^+$ and $D^0 \to \bar{K}^{*0}\rho^0$. We have also included the effects of final state interactions (FSI) by working with the partial wave amplitudes as the dependence of the polarization on the partial wave phase is more obvious in this basis. We have also investigated the final state interaction involving the resonance $\bar{K}_0^*(1950)$ on the decays $D^0 \to \bar{K}^0\eta$ and $D^0 \to \bar{K}^0\eta'$.

The thesis is organized as follows:

- In chapter two we discuss the effective weak Hamiltonian used in the phenomenological analysis of hadronic decays of D mesons. We start by deriving the weak Hamiltonian ignoring QCD corrections. Then we take into account QCD short distance effects, which are summed in the Wilson coefficients $C_1(\mu)$ and $C_2(\mu)$. We have calculated C_1 and C_2 at the scale $\mu = 1.4$ GeV, in the

leading and next to leading order approximation.

- In chapter three we provide a prescription for calculating the hadronic matrix element, $A(D \to M_1 M_2)$, for two-body hadronic D decay in the factorization approximation. Since $A(D \to M_1 M_2)$ depends on the type of particles involved in the final state, we present detailed expressions for final states involving 1) two pseudoscalar mesons, 2) a pseudoscalar and a vector meson, and 3) two vector mesons. For the case of final states with two vectors particles we express the matrix elements in terms of helicity and partial wave amplitudes and we clarify the interrelation between them. We derive expressions for these amplitudes in term of BSW form factors $A_1(q^2)$,$A_2(q^2)$ and $V(q^2)$. We show explicitly that while the P wave contribution depends only on the form factor $V(q^2)$, those for S and D waves are linear combinations of both form factor $A_1(q^2)$ and $A_2(q^2)$. The decay rate $\Gamma(D \to V_1 V_2)$ is an incoherent sum of partial wave amplitudes and is independent of their phases. But the polarization does depend on the phase difference, $\delta_{SD} = \delta_S - \delta_D$, arising from interference between S and D waves.

- In chapter four and five we implement the formalism established in chapter three in the study of decays $D_s^+ \to \rho^+ \phi$ and $D \to K^* \rho$. We evaluate the partial wave ratios $r_{SP} = \frac{|S|}{|P|}$ and $r_{SD} = \frac{|S|}{|D|}$. In these ratios the kinematical and weak coupling constants as well as the Wilson coefficients cancel out. The ratios thus depend only on the particles involved in the final state and on the form factor ratios

$$\begin{aligned} x(q^2) &\equiv \frac{A_2(q^2)}{A_1(q^2)}, \\ y(q^2) &\equiv \frac{V(q^2)}{A_1(q^2)}. \end{aligned} \tag{1.6}$$

  We have also investigated the effect of the interference between S and D waves on the polarization.

- In chapter six we consider the FSI effects of the $K_0^*(1950)$ resonance on $D^0 \to \bar{K}^0\eta$ and $D^0 \to \bar{K}^0\eta'$ decays. We propose that the effect of $\bar{K}_0^*(1950)$ on $D^0 \to \bar{K}^0\eta(\eta')$ could be estimated via a Feynman diagram where we include both $K^-\pi^+$ and $\bar{K}^0\pi^0$ states in the loop. First we estimate the factorized amplitude $A^f(D^0 \to \bar{K}^0\eta)$ and $A^f(D^0 \to \bar{K}^0\eta')$. Second we calculate the contribution of $\bar{K}_0^*(1950)$ by using a factorized input for $D^0 \to \bar{K}_0^*(1950)$ weak transition through a πK loop. We express the resonant amplitude $A^r(D^0 \to \bar{K}^0\eta)$ and $A^r(D^0 \to \bar{K}^0\eta')$ as a function of the unmeasured branching ratio sum $r = B(\bar{K}_0^*(1950) \to \bar{K}^0\eta) + B(\bar{K}_0^*(1950) \to \bar{K}^0\eta')$. Finally we study the dependence of the total amplitude $A(D^0 \to \bar{K}^0\eta(\eta')) = A^f(D^0 \to \bar{K}^0\eta(\eta')) + A^r(D^0 \to \bar{K}^0\eta(\eta'))$ on the variable r.

- chapter seven is devoted to conclusions and a discussion of future prospects for the four body hadronic decay $D \to K\pi\pi\pi$.

Bibliography

[1] M. Bauer, B. Stech, and M. Wirbel, Z. Phys. C **34**, 103 (1987).

[2] A. N. Kamal, R. C. Verma, N. Sinha, Phys. Rev. D **43**, 843 (1991). I. Hinchliffe and T. A. Kaeding, Phys. Rev. D **54**, 914 (1996). P. Bedaque, A. Das, and V. S. Mathur, Phys. Rev. D **49**, 269 (1994).

[3] F. Buccella, M. Lusignoli, A. Pugliese, Phys. Lett. B **379**, 249 (1996); F. Buccella, M. Lusignoli, G. Miele, A. Pugliese, and P. Santorelli, Phys. Rev. D **51**, 3478 (1995).

[4] Particle Data Group, C. Caso et al., Eur. Phys. J. C **3**, 1 (1998).

[5] CLEO Collaboration, V. Balic (private communication).

[6] H. J. Lipkin, Phys. Rev. Lett. **44**, 710 (1980); A. N. Kamal and E. D. Cooper, Z. Phys. C **8**, 67 (1981); C. Sorensen, Phys. Rev. D **23**, 2618 (1981);

[7] A. N. Kamal, Int. J. Mod. Phys. A **7**, 3515 (1992).

[8] J. Wiss, Nuovo Cimento **109A**, 895 (1996).

[9] M. Wirbel, B. Stech and M. Bauer, Z. Phys. C **29**, 637 (1985); M. Bauer and M. Wirbel, *ibid.* **42**, 671 (1989).

[10] M. Gourdin, A. N. Kamal, Y. Y. Keum, and X. Y. Pham, Phys. Lett. **B 339**, 173 (1994).

[11] A. N. Kamal, A. B. Santra, and T. Uppal, R. C. Verma, Phys. Rev. D **53**, 2506 (1996). Hai-Yang Cheng, Z. Phys. C **69**, 647 (1996); Phys. Lett. B **335**, 428 (1994).

[12] A. N. Kamal and A. B. Santra, Z. Phys. **C 71**, 101 (1996).

[13] R. C. Verma, A. N. Kamal, and M. P. Khanna, Z. Phys. C **65**, 255 (1995)

[14] R. C. Verma, Phys. Lett. B **365**, 377 (1996); K. K. Sharma, A. C. Katoch, and R. C. Verma, Z. Phys. C **76**, 311 (1997).

Chapter 2

Effective weak hamiltonian for hadronic D decays

2.1 Weak Hamiltonian

The flavor-changing weak decay of a quark is described by the charged weak current Lagrangian density given by [1]

$$\mathcal{L}_{cc} = \frac{g_w}{2\sqrt{2}}(W_\mu^+ J_-^\mu + h.c), \tag{2.1}$$

where $h.c$ stands for hermitian conjugate, g_w is the weak coupling constant and J_-^μ is the charged current given by

$$\begin{aligned} J_-^\mu &= (\overline{u}, \overline{c}, \overline{t})\gamma^\mu(1-\gamma_5)\begin{pmatrix} d' \\ s' \\ b' \end{pmatrix}, \\ &= (\overline{u}, \overline{c}, \overline{t})\gamma^\mu(1-\gamma_5)\, V\begin{pmatrix} d \\ s \\ b \end{pmatrix}, \end{aligned} \tag{2.2}$$

where V is the Cabibbo-Kobayashi-Maskawa (CKM) mixing matrix [2] connecting the quark weak eigenstates (d', s', b') and the quark mass eigenstates (d, s, b) according

to the linear relation

$$\begin{pmatrix} d' \\ s' \\ b' \end{pmatrix} = \begin{pmatrix} V_{ud} & V_{us} & V_{ub} \\ V_{cd} & V_{cs} & V_{cb} \\ V_{td} & V_{ts} & V_{tb} \end{pmatrix} \begin{pmatrix} d \\ s \\ b \end{pmatrix}. \tag{2.3}$$

The quark field operators $\bar{q}, q = u, d, s, ...,$ in the current J_μ create quarks and annihilate anti-quarks. W_μ^+ is the physical W^+ boson field operator; it annihilates (creates) a W^+ (W^-) particle. Therefore, in first order in perturbation theory, the Lagrangian $\mathcal{L}_{cc}$ describes the coupling of quarks (u, d, s, c, ...) to vector bosons $W^\pm$, i.e the processes with single vertex as shown in (Fig. 2.1). However, none of these processes is physical as the energy and momentum cannot be conserved for any of them with all particles on mass-shell. A known empirical fact is that all weak processes observed so far at low energy, involve four external fermions (quarks and/or leptons). Therefore one needs at least two vertices to describe a physical process, i.e. we must go to second order in perturbation theory of $\mathcal{L}_{cc}$. A typical weak decay is depicted in (Fig. 2.2); $W(q^2)$ is the propagator of the intermediate vector boson given by

$$W(q^2) = -i\frac{g_{\nu\mu} - \frac{q_\nu q_\mu}{M_W^2}}{q^2 - M_W^2} \xrightarrow{q^2 \to 0} i\frac{g_{\nu\mu}}{M_W^2}, \tag{2.4}$$

q^2 is the momentum transfer, q_μ the four-momentum carried by W-boson, and M_W its mass. The energy scale in hadronic decays of mesons is much smaller than the W boson mass, i.e. $q^2 << M_W^2$, therefore, in a second order process the W propagator can be replaced by a constant and the diagram in (Fig. 2.2.a) is replaced by a four-point contact interaction shown in (Fig.2.2.b), where the W boson is integrated out. This is equivalent to using an effective Hamiltonian, of current × current form to order g_w^2 or to first order in the Fermi coupling constant G_F,

$$\begin{aligned} \mathcal{H}_{eff} &= -\mathcal{L}_{eff} \\ &= \frac{G_F}{\sqrt{2}} J_-^\mu J_\mu^+, \end{aligned} \tag{2.5}$$

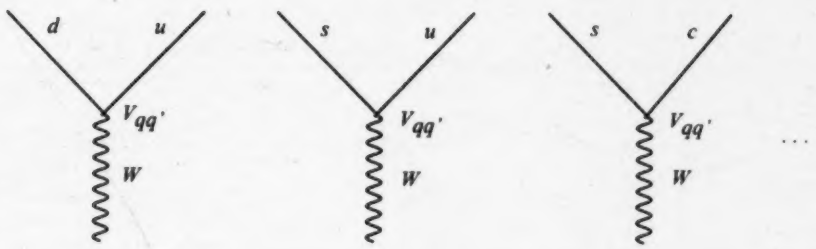

Figure 2.1: Lowest order charged current weak decay of quarks. The vertices describe the coupling of quarks to W-boson with strength $V_{qq'}$.

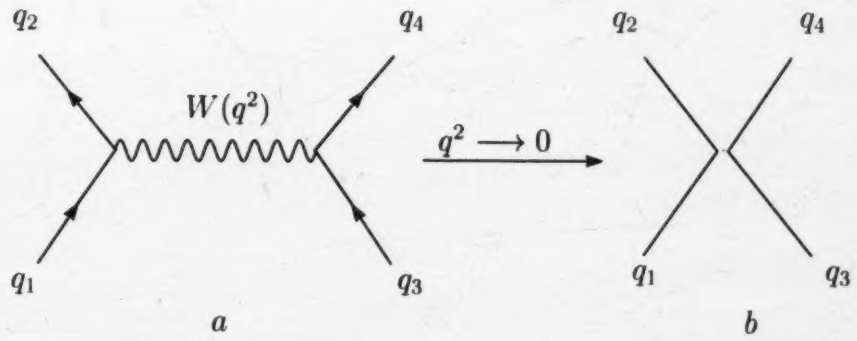

Figure 2.2: a) Tree-level Feynman diagram for the process $q_1 \rightarrow q_2 q_3 \bar{q}_4$, through exchange of intermediate W-boson. b) For $q^2 << M_W^2$ the exchange diagram reduces to a local four point interaction where W-boson is integrated out.

where $J_\mu^+ = J_\mu^{-\dagger}$ and the Fermi coupling constant G_F is defined as [3]

$$\begin{aligned} G_F &= \frac{g_w^2}{4\sqrt{2}M_W^2} \\ &= 1.16639 \times 10^{-5}\, GeV^{-2}. \end{aligned} \tag{2.6}$$

Using Eq. (2.2) and (2.5) we obtain the general effective weak Hamiltonian for flavor changing weak decays of quark

$$\begin{aligned} \mathcal{H}_{eff} &= \frac{G_F}{\sqrt{2}}\Big\{(\bar{u}d')(\bar{d}'u) + (\bar{u}d')(\bar{s}'c) + (\bar{u}d')(\bar{b}'t) + (\bar{c}s')(\bar{d}'u) \\ &\quad +(\bar{c}s')(\bar{s}'c) + (\bar{c}s')(\bar{b}'t) + (\bar{t}b')(\bar{d}'u) + (\bar{t}b')(\bar{s}'c) + (\bar{t}b')(\bar{b}'t)\Big\}, \end{aligned} \tag{2.7}$$

where we have used the notation

$$(\bar{q}_1 q_2) = \sum_{\alpha=1}^{3} \bar{q}_1^\alpha \gamma_\mu (1-\gamma_5) q_2^\alpha, \tag{2.8}$$

where, $\alpha = 1, 2, 3$ is the color index. The relevant part of the weak Hamiltonian for the charm lowering hadronic decay with $\Delta C = -1$:

$$q_1(=c) \;\rightarrow\; q_2\, q_3\, \bar{q}_4 \tag{2.9}$$

where $q_{i=2,3,4} = s, d, u$ is,

$$\begin{aligned} \mathcal{H}(\Delta C = -1) &= \frac{G_F}{\sqrt{2}}\{V_{ud}V_{cs}^*(\bar{u}d)(\bar{s}c) + V_{us}V_{cs}^*(\bar{u}s)(\bar{s}c) \\ &\quad +V_{ud}V_{cd}^*(\bar{u}d)(\bar{d}c) + V_{us}V_{cd}^*(\bar{u}s)(\bar{d}c)\Big\}. \end{aligned} \tag{2.10}$$

We can approximate

$$\begin{aligned} V_{ud} &\simeq V_{cs} \simeq \cos\theta_c, \\ V_{us} &\simeq -V_{cd} \simeq \sin\theta_c, \end{aligned} \tag{2.11}$$

where θ_c is the Cabibbo mixing angle. Therefore we obtain[1]

$$\begin{aligned} \mathcal{H}(\Delta C = -1) &= \frac{G_F}{\sqrt{2}}\Big\{\cos^2\theta_c \bar{u}\gamma^\mu(1-\gamma_5)d\bar{s}\gamma_\mu(1-\gamma_5)c \\ &\quad +cos\theta_c \sin\theta_c \bar{u}\gamma^\mu(1-\gamma_5)s\bar{s}\gamma_\mu(1-\gamma_5)c \\ &\quad -cos\theta_c \sin\theta_c \bar{u}\gamma^\mu(1-\gamma_5)d\bar{d}\gamma_\mu(1-\gamma_5)c \\ &\quad -\sin^2\theta_c \bar{u}\gamma^\mu(1-\gamma_5)s\bar{d}\gamma_\mu(1-\gamma_5)c\Big\}. \end{aligned} \tag{2.12}$$

[1]color indices are omitted

The charm decays induced by different components of the weak Hamiltonian in Eq. (2.12) are classified as follows.

1. Cabibbo-favored decay: Generated by the quark subprocess $c \to su\bar{d}$ (Fig. 2.3.a) described by,

$$\begin{aligned} \mathcal{H}(\Delta C = \Delta S = -1) &= \frac{G_F}{\sqrt{2}} \cos^2\theta_c (\bar{u}d)(\bar{s}c) \\ &= \frac{G_F}{\sqrt{2}} \cos^2\theta_c \times O_1, \end{aligned} \tag{2.13}$$

where we define the notation

$$O_1 = (\bar{u}d)(\bar{s}c), \tag{2.14}$$

for later use.

2. Cabibbo-suppressed decay: Generated by the quark subprocess $c \to su\bar{s}$ (Fig. 2.3.b) or $c \to du\bar{d}$ (Fig. 2.3.c),

$$\begin{aligned} \mathcal{H}(\Delta C = -1, \Delta S = 0) &= \frac{G_F}{\sqrt{2}} \cos\theta_c \sin\theta_c \left\{ (\bar{u}s)(\bar{s}c) - (\bar{u}d)(\bar{d}c) \right\} \\ &= \frac{G_F}{\sqrt{2}} \cos\theta_c \sin\theta_c \times O_1', \end{aligned} \tag{2.15}$$

where

$$O_1' = (\bar{u}s)(\bar{s}c) - (\bar{u}d)(\bar{d}c). \tag{2.16}$$

3. Double-Cabibbo-suppressed decay: Generated by the quark subprocess $c \to du\bar{s}$ (Fig. 2.3.d),

$$\begin{aligned} \mathcal{H}(\Delta C = -\Delta S = -1) &= \frac{G_F}{\sqrt{2}} \sin\theta_c^2 (\bar{u}s)(\bar{d}c) \\ &= \frac{G_F}{\sqrt{2}} \sin\theta_c^2 \times O_1'', \end{aligned} \tag{2.17}$$

where

$$O_1'' = (\bar{u}s)(\bar{d}c). \tag{2.18}$$

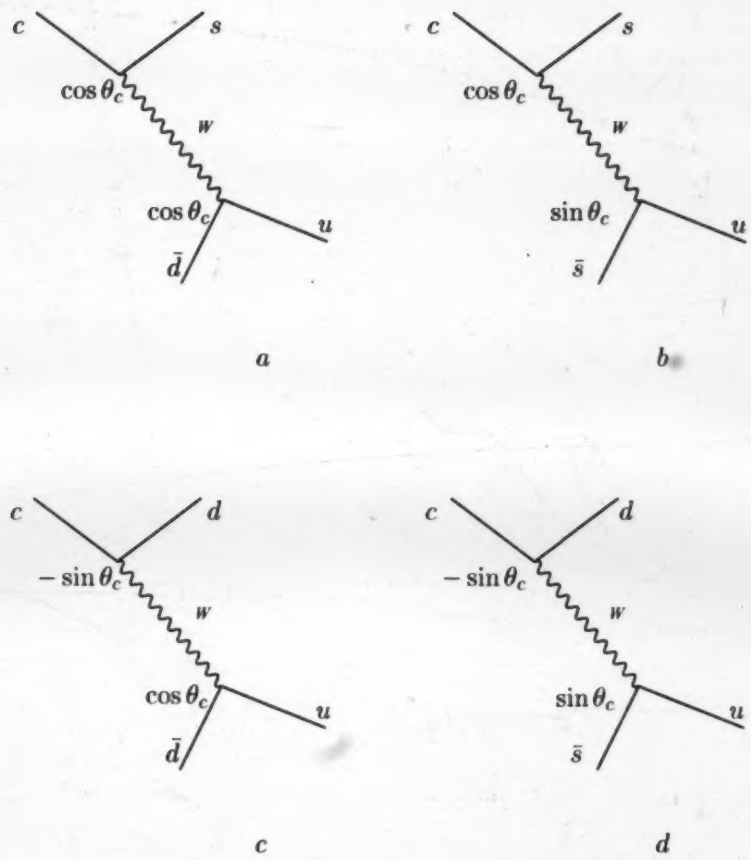

Figure 2.3: Classification of non leptonic charm decays: a) Cabibbo-favored decay, amplitude $\propto \cos^2\theta_c$, b) and c) Cabibbo-suppressed decay, amplitude $\propto \sin\theta_c \cos\theta_c$, d) Double Cabibbo-suppressed decay amplitude $\propto \sin^2\theta_c$.

From the expressions of the Hamiltonian in Eqns. (2.13), (2.15) and (2.17), a simple picture of nonleptonic weak decay of charm meson starts to emerge (Fig. 2.4). Since quarks exist only in bound states inside hadrons (baryons and mesons), the weak decay of the charm quark results in 3 quarks (two quarks and one anti-quark) which combine with the other "spectator" anti-quark $\bar{q}_s$ from the initial state to form the appropriate final state. The spectator $\bar{q}_s$ can combine either with q_2 as shown in (Fig. 2.4.a), or with q_3 as shown in (Fig. 2.4.b), leading to two different final states. The diagram in (Fig. 2.4.a) is called the external W-emission diagram and that in (Fig. 2.4.b) the internal W-emission diagram. In this picture the antiquark $\bar{q}_s$ is inert (a spectator) and does not contribute in the weak process except in combining with other quarks to form the initial and final hadrons. This picture is called spectator model. However, strong interactions significantly modify this simple picture as we discuss below.

2.2 Strong Interaction Effects

Compared to the electromagnetic and the strong interactions, the weak interactions are very feeble. In decays of resonances or excited states the weak interaction effects are usually masked by strong and/or electromagnetic interaction effects. The only place where one can observe weak phenomena is in the decays of ground state hadrons (baryons and mesons) where conservation laws prohibit their strong decay and strong interactions play no role except to confine the quarks inside the hadrons. Therefore the hadronic weak decay of the ground state of a heavy meson is basically triggered by the weak decay of the heavy quark resulting in the appearance of three new quarks rearranged with the spectator by strong interactions into appropriate final hadronic states. Although the weak Hamiltonian we have developed so far, Eq. (2.12), is valid at the energy scale, $q^2 \ll M_W^2$, much smaller than W boson mass ($\sim$ 80 GeV) and represents physics at very short distances, it was derived ignoring QCD corrections.

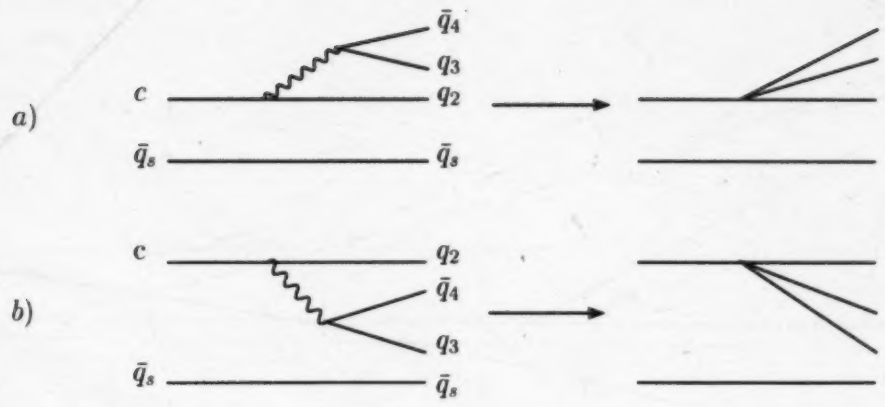

Figure 2.4: Quark diagrams for the decay of a charm-meson generated by the effective weak Hamiltonian in Eq. (2.12), $\bar{q}_s$ is a spectator quark: a) External W-emission, b) Internal W-emission.

However weak decays of heavy mesons occur at a scale of $\mu \sim$ few GeV ($\mu \sim m_c$ for D decays and $\mu \sim m_b$ for B decays). Therefore we must allow the evolution of the Hamiltonian from the W - mass scale down to the physical scale μ, of the order of the heavy quark mass, relevant for hadronic decays.

The theory of strong interactions, Quantum Chromodynamics (QCD), describes strong interactions among quarks through exchange of gluons. The QCD Lagrangian density $\mathcal{L}_{QCD}$ is given by [1]

$$\mathcal{L}_{QCD} = -\frac{1}{4} F^i_{\mu\nu} F_i^{\mu\nu} + \bar{q}^f_a \left(i\gamma^\mu \mathcal{D}_\mu - m_f \right) q^f_a, \tag{2.19}$$

where repeated indices are summed over. $F^i_{\mu\nu}$ is given in term of eight gluon fields G^i_ν, $i = 1, ..., 8$

$$F^i_{\mu\nu} = \partial_\mu G^i_\nu - \partial_\nu G^i_\mu - g_s f_{ijk} G^j_\mu G^k_\nu, \tag{2.20}$$

where g_s is a coupling constant and the covariant derivative $\mathcal{D}_\mu$ are given by,

$$\mathcal{D}_\mu q^f_a = \partial_\mu q^f_a + i \frac{g_s}{2} G^\alpha_\mu (\lambda_\alpha)_{ab} q^f_b, \tag{2.21}$$

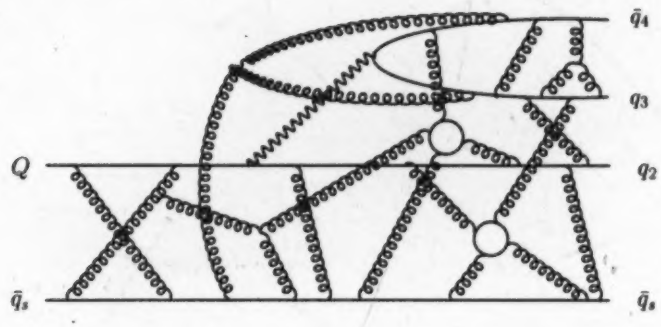

Figure 2.5: A more realistic picture of two-body hadronic decay of a heavy flavor. The solid straight lines represent quarks, wavy and curly lines represents W-boson and gluons, respectively (compare with Fig. 2.4).

where λ_α, α =1, ..., 8 are the Gell-Mann matrices, f_{ijk} are the SU(3) antisymmetric structure constants given in Appendix A and q_a^f denote the four-component Dirac spinors associated with each quark field of flavor f and color a. There are six flavors and three colors, hence the 18 quark fields are

$$q_a^f = \begin{pmatrix} u_1 \\ u_2 \\ u_3 \end{pmatrix}, \begin{pmatrix} d_1 \\ d_2 \\ d_3 \end{pmatrix}, \begin{pmatrix} s_1 \\ s_2 \\ s_3 \end{pmatrix}, \begin{pmatrix} c_1 \\ c_2 \\ c_3 \end{pmatrix}, \begin{pmatrix} b_1 \\ b_2 \\ b_3 \end{pmatrix}, \begin{pmatrix} t_1 \\ t_2 \\ t_3 \end{pmatrix}. \tag{2.22}$$

Since in hadronic decays of mesons, quarks are involved in the initial, as well as the final state, one would expect QCD effects arising from interaction between gluons and quarks to have a dramatic effect on hadronic weak decays of heavy flavors. The complexity of these effects increases with the number of quarks involved in the final state. Consequently the spectator model (Fig. 2.4) is far from representing a real picture of the hadronic decay. A more realistic picture for a typical two-body hadronic decay of heavy flavors is shown in (Fig. 2.5). All types of gluons, soft and hard, are involved. It is evident that it is almost impossible to evaluate the contributions from such diagrams. So far only short distance QCD effects have been

treated systematically as we discuss in the following.

Due to the nature of strong interactions, the QCD contributions, are divided into two different regimes separated by the scale μ:

1. Short-distance contributions arising from hard gluon exchanges between quark lines as shown in (Fig. 2.6) with energy scale higher that μ. They are systematically treated within QCD perturbative theory due to the asymptotic freedom [4]. Usually short distance effects are included in the Wilson coefficients which are known up to next-to-leading order QCD corrections, and their effects result in the modification of the strength as well as the structure of the weak Hamiltonian (see below).

2. Long-distance contributions responsible for the binding of quarks inside hadrons arising from soft gluons with energy scale lower than μ. They are nonperturbative and difficult to calculate and they constitute the major source of uncertainty in theoretical calculations of hadronic matrix elements. Their effects are usually included in the hadronic matrix element.

In what follows we will concentrate on the quark process $c \to su\bar{d}$ relevant for Cabibbo-favored decays of charm mesons described by the Hamiltonian in Eq. (2.13). To order α_s the QCD corrections to the weak Hamiltonian arising from one gluon exchanges between the quark lines in all possible ways are shown in (Fig. 2.6). Calculation of these corrections leads to the modification of the weak Hamiltonian as follows [5].

$$\begin{aligned}\mathcal{H}(\Delta C = \Delta S = -1) &= \frac{G_F}{\sqrt{2}} \cos^2\theta_c \left[\left(1 + \frac{\alpha_s(\mu)}{4\pi} \ln\left(\frac{M_W^2}{\mu^2}\right)\right) (\bar{u}_i d_i)(\bar{s}_j c_j) \right. \\ &\left. -3\frac{\alpha_s(\mu)}{4\pi} \ln\left(\frac{M_W^2}{\mu^2}\right) (\bar{u}_k c_k)(\bar{s}_l d_l) \right], \end{aligned} \tag{2.23}$$

where i, j, k and l are color indices, summation over repeated indices is understood [2], μ is the normalization scale and $\alpha_s(\mu)$ is the running strong coupling constant given

[2] In what follows we drop the color indices and adopt the convention that repeated indices are summed over unless otherwise stated.

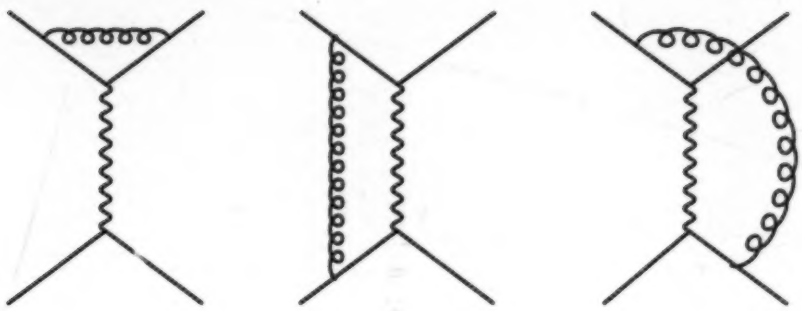

Figure 2.6: First order ($O(\alpha_s)$) QCD corrections to the 4-quark nonleptonic weak Hamiltonian. The solid straight lines represent quarks, wavy and curly lines represent W-boson and gluons, respectively. Diagrams differing by left-right and up-down reflection are not shown.

in the leading order calculation by [4]

$$\alpha_s^{(f)}(\mu) = \frac{4\pi}{\beta_0(f)\ln(\mu^2/\Lambda^2_{QCD})}, \tag{2.24}$$

Λ_{QCD} is the QCD scale to be determined from experiment and the functions $\beta_0(f)$ is given by [3]

$$\beta_0(f) = 11 - \frac{2}{3}f, \tag{2.25}$$

where f is the number of active flavors (quarks with mass less than μ). In the next-to-leading-order (NLO) calculation [3]

$$\alpha_s^{(f)}(\mu) = \frac{4\pi}{\beta_0(f)\ln(\mu^2/\Lambda^2_{QCD})}\left\{1 - \frac{\beta_1(f)}{\beta_0^2(f)}\frac{\ln\left[\ln(\mu^2/\Lambda^2_{QCD})\right]}{\ln(\mu^2/\Lambda^2_{QCD})}\right\}, \tag{2.26}$$

where the function $\beta_1(f)$ is given by [3]

$$\beta_1(f) = 102 - \frac{38}{3}f. \tag{2.27}$$

It is clear from the Eq. (2.23) that the first order QCD corrections modify the bare weak Hamiltonian of Eq. (2.13) in two ways; first by altering the normalization

of the original operator O_1, and second by generating a new operator O_2 having a structure different than that of O_1,

$$O_2 = (\bar{s}d)(\bar{u}c). \tag{2.28}$$

This new operator is a product of two color-singlet flavor-changing neutral currents $s \longleftrightarrow d$ and $c \longleftrightarrow u$. However such currents are not observed experimentally. It is important to realize that this structure appears as a consequence of Fierz transformation and completeness of the $SU(3)$ algebra. The modification of the weak Hamiltonian $\mathcal{H} \equiv O_1$ to first order QCD is

$$\begin{aligned} \mathcal{H} \equiv O_1 \quad &\longrightarrow \quad O_1 + \frac{\alpha_s}{4\pi} \ln\left(\frac{M_W^2}{\mu^2}\right) \{O_1 - 3O_2\}, \\ &= \quad \left(1 + \frac{\alpha_s}{4\pi} \ln\left(\frac{M_W^2}{\mu^2}\right)\right) O_1 - 3\frac{\alpha_s}{4\pi} \ln\left(\frac{M_W^2}{\mu^2}\right) O_2. \end{aligned} \tag{2.29}$$

In a similar way QCD corrections arising from one gluon exchange modify the operator O_2 as follows [4, 6]

$$O_2 \longrightarrow O_2 + \frac{\alpha_s}{4\pi} \ln\left(\frac{M_W^2}{\mu^2}\right) \{O_2 - 3O_1\}. \tag{2.30}$$

This means that the two operators mix by QCD corrections. It is convenient to express the weak Hamiltonian in terms of operators which are form invariant under QCD. This is achieved by the use of operators of definite symmetry. An operator of the kind under discussion can always be decomposed into its symmetric and anti-symmetric parts for example,

$$\begin{aligned} O &= (\bar{q}_1 q_2)(\bar{q}_3 q_4) \\ &= \frac{1}{2}\{(\bar{q}_1 q_2)(\bar{q}_3 q_4) + (\bar{q}_3 q_2)(\bar{q}_1 q_4)\} + \frac{1}{2}\{(\bar{q}_1 q_2)(\bar{q}_3 q_4) - (\bar{q}_3 q_2)(\bar{q}_1 q_4)\} \\ &= O_+ + O_-. \end{aligned} \tag{2.31}$$

The operators O_+ and O_- are symmetric and anti-symmetric under the exchange of indices $1 \longleftrightarrow 3$ and $2 \longleftrightarrow 4$. Therefore we can express the operators O_1 and O_2 as

follows,

$$\begin{aligned} O_1 &= \frac{1}{2}\{(\bar{u}d)(\bar{s}c) + (\bar{u}c)(\bar{s}d)\} + \frac{1}{2}\{(\bar{u}d)(\bar{s}c) - (\bar{u}c)(\bar{s}d)\} \\ &= O_+ + O_-, \\ O_2 &= \frac{1}{2}\{(\bar{u}d)(\bar{s}c) + (\bar{u}c)(\bar{s}d)\} - \frac{1}{2}\{(\bar{u}d)(\bar{s}c) - (\bar{u}c)(\bar{s}d)\} \\ &= O_+ - O_-, \end{aligned} \tag{2.32}$$

with

$$O_\pm = \frac{1}{2}(O_1 \pm O_2). \tag{2.33}$$

Since the quark field q_i carries flavors and color indices, the operators O_+ and O_- differ by their internal (flavor) symmetry as well as their color symmetry.

Using Eqns. (2.23) and (2.33), the first-order-corrected weak Hamiltonian takes the following form,

$$\mathcal{H}(\Delta C = \Delta S = -1) = \frac{G_F}{\sqrt{2}} \cos^2\theta_c \left\{ C_+^{(1)} O_+ + C_-^{(1)} O_- \right\}, \tag{2.34}$$

where

$$\begin{aligned} C_+^{(1)}(\mu) &= 1 - \frac{\alpha_s(\mu)}{2\pi} \ln\left\{\frac{M_W^2}{\mu^2}\right\} \\ C_-^{(1)}(\mu) &= 1 + \frac{\alpha_s(\mu)}{\pi} \ln\left\{\frac{M_W^2}{\mu^2}\right\}. \end{aligned} \tag{2.35}$$

At the scale $\mu = M_W$ we have

$$C_+^{(1)}(M_W) = C_-^{(1)}(M_W) = 1, \tag{2.36}$$

QCD does not bring any corrections and Eq. (2.34) reduces to the bare Hamiltonian of Eq. (2.13). Although at the scale $\mu \sim m_Q$ ($Q = b, c$), $\alpha_s(m_Q)$ is small enough to serve as an expansion parameter, the first order QCD correction from one gluon exchange contains a large logarithmic term $\ln(M_W^2/\mu^2)$. For a hadronic scale $\mu \sim m_c = 1.4\,GeV$

$$\frac{\alpha_s(m_c)}{2\pi} \simeq 0.06, \quad \text{and} \quad \ln\left[M_W^2/\mu^2\right] \simeq 8, \tag{2.37}$$

then

$$C_+^{(1)}(m_c) \simeq 1 - 0.48,$$
$$C_-^{(1)}(m_c) \simeq 1 + 0.96. \tag{2.38}$$

Hence the first order QCD correction to $C_+^{(1)}$ is about 50% and 100% to $C_-^{(1)}$. These corrections are very large and consequently higher order QCD corrections $[\alpha_s(\mu)\ln(M_W^2/\mu^2)]^n$, corresponding to multiple gluon exchanges, cannot be neglected, and the series in powers of $\alpha_s(\mu)\ln(M_W^2/\mu^2)$ must be summed up to all orders. This is usually achieved by using the renormalization group equation techniques [4, 5, 6]. The coefficients $C_\pm$ satisfy the differential equation

$$\left(\frac{d}{d\ln\mu} - D_\pm\right) C_\pm(\mu) = 0, \tag{2.39}$$

where

$$D_\pm = d_\pm \frac{\alpha_s(\mu)}{4\pi}, \quad d_- = -2d_+ = 8, \tag{2.40}$$

with the initial condition

$$C_+(M_W) = C_-(M_W) = 1. \tag{2.41}$$

We can easily integrate the differential equation, Eq. (2.39), using Eqns. (2.24) and (2.40) with the initial condition (2.41). The solution we obtain, known as leading order approximation (LO), is given by [4, 5, 7],

$$C_\pm(\mu) = \left[\frac{\alpha_s(\mu)}{\alpha_s(M_W)}\right]^{\frac{d_\pm}{2\beta_0}}. \tag{2.42}$$

We note that in the leading order, the QCD coefficients C_+ and C_- satisfy the following relations

$$C_+^2 C_- = 1, \quad \text{and} \quad C_+ < 1 < C_-. \tag{2.43}$$

Calculations, of the coefficients C_+ and C_-, including next-to-leading-order (NLO) corrections, exist in the literature [7, 8],

$$C_\pm(\mu) = \left[\frac{\alpha_s(\mu)}{\alpha_s(M_W)}\right]^{\frac{d_\pm}{2\beta_0}} \left\{1 + R_\pm \frac{\alpha_s(\mu) - \alpha_s(M_W)}{4\pi}\right\}, \tag{2.44}$$

where $R_\pm$ is a function of f, given by

$$R_+(f) = -\frac{11}{3} + \frac{1}{6\beta_0(f)}\left(21 - \frac{4}{3}f\right) + \frac{2\beta_1(f)}{\beta_0^2(f)}$$
$$R_-(f) = \frac{22}{3} + \frac{1}{3\beta_0(f)}\left(21 + \frac{4}{3}f\right) - \frac{4\beta_1(f)}{\beta_0^2(f)}. \quad (2.45)$$

2.2.1 Quark mass effects

The running coupling constant $\alpha_s^f(\mu)$ depends on the number of active flavors f as can be seen from β functions Eqns. (2.24) - (2.27). Therefore when the bare weak Hamiltonian is evolved down to the physical scale $\mu < m_Q$ one crosses quark threshold at $\mu = m_Q$ and the number of effective flavors changes by one each time a flavor threshold is crossed. For the equations (2.24) or (2.26) for $\alpha_s^f(\mu)$ to remain valid for all values of μ the QCD scale Λ_{QCD}^f must change, $\Lambda^f \longrightarrow \Lambda^{f-1}$, as quark thresholds are crossed and the running coupling constants $\alpha_s^f(\mu)$ and $\alpha_s^{f-1}(\mu)$ are related to order $O((\alpha_s^f)^3)$ according to [9],

$$\alpha_s^{f-1}(m_Q) = \alpha_s^f(m_Q) + \frac{7}{72\pi^2}(\alpha_s^f(m_Q))^3. \quad (2.46)$$

Therefore in order to calculate the Wilson coefficients relevant for D decays we have to evolve the weak Hamiltonian $\mathcal{H}$ Eq. (2.13) down to the scale $\mu = m_c$, which is below the mass of b quark. Hence, a quark threshold is crossed at $\mu = m_b$. We distinguish two regions, $m_b < \mu < M_W$ with $f = 5$ and $m_c < \mu < m_b$ with $f = 4$. The calculation is done in each region in a similar way as before, i.e. the coefficients are evolved from $\mu \sim M_W$ mass scale down to $\mu = m_b$ mass scale with $f = 5$ and the initial condition $C_\pm(M_W) = 1$, then from m_b scale down to m_c scale with $f = 4$ and $C_\pm(m_b)$ as initial conditions. The QCD scale $\Lambda_{QCD} \equiv \Lambda^{f=4}$ relevant for the region $m_c < \mu < m_b$ is determined by imposing the continuity of the running coupling constant, Eq. (2.47), to order $O((\alpha_s^f)^2)$ at the scale $\mu = m_b$,

$$\alpha_s^{f=5}(m_b) = \alpha_s^{f=4}(m_b). \quad (2.47)$$

The results for the QCD coefficients in the leading order at a scale $m_c < \mu < m_b$ relevant for D decay are given by [10]

$$C_{\pm}(\mu) = \left[\frac{\alpha_s^{(4)}(\mu)}{\alpha_s^{(4)}(m_b)}\right]^{\frac{d_\pm}{2\beta_0^{(4)}}} \times \left[\frac{\alpha_s^{(5)}(m_b)}{\alpha_s^{(5)}(M_W)}\right]^{\frac{d_\pm}{2\beta_0^{(5)}}} . \tag{2.48}$$

Tracking the calculation down to the charm scale, the next-to-leading-order calculation for $C_{\pm}(\mu)$ at a scale $m_c < \mu < m_b$ gives

$$\begin{aligned} C_{\pm}(\mu) &= \left[\frac{\alpha_s^{(4)}(\mu)}{\alpha_s^{(4)}(m_b)}\right]^{\frac{d_\pm}{2\beta_0^{(4)}}} \times \left\{1 + R_{\pm}(4)\frac{\alpha_s^{(4)}(\mu) - \alpha_s^{(4)}(m_b)}{4\pi}\right\} \\ &\quad \times \left[\frac{\alpha_s^{(5)}(m_b)}{\alpha_s^{(5)}(M_W)}\right]^{\frac{d_\pm}{2\beta_0^{(5)}}} \times \left\{1 + R_{\pm}(5)\frac{\alpha_s^{(5)}(m_b) - \alpha_s^{(5)}(M_W)}{4\pi}\right\}. \end{aligned} \tag{2.49}$$

2.3 Effective weak Hamiltonian

The QCD-corrected Cabibbo-favored weak Hamiltonian at a scale $\mu \sim m_c$ is then

$$\mathcal{H}(\Delta C = \Delta S = -1) = \frac{G_F}{\sqrt{2}} \cos\theta_c{}^2 \left\{C_+ O_+ + C_- O_-\right\}, \tag{2.50}$$

where $C_{\pm}$ are given in the leading order and next-to-leading order by Eqns. (2.48) and (2.49) respectively.

In a similar way the calculation of QCD effects on the Cabibbo-suppressed part, Eq. (2.15) and double Cabibbo-suppressed part, Eq. (2.17) of the weak Hamiltonian gives

$$\begin{aligned} \mathcal{H}(\Delta C = -1, \Delta S = 0) &= \frac{G_F}{\sqrt{2}} \cos\theta_c \sin\theta_c \left\{C_+ O'_+ + C_- O'_-\right\}, \\ \mathcal{H}(\Delta C = -\Delta S = -1) &= \frac{G_F}{\sqrt{2}} \sin^2\theta_c \left\{C_+ O''_+ + C_- O''_-\right\}, \end{aligned} \tag{2.51}$$

where $O'_{\pm}$ and $O''_{\pm}$ are defined in terms of O'_1, O'_2 and O''_1, O''_2 as follow,

$$O'_{\pm} = \frac{1}{2}\left\{(\bar{u}s)(\bar{s}c) \pm (\bar{s}s)(\bar{u}c)\right\} - \frac{1}{2}\left\{(\bar{u}d)(\bar{d}c) \pm (\bar{d}d)(\bar{u}c)\right\}$$

$$
\begin{aligned}
&= \frac{1}{2}(O_1' \pm O_2'), \\
O_\pm'' &= \frac{1}{2}\left\{(\bar{u}s)(\bar{d}c) \pm (\bar{d}s)(\bar{u}c)\right\} \\
&= \frac{1}{2}(O_1'' \pm O_2'').
\end{aligned} \tag{2.52}
$$

The neutral current operators O_2' and O_2'' are associated with the charged current operators O_1' and O_1'' respectively. They are given by

$$
\begin{aligned}
O_2' &= (\bar{s}s)(\bar{u}c) - (\bar{d}d)(\bar{u}c) \\
O_2'' &= (\bar{d}s)(\bar{u}c),
\end{aligned} \tag{2.53}
$$

and they emerge when QCD effects from gluons exchange between quark lines are taken into account in the same manner as the operator O_2 does.

It is useful to express the weak Hamiltonian for hadronic charm lowering decays in terms of the operators O_1, O_1', O_1'' and O_2, O_2', O_2''. Using Eqns. (2.33) and (2.50) - (2.52) we obtain,

$$
\begin{aligned}
\mathcal{H} &= \frac{G_F}{\sqrt{2}}\cos^2\theta_c\left\{\frac{1}{2}(C_+ + C_-)O_1 + \frac{1}{2}(C_+ - C_-)O_2\right\} \\
&\quad + \frac{G_F}{\sqrt{2}}\cos\theta_c\sin\theta_c\left\{\frac{1}{2}(C_+ + C_-)O_1' + \frac{1}{2}(C_+ - C_-)O_2'\right\} \\
&\quad - \frac{G_F}{\sqrt{2}}\sin^2\theta_c\left\{\frac{1}{2}(C_+ + C_-)O_1'' + \frac{1}{2}(C_+ - C_-)O_2''\right\} \\
&= \frac{G_F}{\sqrt{2}}\cos^2\theta_c\left\{C_1(\mu)O_1 + C_2(\mu)O_2\right\} \\
&\quad + \frac{G_F}{\sqrt{2}}\cos\theta_c\sin\theta_c\left\{C_1(\mu)O_1' + C_2(\mu)O_2'\right\} \\
&\quad - \frac{G_F}{\sqrt{2}}\sin^2\theta_c\left\{C_1(\mu)O_1'' + C_2(\mu)O_2''\right\},
\end{aligned} \tag{2.54}
$$

where the coefficients $C_1(\mu)$ and $C_2(\mu)$ given by

$$
\begin{aligned}
C_1(\mu) &= \frac{1}{2}(C_+(\mu) + C_-(\mu)), \\
C_2(\mu) &= \frac{1}{2}(C_+(\mu) - C_-(\mu)),
\end{aligned} \tag{2.55}
$$

are the Wilson coefficients. They describe the strength by which each of the operators O_1, O_1', O_1'' and O_2, O_2', O_2'' enters the weak Hamiltonian. Eq.(2.54) represents the

effective weak Hamiltonian used in the phenomenological analysis of hadronic decays of the heavy flavor. Given Eq. (2.54) the amplitude for two-body hadronic decays of heavy meson such as $D \to M_1 M_2$, ($M_1 M_2$ are two charmless mesons), has the following generic form,

$$\begin{aligned} A(D \to M_1 M_2) &\equiv \frac{G_F}{\sqrt{2}}(CKM)\{C_1(\mu)\langle M_1 M_2|X_1(\mu)|D\rangle \\ &\quad + C_2(\mu)\langle M_1 M_2|X_2(\mu)|D\rangle\} \\ &\equiv \frac{G_F}{\sqrt{2}}(CKM)\{C_1(\mu)\langle X_1(\mu)\rangle + C_2(\mu)\langle X_2(\mu)\rangle\}. \end{aligned} \tag{2.56}$$

where $X = O,\ O',\ O''$ and the CKM matrix elements are fixed once the final state particles $M_1 M_2$ are specified. For example the decays of D meson induced by the operator $X = O$ are Cabibbo favored. Typical decay of this kind are $D \longrightarrow K\pi,\ K^*\rho, K\eta,\ ....$ The decay amplitude for $D \longrightarrow K\pi$, for example, is

$$\begin{aligned} A(D \to K\pi) &\equiv \frac{G_F}{\sqrt{2}}\cos^2\theta_c\{C_1(\mu)\langle K\pi|O_1(\mu)|D\rangle \\ &\quad + C_2(\mu)\langle K\pi|O_2(\mu)|D\rangle\} \\ &\equiv \frac{G_F}{\sqrt{2}}\cos^2\theta_c\{C_1(\mu)\langle O_1(\mu)\rangle + C_2(\mu)\langle O_2(\mu)\rangle\}. \end{aligned} \tag{2.57}$$

From Eq. (2.56) we make the following observations:

- The QCD corrections to charged current operators O_1, O_1' and O_1'' generate new operators O_2, O_2', O_2'' having neutral current structure. These neutral currents can always be transformed to charged currents by Fierz transformation (Sec. 3.3).

- Although QCD brings the same corrections $C_1(\mu)$ ($C_2(\mu)$) to currents carrying the same charge, the weak interaction on the other hand distinguishes between currents carrying the same charge through the CKM matrix element.

- Both the coefficients $C_i(\mu)$ as well as the hadronic matrix elements $\langle O_i(\mu)\rangle$ depend on the scale μ. However the total physical amplitude $A(D \to M_1 M_2)$ is μ independent. Therefore the $\mu-$dependence of the coefficients $C_i(\mu)$ must cancel

that of the matrix element $\langle O_i(\mu)\rangle$ in the product $C_i(\mu)\langle O_i(\mu)\rangle$. Consequently, the choice of the scale μ is arbitrary and should, in principle, have no effect on the final result. Usually μ is chosen to be $\mu \sim m_b$ for B decay and $\mu \sim m_c$ for D decay.

- The calculation of the amplitude reduces to the calculation of the Wilson coefficients $C_i(\mu)$ and the calculation of the matrix elements $\langle O_i(\mu)\rangle$.

We have seen that the Wilson coefficients are known in the leading and next-to-leading order QCD from Eqns. (2.42), (2.48) and (2.44), (2.49). However the calculation of the matrix elements of hadronic decay of heavy flavor, from first principles, is not yet possible. We calculate the values of Wilson coefficients relevant for B and D decay in the next section while we leave the evaluation of the matrix element $\langle O_i(\mu)\rangle$ for the next chapter.

2.4 Numerical results for Wilson coefficients C_1 and C_2

2.4.1 B decays

The calculation of the coefficients C_+, C_-, C_1 and C_2 in the leading order proceeds as follows. First, we determine the QCD scale Λ_{QCD} using the experimental values of the running coupling constant [3]

$$\alpha_s(M_z) = 0.119 \pm 0.002, \tag{2.58}$$

with $M_Z = 91.187\ GeV$ in conjunction with Eqns. (2.24) and (2.25) with $f = 5$ to extract $\Lambda_{QCD} \equiv \Lambda^{(f=5)}$. Then, we substitute the value of Λ so obtained in Eq. (2.42) with $f = 5$ and choose the scale $\mu = 4.4\ GeV$ relevant for B decay. The numerical results are presented in Table 2.1. In a similar way we obtain Wilson coefficients

including the next-to-leading order corrections using Eqns. (2.26), (2.27) and (2.44). The results are presented in Table 2.2.

2.4.2 D decays

First we derive the QCD scale $\Lambda_{QCD} \equiv \Lambda^{(f=4)}$ by imposing the continuity equation (2.47). Then, using Eqns. (2.24), (2.25) and (2.48) with $f = 4$, we calculate the Wilson coefficients C_1 and C_2 at the scale $\mu = 1.4\ GeV$ relevant for D decays in the leading order. The results are presented Table 2.3. In the next-to-leading order numerical calculation of Wilson coefficients, we use Eqns. (2.26), (2.27) and (2.49) and we neglect terms of order $(R_{\pm}(f)\alpha_s(\mu))^2$ in Eq. (2.49). The results so obtained are presented in Table 2.4. There are two important remarks to be made about the above results:

1. If we compare the leading and next-to-leading order results obtained for Wilson coefficients we observe that the difference is large specially for C_2 [3]. This difference is even larger in D than in B because of the large QCD coupling constant at low scale $\mu \sim m_c$, $\alpha_s(m_c) > \alpha_s(m_b)$. A careful examination of the leading order and next-to-leading order results shows that the QCD scale in the leading order (LO) is

$$\begin{aligned} \Lambda^{(5)} &= 93 \pm 11\ MeV \quad \text{for } B \text{ meson,} \\ \Lambda^{(4)} &= 127 \pm 13\ MeV \quad \text{for } D \text{ meson.} \end{aligned} \tag{2.59}$$

   These number are far below the accepted values extracted from experiments $\Lambda^{(5)} \sim 237 \pm 25\ MeV$ [3].

   It is informative to repeat the LO calculation using the next-to-leading order (NLO) expression for $\alpha_s(\mu)$ in Eq. (2.26) instead of the LO $\alpha_s(\mu)$ in Eq. (2.24) the results obtained this way are shown in Tables 2.5 and 2.6 for B and D, respectively. The discrepancies between LO and NLO are reduced to a reasonable

[3] Note that without QCD corrections $C_2 = 0$

size. Therefore the large difference between LO and NLO is partly due to the small values of Λ_{QCD} used in the calculation.

2. We note that we can reproduce the numerical values of Wilson coefficients $C_{\pm}$ and $C_{1,2}$, in the leading as well as the next-to-leading order relevant for D decays (with an accuracy of 1% or better for the next-to-leading order), by using the simple Eqns. (2.42) and (2.44), with a minor modification [11], instead of the complicated Eqns. (2.48) and (2.49). Simply, we use Eqs. (2.42) and (2.44) with the QCD scale $\Lambda^{(5)}$ replaced by $\Lambda^{(4)}$ and an effective number of active flavors, $f = 4.15$. The results obtained in this way at a scale $\mu = 1.4\ GeV$, for both leading and next-to-leading order are presented in Tables 2.7 and 2.8, respectively.

Table 2.1: The QCD scale $\Lambda^{(5)}$ and the Wilson coefficients C_+, C_-, C_1 and C_2 for B decays at the scale $\mu = 4.4\ GeV$ in the leading order approximation. These values were obtained from Eqns. (2.24) and (2.42) with $f = 5$ and the running coupling constant normalized to $\alpha_s(M_Z) = 0.119 \pm 0.002$ as explained in the text.

$\alpha_s(M_Z)$	$\Lambda^{(5)}$	C_+	C_-	C_1	C_2
0.117	0.0828	0.866	1.331	1.099	- 0.232
0.119	0.0931	0.864	1.3405	1.102	-0.238
0.121	0.104	0.861	1.350	1.105	-0.244

Table 2.2: The QCD scale $\Lambda^{(5)}$ and the Wilson coefficients C_+, C_-, C_1 and C_2 for B decays at scale $\mu = 4.4\ GeV$, in the next-to-leading order approximation. These values were obtained from Eqns. (2.26) and (2.44) with $f = 5$ and the running coupling constant normalized to $\alpha_s(M_Z) = 0.119 \pm 0.002$.

$\alpha_s(M_Z)$	$\Lambda^{(5)}$	C_+	C_-	C_1	C_2
0.117	0.214	0.841	1.433	1.137	-0.296
0.119	0.239	0.836	1.449	1.143	-0.306
0.121	0.267	0.832	1.466	1.149	-0.317

Table 2.3: The QCD scale $\Lambda^{(4)}$ and the Wilson coefficients C_+, C_-, C_1 and C_2 for D decays at the scale $\mu = 1.4\ GeV$, in the leading order approximation. These values were obtained using Eqns. (2.24) and (2.48) with an effective number of flavors $f = 4$ and the running coupling constant normalized to $\alpha_s(M_Z) = 0.119 \pm 0.002$.

$\alpha_s(M_Z)$	$\Lambda^{(4)}$	C_+	C_-	C_1	C_2
0.117	0.114	0.792	1.595	1.193	- 0.401
0.119	0.127	0.787	1.616	1.201	-0.415
0.121	0.141	0.781	1.639	1.210	-0.429

Table 2.4: The QCD scale $\Lambda^{(4)}$ and the Wilson coefficients C_+, C_-, C_1 and C_2 for D decays at the scale $\mu = 1.4\ GeV$, in the next-to-leading order approximation. These values were obtained using Eqns. (2.26) and (2.49) with an effective number $f = 4$ and the running coupling constant normalized to $\alpha_s(M_Z) = 0.119 \pm 0.002$.

$\alpha_s(M_Z)$	$\Lambda^{(4)}$	C_+	C_-	C_1	C_2
0.117	0.309	0.727	1.944	1.336	-0.609
0.119	0.342	0.715	2.011	1.363	-0.648
0.121	0.376	0.703	2.086	1.394	-0.692

Table 2.5: The QCD scale $\Lambda^{(5)}$ and the Wilson coefficients C_+, C_-, C_1 and C_2 for B decays at scale $\mu = 4.4\ GeV$ in the leading order approximation. These values were obtained from Eqns. (2.26) and (2.42) with $f = 5$ and the running coupling constant normalized to $\alpha_s(M_Z) = 0.119 \pm 0.002$ as explained in the text.

$\alpha_s(M_Z)$	$\Lambda^{(5)}$	C_+	C_-	C_1	C_2
0.117	0.214	0.854	1.370	1.112	- 0.258
0.119	0.239	0.851	1.3815	1.116	-0.265
0.121	0.267	0.847	1.394	1.120	-0.273

Table 2.6: The QCD scale $\Lambda^{(4)}$ and the Wilson coefficients C_+, C_-, C_1 and C_2 for D decays at the scale $\mu = 1.4\ GeV$, in the leading order approximation. These values were obtained using Eqns. (2.26) and (2.48) with an effective number $f = 4$ and the running coupling constant normalized to $\alpha_s(M_Z) = 0.119 \pm 0.002$.

$\alpha_s(M_Z)$	$\Lambda^{(4)}$	C_+	C_-	C_1	C_2
0.117	0.309	0.755	1.752	1.254	- 0.500
0.119	0.342	0.746	1.796	1.271	-0.525
0.121	0.376	0.736	1.844	1.290	-0.554

Table 2.7: The QCD scales and Wilson coefficients C_+, C_-, C_1 and C_2 for D decays at the scale $\mu = 1.4\ GeV$, in the leading order approximation. These values are obtained using Eq. (2.42), instead of the correct Eq. (2.48), with QCD scale $\Lambda^{(5)}$ replaced by $\Lambda^{(4)}$ and an effective number of active flavors $f = 4.15$.

$\alpha_s(M_Z)$	f	$\Lambda^{(5)}$	$\Lambda^{(4)}$	C_+	C_-	C_1	C_2
0.117	4.15	0.214	0.309	0.754	1.761	1.257	- 0.500
0.119	4.15	0.239	0.342	0.744	1.805	1.275	-0.530
0.121	4.15	0.267	0.376	0.734	1.854	1.294	-0.560

Table 2.8: The QCD scales and Wilson coefficients C_+, C_-, C_1 and C_2 for D decays at the scale $\mu = 1.4\ GeV$, in the next-to-leading order approximation. These values were obtained using Eq. (2.44), instead of the correct Eq. (2.49), with $\Lambda^{(5)}$ replaced by $\Lambda^{(4)}$ and an effective number of active flavors $f = 4.15$.

$\alpha_s(M_Z)$	f	$\Lambda^{(5)}$	$\Lambda^{(4)}$	C_+	C_-	C_1	C_2
0.117	4.15	0.214	0.309	0.725	1.957	1.341	-0.616
0.119	4.15	0.239	0.342	0.713	2.025	1.369	-0.656
0.121	4.15	0.267	0.376	0.701	2.101	1.401	-0.700

Bibliography

[1] O. Nachtmann, Elementary Particle Physics: Concepts and Phenomena, 1990 (Springer-Verlag). Fayyazuddin and Riazuddin, A modern Introduction to Particle Physics, 1992 (World Scientific).

[2] M. Kobayashi and T. Maskawa, Prog. Theor. Phys. 49, 652 (1973).

[3] Particle Data Group, C. Caso et al., Eur. Phys. J. C3, 1 (1998).

[4] Quang Ho-Kim and Pham Xuan Yem, Elementary Particles and their Interactions: Concepts and Phenomena, 1998 (Springer-Verlag). M. E. Peskin and D. V. Schroeder, An Introduction to Quantum Field Theory, 1995 (Addison-Wesley).

[5] G. Buchalla, A. Buras and M. Lautenbacher, Rev. M. Phys. **68**, 1125 (1996); M. Wirbel, Prog. Nucl. Part. Phys. 21, 33 (1988); Rückl R., Weak Decays of Heavy Flavours, Habilitationsschrift, submitted to University of Munich, CERN print (1983);*ibid*, Proceedings of the International School of Physics "Enrico Fermi" Course XCII, ed. N. Cabibbo, 1987(North-Holland, Amesterdam), p.43. For more detailed calculations see Ref.[4].

[6] J. F. Donoghue, E. G. Golowich, B. R. Holstein, Dynamics of the Standard Model, 1994 (Cambridge University Press).

[7] M. Neubert and B. Stech, Weak Decays of B meson, to appear in second edition of Heavy Flavors, ed. by A. J. Buras and M. Lindner, (World Scientific Singapore), hep-ph/9705292. A. Buras, Nucl. Phys. B434, 606(1995).

[8] G. Altarelli, G. Curci, G. Martinelli and S. Petrarca, Phys. Lett. B99, 141(1981); *ibid*, Nucl. Phys. B187, 461(1981), A. J. Buras and P. H. Weisz, Nucl. Phys. B333, 66(1990); R. Rückl, hep-ph/9810338.

[9] S. Bethke, Nucl. Phys. Proc. Suppl. 39BC, 198 (1995); W. Bernreuther and W. Wetzel, Nucl. Phys. B 197, 228 (1982).

[10] F. J. Gilman and M. B. Wise, Phys. Rev. D 20, 2392(1979).

[11] see A. Buras, in [7], G. Buchalla et al. in [5].

Chapter 3

Hadronic matrix elements

3.1 Introduction

The importance of the hadronic matrix elements for the physical processes stems from two important aspects; the first one is dynamical – all the information about the underlying long-distance dynamics of the process is contained in this matrix element; the second aspect is rather experimental – measurable quantities such as decay rates and cross sections are directly related to the matrix element. Hence its theoretical estimation is crucial. Unfortunately, a systematic calculation of the matrix element for hadronic weak decays from first principles is not yet possible. The complexity of hadronic decays arises from the fact that final states involve hadrons and, consequently, hadronic effects in the final state cannot be overlooked – being non-perturbative such effects are difficult to treat. In the case of low energy hadronic decays induced by an effective weak Hamiltonian $\mathcal{H}$ involving soft pions in the final state such as in the strange decay $K \to \pi\pi$, the estimation of the hadronic matrix element is, usually, based on the use of current algebra and soft-pion theorem techniques to relate the matrix element of the process $K \to \pi\pi$ in the limit of small vanishing

momentum of the pion to that of the much simpler process $K \to \pi$ according to [1].

$$\lim_{q_3^2 \to 0} \langle \pi(q_3)\pi(q_2)|\mathcal{H}|K(q_1)\rangle \equiv \langle \pi(q_2)|[Q_5, \mathcal{H}]|K(q_1)\rangle, \tag{3.1}$$

where q_i, $i = 1, 2, 3$ are the four momenta and Q_5 is the axial charge.

However these techniques cannot be extended to the case of hadronic weak decays of heavy flavor such as D and B mesons because the final state is energetic and the soft limit is not usually satisfied. Faced with such a situation, it becomes evident that the use of some symmetry principle or approximations and/or models as tools to get reliable estimation of matrix element for hadronic weak decay will be fruitful. In fact, more progress has been made in this direction and different phenomenological approaches and techniques have been developed specifically to achieve this goal. Some of the popular approaches are :

1. The diagrammatic technique [2, 3],

2. the factorization approximation [4].

The work in this thesis is based on the use of the factorization approximation. However, in the following we give a brief description of the diagramatical approach.

3.2 Diagrammatic Approach

The use of the diagrammatical approach in the analysis of two-body hadronic weak decays of heavy flavor consists of decomposing the total amplitude associated with the transition of the charm quark,

$$c \to q_2\, q_3\, \bar{q}_4, \tag{3.2}$$

into quark-diagrams (amplitudes) with different topologies. Each of these diagrams results in a contribution to the hadronic matrix element [2, 3]. The resulting shapes are illustrated in (Fig. 3.1). In total there are six relevant topologies:

1. The external W-emission, (Fig. 3.1.a), known as color-favored "tree" amplitude, T, in which the W-boson materializes into a quark-antiquark ($q_3\bar{q}_4$) pair which combine to form a color-singlet pseudoscalar or vector meson, while the other quark q_2, coming from the heavy flavor, combines with the spectator antiquark $\bar{q}_s$ to form the other meson.

2. The internal W-emission, (Fig. 3.1.b), known as color-suppressed tree amplitude, C, in which the quark-antiquark ($q_3\bar{q}_4$) pair coming from the W-boson split and end up in different hadrons: $\bar{q}_4$ combines with q_2 to form a color-singlet meson and q_3 combines with the spectator antiquark $\bar{q}_s$ to form the other meson.

3. The annihilation amplitude, A, (Fig. 3.1.c), in which the charm quark and the spectator $\bar{q}_s$ annihilate to a final state by means of W-boson through the subprocess

$$c\,\bar{q}_s \rightarrow W \rightarrow u\bar{q}, \ (q = d, s). \tag{3.3}$$

   This diagram contributes to decays of charged heavy flavor[1] only.

4. The W-exchange amplitude, E, (Fig. 3.1.d), in which the charm quark and the spectator antiquark $\bar{q}_s$ in the decaying heavy meson exchange a W-boson. This diagram contributes to weak decays of neutral mesons only.

5. The penguin-annihilation amplitude, PA, (Fig. 3.1.e) , in which the charm quark and the spectator anti-quark $\bar{q}_s$ annihilate into vacuum. The final state is generated by strong interactions, therefore this diagram contributes to weak decays of neutral meson only.

6. The penguin diagram amplitude, P, (Fig. 3.1.f), associated with transition $Q \rightarrow q_2$ involving virtual quarks in the loop coupling with gluons to form the final state.

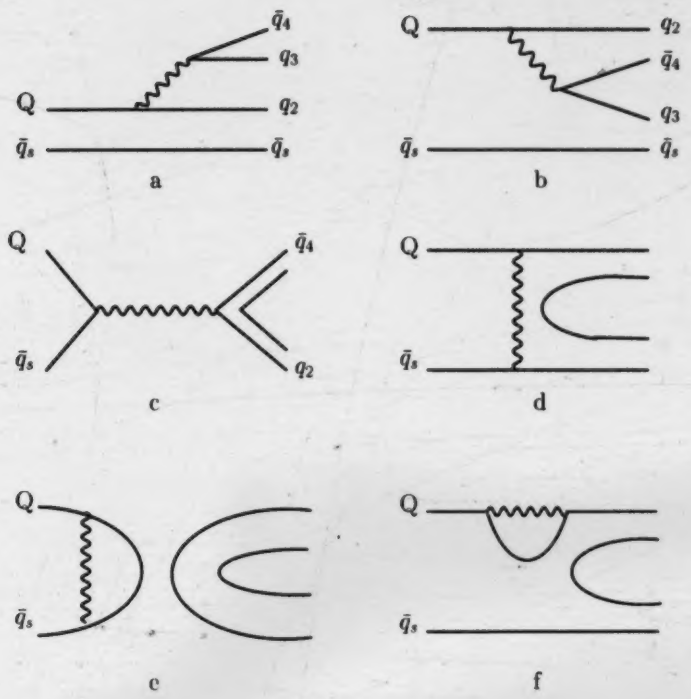

Figure 3.1: The six quark-diagrams contributing to heavy flavor decays (Q is a heavy quark c or b and $\bar{q}_s$ is a light antiquark $\bar{u}$, $\bar{d}$ or $\bar{s}$: a) color-favored tree diagram, b) color-suppressed tree diagram, c) annihilation, d) W-exchange diagram , e) penguin annihilation diagram, f) penguin diagram.

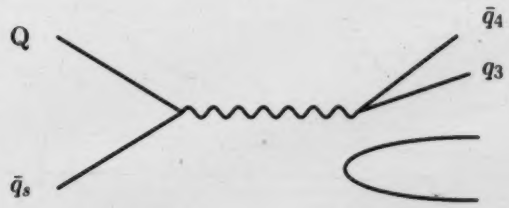

Figure 3.2: Hair-pin diagram contributing to final state with SU(3) singlet $\bar{q}q$ in the final state

There is another diagram, known as hair-pin diagram, (Fig. 3.2), which appears in channels involving SU(3) singlets in the final-state meson. The quark-antiquark pair forming the color and flavor singlet meson is created from the vacuum. Recent analysis of the data on charm decays showed that there is no compelling evidence for contributions from such a diagram [5].

The next step in the diagrammatic approach is to express the total amplitude for each decay of a heavy flavor to a certain final state as a linear combination of all the amplitudes associated with the quark diagrams leading to the specified final state. Then one uses experimental data to fix the different amplitudes which are used subsequently in making predictions for other decays. This approach has been used extensively in the analysis of D and B decays [2, 3, 6].

In charm decays penguin diagrams are Cabibbo-suppressed, and the contribution from the b quark in the loop are suppressed by CKM elements $V_{ub}V_{cb} \sim 10^{-5}$, and the contributions from the other quarks, d and s, in the loop cancel each other because $V_{us} \sim -V_{cd}$. Adding to that, recent calculations of the Wilson coefficients associated with penguin operators show that they are smaller, at least by one order of magnitude [7] than those associated with the amplitude T and C, hence penguin contributions are negligible in charm decay.

Although, the diagrammatic approach can help in understanding the mechanism of hadronic weak decays of heavy flavor it does not provide an explanation for the underlying dynamics of each process; the physics of the process remains obscure. It was pointed out a long time ago [2] that quark diagram amplitudes form an over complete set [8] and provide a redundant parameterization of the decay amplitude. In addition, final-state interactions can mix the amplitudes arising from different diagrams thereby spoiling the distinction by topology [9].

[1]The decay of D^+ through annihilation is Cabbibo-suppressed.

3.3 Factorization

3.3.1 General Idea

The current operators $(\bar{u}d)$, $(\bar{s}c)$, ... in the effective weak Hamiltonian

$$\begin{aligned} \mathcal{H} &= \frac{G_F}{\sqrt{2}} \cos^2\theta_c \left\{ C_1(\bar{u}d)(\bar{s}c) + C_2(\bar{s}d)(\bar{u}c) \right\} \\ &= \frac{G_F}{\sqrt{2}} \cos^2\theta_c \left\{ C_1 O_1 + C_2 O_2 \right\}, \end{aligned} \tag{3.4}$$

are expressed in terms of the fundamental quark fields. Each of these currents have the same quantum numbers (spin, isospin, flavor, ...) as the corresponding quark and antiquark combination. It is convenient to have the Hamiltonian in a form such that one of these currents carries the same quantum numbers as one of the mesons in the final state. This can be achieved by using Fierz transformation to rearrange the order of quark fields in $\mathcal{H}$. We observe that the operators O_1 and O_2 in Eq. (3.4) contain the currents $(\bar{u}d)$ and $(\bar{s}d)$, which have the same quark structure as π and K meson, respectively. Consequently one would expect the decays induced by these operators to be different. But we have seen that O_1 and O_2 are not independent; O_1 contains O_2 in itself and vice versa. We project O_1 on O_2 by Fierz transformation as follows. Using the identity

$$[\gamma^\mu(1-\gamma^5)]_{\alpha\beta}[\gamma^\mu(1-\gamma^5)]_{\delta\epsilon} = -[\gamma^\mu(1-\gamma^5)]_{\alpha\epsilon}[\gamma^\mu(1-\gamma^5)]_{\delta\beta}, \tag{3.5}$$

with the following relation for $SU(N)$ matrices

$$\lambda^a_{\alpha\beta}\lambda^a_{\gamma\delta} = -\frac{2}{N}\delta_{\alpha\beta}\delta_{\gamma\delta} + 2\delta_{\alpha\delta}\delta_{\gamma\beta}, \tag{3.6}$$

for SU(3) ($N = 3$) we obtain

$$\begin{aligned} (\bar{u}d)(\bar{s}c) &= \frac{1}{3}(\bar{s}d)(\bar{u}c) + \frac{1}{2}(\bar{s}\lambda^a d)(\bar{u}\lambda^a c) \\ O_1 &= \frac{1}{3}O_2 + \tilde{O}_8. \end{aligned} \tag{3.7}$$

In the same manner we can also Fierz transform O_2 with the result

$$O_2 = \frac{1}{3}O_1 + O_8, \tag{3.8}$$

where O_8 and $\tilde{O}_8$ are products of color octet currents:

$$\begin{aligned} O_8 &= \frac{1}{2}\sum_{a=1}^{8}(\bar{u}\lambda^a d)(\bar{s}\lambda^a c), \\ \tilde{O}_8 &= \frac{1}{2}\sum_{a=1}^{8}(\bar{s}\lambda^a d)(\bar{u}\lambda^a c), \end{aligned} \tag{3.9}$$

with λ^a are the Gell-Mann matrices given in Appendix A, and

$$(\bar{q}\lambda^a q') = \bar{q}\gamma^\mu(1-\gamma_5)\lambda^a q'. \tag{3.10}$$

Using Eqns. (3.7) and (3.8) the effective weak Hamiltonian $\mathcal{H}$ can be reduced to the following color-favored (CF) form

$$\mathcal{H}_{CF} = \frac{G_F}{\sqrt{2}}\cos^2\theta_c[a_1(\bar{u}d)(\bar{s}c) + C_2 O_8], \tag{3.11}$$

and to a color-suppressed (CS) form

$$\mathcal{H}_{CS} = \frac{G_F}{\sqrt{2}}\cos^2\theta_c[a_2(\bar{u}c)(\bar{s}d) + C_1\tilde{O}_8], \tag{3.12}$$

where the scale-dependent parameters a_1 and a_2 are related to Wilson coefficients $C_1(\mu)$ and $C_2(\mu)$ by

$$\begin{aligned} a_1(\mu) &= C_1(\mu) + \frac{C_2(\mu)}{3}, \\ a_2(\mu) &= C_2(\mu) + \frac{C_1(\mu)}{3}. \end{aligned} \tag{3.13}$$

Equations (3.11) and (3.12) represent the same interaction as Eq. (3.4) but are expressed in different but equivalent ways.

After such transformations the quark bilinears built up from the fundamental quark fields are treated as interpolating fields and can be replaced, in the weak Hamiltonian $\mathcal{H}$, by meson fields using the current field identity [10],

$$\bar{q}\gamma^\mu(1-\gamma^5)q' \longrightarrow (\bar{q}\gamma^\mu(1-\gamma^5)q')_H = J_\mu, \tag{3.14}$$

where the subscript H indicates the change from quark currents to hadronic currents. Thus we can express the effective Hamiltonian as a product of hadronic currents, instead of quark currents, as follows

$$\begin{aligned} \mathcal{H}_{CF} &= \frac{G_F}{\sqrt{2}} \cos^2\theta_c [a_1(\bar{u}d)_H(\bar{s}c)_H + C_2 O_8], \\ \mathcal{H}_{CS} &= \frac{G_F}{\sqrt{2}} \cos^2\theta_c [a_2(\bar{u}c)_H(\bar{s}d)_H + C_1 \tilde{O}_8]. \end{aligned} \tag{3.15}$$

Neglecting the contribution from the operators O_8 and $\tilde{O}_8$, the effective weak Hamiltonian reduces to the product of two hadronic currents

$$\mathcal{H} \equiv G J'_\mu J^\mu, \tag{3.16}$$

where J_μ has the usual $(V-A)_\mu$ structure and G is a constant which involves the Fermi coupling constant G_F, CKM matrix elements and any other constant parameters.

It is known that in weak interactions mesons can be generated by hadronic currents carrying the appropriate quantum numbers. We can consider one of the mesons in the final state of two-body hadronic decays to be created directly by one of the currents in the Hamiltonian, Eq. (3.16). In order to illustrate how this phenomenological approach works in the calculation of the hadronic matrix elements, we consider the hadronic weak decays of a heavy pseudoscalar meson

$$F \longrightarrow M_1 M_2, \tag{3.17}$$

where $M_1 M_2$ are two light mesons. We need to calculate the hadronic matrix elements $\langle M_1 M_2 | J_\mu J'_\mu | F \rangle$.

In the factorization assumption one writes the matrix elements of the current product as the product of matrix elements of the currents in all possible ways. Thus,

$$\begin{aligned} \langle M_1 M_2 \mid \mathcal{H} \mid P \rangle &= \langle M_1 \mid J' \mid 0 \rangle \langle M_2 \mid J \mid F \rangle \\ &\quad + \langle M_2 \mid J' \mid 0 \rangle \langle M_1 \mid J \mid F \rangle \\ &\quad + \langle M_1 M_2 \mid J' \mid 0 \rangle \langle 0 \mid J \mid F \rangle. \end{aligned} \tag{3.18}$$

Subsequently Lorentz invariance is used to express the matrix element of weak currents, namely $\langle M_i \mid J' \mid 0\rangle$ and $\langle M_j \mid J \mid F\rangle$, in terms of invariant form factors and decay constants as will be explained later. The first two terms in Eq. (3.18) represent the spectator contribution and the last term the weak annihilation contribution.

In order to make the idea of factorization more clear let us be more specific and consider for example the following decay channels, $D^0 \to K^-\pi^+$, $D^0 \to \bar{K}^0\pi^0$ and $D^+ \to \bar{K}^0\pi^+$.

3.3.2 Classification of two-body hadronic decays in the factorization approximation

The decays induced by the weak Hamiltonian are classified into three different classes, depending on which part of $\mathcal{H}$ is involved [4]

1. Class I process :

   Decays in this class get contributions from the color favored part, $\mathcal{H}_{CF}$, of the weak Hamiltonian, hence the name "color favored". An example of such a decay is $D^0 \longrightarrow K^-\pi^+$, (Fig. 3.3.a). This decay proceeds via the charged current operator $(\bar{u}d) \times (\bar{s}c)$. The π^+ meson is created from the vacuum by the weak current $(\bar{u}d)$ while the transition $D^0 \longrightarrow K^-$ is induced by the current $(\bar{s}c)$. The factorized amplitude is given by

   $$\begin{aligned} A(D^0 \longrightarrow K^-\pi^+) &\equiv a_1\langle K^-\pi^+|(\bar{u}d)(\bar{s}c)|D^0\rangle \\ &= a_1\langle\pi^+|(\bar{u}d)|0\rangle\langle K^-|(\bar{s}c)|D^0\rangle. \end{aligned} \tag{3.19}$$

   The amplitude A is proportional to a_1 and color favored decays get contribution from external W-emission diagram. The decay amplitudes for class I processes are determined by the parameter a_1.

2. Class II process:

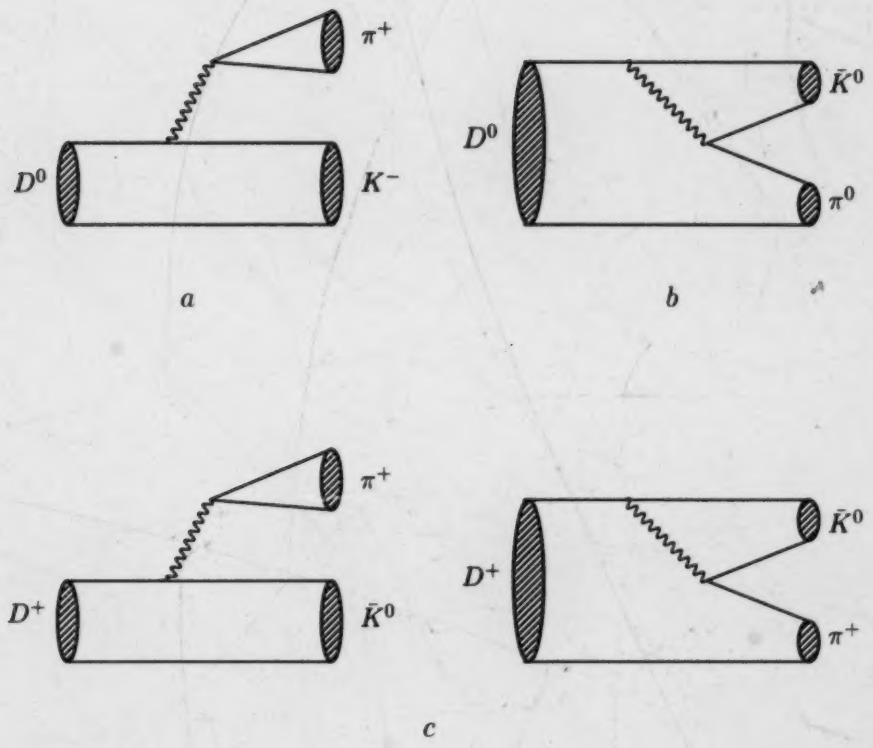

Figure 3.3: Classification of nonleptonic two-body hadronic decays of charm meson, a) class I or color favored tree diagram determined by a_1, b) class II or color suppressed tree diagram determined by a_2, c) class III decay determined by $a_1 + xa_2$.

Decays in this class get contributions from the color suppressed part, $\mathcal{H}_{CS}$, of the weak Hamiltonian, hence the name "color suppressed". An example of such a decay is $D^0 \longrightarrow \bar{K}^0\pi^0$, (Fig. 3.3.b). This decay proceeds via the neutral current operator $(\bar{s}d) \times (\bar{u}c)$. The $\bar{K}^0$ meson is generated from vacuum by the weak current $(\bar{s}d)$ while the transition $D^0 \longrightarrow \pi^0$ is induced by the other current $(\bar{u}c)$. The factorized amplitude is given by

$$\begin{aligned} A(D^0 \longrightarrow \bar{K}^0\pi^0) &\equiv \frac{a_2}{\sqrt{2}}\langle \bar{K}^0\pi^0|(\bar{s}d)(\bar{u}c)|D^0\rangle \\ &= \frac{a_2}{\sqrt{2}}\langle \bar{K}^0|(\bar{s}d)|0\rangle\langle \pi^0(\bar{u}c)|D^0\rangle \end{aligned} \tag{3.20}$$

The amplitude A is proportional to a_2 and color suppressed decays get contribution from internal W-emission diagram. The decay amplitudes for class II processes are determined by the parameter a_2.

3. Class III process:

Decays in this class get contributions from both parts, color favored $\mathcal{H}_{CF}$ and color suppressed $\mathcal{H}_{CS}$, of the Hamiltonian. An example of such a decay is $D^+ \longrightarrow \bar{K}^0\pi^+$, (Fig. 3.3.c). This decay proceeds via both the charged current as well as the neutral current. The amplitude is given by

$$\begin{aligned} A(D^+ \longrightarrow \bar{K}^0\pi^+) &\equiv a_1\langle \pi^+|(\bar{u}d)|0\rangle\langle \bar{K}^0|(\bar{s}c)|D^+\rangle \\ &\quad + a_2\langle \bar{K}^0|(\bar{s}d)|0\rangle\langle \pi^+|(\bar{u}c)|D^+\rangle. \end{aligned} \tag{3.21}$$

The decay amplitude A is proportional to $(a_1 + xa_2)$. Thus class III decay amplitudes get contributions from both external and internal W-emission diagrams. As they are determined by both parameters a_1 and a_2, this class involves interference between terms with a_1 and a_2. This interference effect, known as Pauli interference, shows up whenever the final state has two identical fermions in the final state; in this case there are two $\bar{d}$ quarks in the final state, see (Fig. 3.3). We note that the interference between a_1 and a_2 terms is present in

D^+ and absent in D^0. From Chapter 1, we have

$$\begin{aligned} C_1(m_c) &= 1.363, \\ C_2(m_c) &= -0.648. \end{aligned} \tag{3.22}$$

substituting these values in Eq. (3.13) for the a_1 and a_2 we obtain,

$$\begin{aligned} a_1 &= 1.147, \\ a_2 &= -0.194. \end{aligned} \tag{3.23}$$

Since a_1 and a_2 have opposite sign the interference is destructive. The large difference in lifetime between D^+ and D^0 is attributed to this effect.

Summarizing: if both particles in the final state are charged then the decay is induced by the charged current part of the Hamiltonian; these decays belong to Class I. If both particles are neutral then the decay proceeds via the neutral current part; decays of this kind belong to Class II. If one of the particles is neutral and the other charged then the decay can proceed via both charged and neutral currents; such decays belong to class III.

3.4 Decay Amplitude in factorization scheme

The Lorentz structure of the matrix element depends on the type of particles M_1 and M_2 involved in the final state. There are three cases to be distinguished :

1. both M_1 and M_2 are pseudoscalar mesons, P_1 P_2;
2. a pseudoscalar meson P and a vector meson V or;
3. two vector mesons, V_1, V_2.

Let $|F\rangle$ and $|P\rangle$ represent pseudoscalar meson states (F is the decaying heavy mesons), and $|V\rangle$ a vector meson state. Therefore, in the factorization scheme, we need to

evaluate the following matrix elements, $\langle P|J_\mu|0\rangle$, $\langle V|J_\mu|0\rangle$, $\langle P|J_\mu|F\rangle$, and $\langle V|J_\mu|F\rangle$. The current J_μ has $V_\mu - A_\mu$ structure.

Since P and F are pseudoscalars mesons ($J^P = 0^-$), we have

$$\begin{aligned} \langle P|A_\mu|F\rangle &= 0, \\ \langle P|V_\mu|0\rangle &= 0. \end{aligned} \tag{3.24}$$

The matrix elements $\langle P|J_\mu|0\rangle$ and $\langle P|J_\mu|F\rangle$ have the following covariant structures [11]:

$$\begin{aligned} \langle P|J_\mu|0\rangle &\equiv \langle P(k_P)|A_\mu|0\rangle \\ &= -if_P(k_P)_\mu, \\ \langle P|J_\mu|F\rangle &= \langle P(k_P)|V_\mu|F(k_F)\rangle \\ &= (k_F + k_P)_\mu f_+(q^2) + (k_F - k_P)_\mu f_-(q^2), \end{aligned} \tag{3.25}$$

with the momentum transfer

$$q_\mu = (k_F - k_P)_\mu, \tag{3.26}$$

where k_X is the four momentum of the particle X and f_P is the decay constant of the pseudoscalar meson P. The scalar functions $f_-(q^2)$ and $f_+(q^2)$ are the invariant weak transition $F \longrightarrow P$ form factors. There is another parameterization of the matrix element in Eq. (3.25) which we determine as follows. Let us calculate the divergence of Eq. (3.25), we obtain

$$\begin{aligned} \langle P|\partial_\mu V_\mu|F\rangle &= \langle P|q_\mu V_\mu|F\rangle \\ &= q_\mu \left\{(k_F + k_P)_\mu f_+(q^2) + (k_F - k_P)_\mu f_-(q^2)\right\}, \\ &= (k_F^2 - k_P^2) f_+(q^2) + q^2 f_-(q^2). \end{aligned} \tag{3.27}$$

In the limit that SU(4) is a good symmetry we have

$$k_F^2 - k_P^2 \simeq 0, \tag{3.28}$$

and hence,

$$\langle P|\partial_\mu V_\mu|F\rangle = q^2 f_-(q^2). \tag{3.29}$$

If the vector current V_μ is conserved, i.e.

$$\partial_\mu V_\mu = 0, \tag{3.30}$$

then the form factor $f_-(q^2)$ has to vanish while $f_+(q^2)$ is nonzero. However, $SU(4)$ is badly broken,i.e.

$$k_F^2 - k_P^2 \neq 0, \tag{3.31}$$

and the weak vector current

$$V_\mu = (\bar{q}\gamma_\mu c), \tag{3.32}$$

where $q = u, d, s$, is not conserved. Using Dirac equation for the quark field q and c we calculate the divergence of V_μ to be

$$\begin{aligned} \partial_\mu V_\mu &= \partial_\mu(\bar{q}\gamma_\mu c) \\ &\equiv (m_c - m_q)\bar{q}c \\ &\simeq m_c\bar{q}c \\ &\neq 0. \end{aligned} \tag{3.33}$$

Consequently both form factors, $f_-(q^2)$ and $f_-(q^2)$ in Eq. (3.27) will survive.

Let us introduce a new function $F_0(q^2)$ such that

$$(k_F^2 - k_P^2)f_+(q^2) + q^2 f_-(q^2) = (m_F^2 - m_P^2)F_0(q^2). \tag{3.34}$$

Therefore, using Eq. (3.34), we can express the matrix element in Eq. (3.25) in the following equivalent form

$$\langle P|V_\mu|F\rangle = \left\{(k_F + k_P)_\mu - \frac{m_F^2 - m_P^2}{q^2}q_\mu\right\}F_1(q^2) + \frac{m_F^2 - m_P^2}{q^2}q_\mu F_0(q^2), \tag{3.35}$$

where the form factors f_-, f_+ and F_0, F_1 are related by

$$\begin{aligned} f_+(q^2) &= F_1(q^2), \\ f_-(q^2) &= \frac{(m_F^2 - m_P^2)}{q^2}\{F_0 - F_1\}. \end{aligned} \tag{3.36}$$

In order to avoid the singularity at $q^2 = 0$, we must have the following constraint,

$$F_0(0) = F_1(0). \tag{3.37}$$

The decomposition in Eq. (3.35) is known as Bauer, Stech and Wirbel (BSW) decomposition [4]. The advantage of this decomposition is that it reflects the spin structure of the weak vector current V_μ. This can be easily seen as follows: If we multiply both sides of Eq. (3.35) by q_μ, we obtain

$$\begin{aligned}\langle P|q_\mu V_\mu|F\rangle &= q_\mu\left\{(k_F+k_P)_\mu - \frac{m_F^2-m_P^2}{q^2}q_\mu\right\}F_1(q^2) \\ &\quad + \frac{m_F^2-m_P^2}{q^2}q^2F_0(q^2) \\ &= (m_F^2-m_P^2)F_0(q^2).\end{aligned} \tag{3.38}$$

Equation (3.38) shows that $F_0(q^2)$ represents the matrix elements of the quantity $\partial_\mu V_\mu = q_\mu V_\mu$ which behaves as a scalar operator with spin parity $J^P = 0^+$. We also have

$$q_\mu\left\{(k_F+k_P)_\mu - \frac{m_F^2-m_P^2}{q^2}q_\mu\right\} = 0. \tag{3.39}$$

Therefore the associated operator of the form factor $F_1(q^2)$ in Eq. (3.35) is orthogonal to q_μ. Consequently the contribution of $F_1(q^2)$ corresponds to spin 1 part of the current V_μ.

In the case the final state involves a vector particle, we need the matrix element $\langle V|J_\mu|0\rangle$ and $\langle V|J_\mu|F\rangle$. Since V is a vector particle we have

$$\begin{aligned}\langle V(k,\epsilon)|A_\mu|0\rangle &= 0 \\ \langle V(k,\epsilon)|V_\mu|0\rangle &= m_V f_V \epsilon_\mu^*,\end{aligned} \tag{3.40}$$

where ϵ_μ is the polarization vector of the vector meson. By Lorentz invariance the quantity $\langle V|J_\mu|F\rangle$ has the following covariant structure [11],

$$\begin{aligned}\langle V(k_V,\epsilon)|V_\mu|F(k_F)\rangle &= ig\varepsilon_{\mu\nu\rho\sigma}\epsilon^{*\nu}(k_F+k_V)^\rho(k_F-k_V)^\sigma \\ \langle V(k_V,\epsilon)|A_\mu|F(k_F)\rangle &= f\epsilon_\mu^* + a_+(\epsilon^*.k_F)(k_F+k_V)_\mu \\ &\quad + a_-(\epsilon^*.k_F)(k_F-k_V)_\mu.\end{aligned} \tag{3.41}$$

Bauer, Stech and Wirbel [4] choose to write these matrix elements in a different, but equivalent form,

$$\langle V(k_V,\epsilon)|V_\mu|F(k_F)\rangle = \frac{2}{m_F+m_V}\varepsilon_{\mu\nu\rho\sigma}\epsilon^{*\nu}k_F^\rho\, k_V^\sigma\, V(q^2), \tag{3.42}$$

$$\begin{aligned}\langle V(k_V)|A_\mu|F(k_F)\rangle &= -i\epsilon_\mu^*(m_F+m_V)A_1(q^2)+i\frac{\epsilon^*.q}{m_F+m_V}(k_F+k_V)_\mu\, A_2(q^2)\\ &\quad +i\frac{\epsilon^*.q}{q^2}2\,m_V q_\mu\left(A_3(q^2)-A_0(q^2)\right),\end{aligned} \tag{3.43}$$

where

$$q_\mu = (k_F-k_V)_\mu, \tag{3.44}$$

and the form factors A_1, A_2 and A_3 satisfy the following relation,

$$A_3(q^2) = \frac{m_F+m_V}{2m_V}A_1(q^2) - \frac{m_F-m_V}{2m_V}A_2(q^2), \tag{3.45}$$

with the condition,

$$A_3(0) = A_0(0), \tag{3.46}$$

so that no pole occurs at $q^2=0$. Using Eq. (3.45) in Eq. (3.43), we obtain

$$\begin{aligned}\langle V(k_V,\epsilon)|A_\mu|F(k_F)\rangle &= -i(m_F+m_V)\left[\epsilon_\mu^*-\frac{\epsilon^*.q}{q^2}q_\mu\right]A_1(q^2)\\ &\quad +i\epsilon^*.q\left[\frac{(k_F+k_V)_\mu}{m_F+m_V}-\frac{m_F-m_V}{q^2}q_\mu\right]A_2(q^2)\\ &\quad -2i\,m_V\frac{\epsilon^*.q}{q^2}q_\mu A_0(q^2).\end{aligned} \tag{3.47}$$

The BSW form factors $V(q^2)$, $A_0(q^2)$, $A_1(q^2)$, $A_2(q^2)$, $A_3(q^2)$ in Eqns. (3.42), (3.43) are related to the form factors f, a_-, a_+ and g in Eq. (3.41) by

$$\begin{aligned}A_1(q^2) &= \frac{i}{m_F+m_V}f(q^2),\\ A_2(q^2) &= -i(m_F+m_V)a_+(q^2),\\ A_3(q^2) &= \frac{i}{2m_V}\left(f(q^2)+(m_F^2-m_V^2)a_+(q^2)\right),\\ V(q^2) &= -i(m_F+m_V)g(q^2),\\ A_0(q^2) &= \frac{i}{2m_V}\left(f(q^2)+(m_F^2-m_V^2)a_+(q^2)+q^2a_-(q^2)\right).\end{aligned} \tag{3.48}$$

We note that the tensor structures in Eq. (3.42) and in the square brackets of Eq. (3.47) have a vanishing divergence, i.e.

$$\begin{aligned} q_\mu \varepsilon_{\mu\nu\rho\sigma} \epsilon^{*\nu} k_F^\rho k_V^\sigma &= 0 \\ q_\mu \left[\epsilon_\mu^* - \frac{\epsilon^*.q}{q^2} q_\mu \right] &= 0 \\ q_\mu \left[\frac{(k_F + k_V)_\mu}{m_F + m_V} - \frac{m_F - m_V}{q^2} q_\mu \right] &= 0, \end{aligned} \tag{3.49}$$

hence it follows from Eqns. (3.42), (3.47) and (3.49) that the contributions of the form factors $V(q^2)$ and $A_1(q^2)$, $A_2(q^2)$ are orthogonal to q_μ, therefore their contributions correspond to the spin 1 part of the currents V_μ and A_μ respectively. Eqns. (3.47) and (3.49) gives

$$\langle V | q_\mu A_\mu | F \rangle = -2im_V A_0(q^2) \epsilon^*.q. \tag{3.50}$$

Thus, $A_0(q^2)$ represents the matrix element of the quantity $q_\mu A_\mu$ which behaves as a pseudoscalar operator with spin parity $J^P = 0^-$.

Now we proceed to calculate the decay amplitudes and decay rates, within the factorization approximation, for the processes

$$F \longrightarrow M_1 \, M_2, \tag{3.51}$$

where $(M_1, M_2) = (P_1, P_2)$, (P, V), (V_1, V_2).

3.4.1 $F \longrightarrow P_1 P_2$

Here we have a decay of a pseudoscalar into two pseudoscalars:

$$0^- \longrightarrow 0^- \, 0^-. \tag{3.52}$$

Conservation of angular momentum requires that the particles P_1 and P_2 be in a relative S state. Assuming factorization, the decay amplitude for this process is given by,

$$A_{pp}(F \longrightarrow P_1 P_2) = G \langle P_2(k_2) | J_\mu | 0 \rangle \langle P_1(k_1) | J'_\mu | F(K) \rangle, \tag{3.53}$$

where the four-momenta are related by

$$\begin{aligned} q_\mu &= (K - k_1)_\mu \\ K_\mu &= (k_1 + k_2)_\mu. \end{aligned} \tag{3.54}$$

In the center of mass we have

$$\begin{aligned} K &= (m_F, 0, 0, 0), \\ \mathbf{k}_1 &= -\mathbf{k}_2 = \mathbf{k}, \\ k_1 &= (E_1, \mathbf{k}),\ k_2 = (E_2, -\mathbf{k}). \end{aligned} \tag{3.55}$$

Using Eqns. (3.25) and (3.35) in Eq. (3.53) we obtain

$$\begin{aligned} A_{pp}(F \longrightarrow P_1 P_2) &= -iGf_2 k_{2\mu} \left[\left((K + k_1)_\mu - \frac{m_F^2 - m_1^2}{q^2} q_\mu \right) F_1 + \frac{m_F^2 - m_1^2}{q^2} q_\mu F_0 \right] \\ &= -iGf_2 (m_F^2 - m_1^2) F_0^{FP_1}(m_2^2). \end{aligned} \tag{3.56}$$

The decay rate is given by

$$\begin{aligned} \Gamma(F \longrightarrow P_1 P_2) &= \frac{|\mathbf{k}|}{8m_F^2 \pi} |A_{pp}(F \longrightarrow P_1 P_2)|^2 \\ &= \frac{G^2 f_2^2 (m_F^2 - m_1^2)^2}{8m_F^2 \pi} \left(F_0^{FP_1}(m_2^2) \right)^2 |\mathbf{k}|. \end{aligned} \tag{3.57}$$

3.4.2 $F \longrightarrow PV$

This a decay of the type

$$0^- \longrightarrow 0^- 1^-. \tag{3.58}$$

Conservation of angular momentum requires the final state PV to be in a relative P state. There are two cases to be distinguished depending on which particle, the pseudoscalar or the vector, is created out of the vacuum. We have the following amplitudes

$$\begin{aligned} A_{vp}(F \longrightarrow VP) &= G\langle P(k_2)|J_\mu|0\rangle\langle V(k_1)|J'_\mu|F(K)\rangle, \\ A_{pv}(F \longrightarrow PV) &= G\langle V(k_1)|J_\mu|0\rangle\langle P(k_2)|J'_\mu|F(K)\rangle. \end{aligned} \tag{3.59}$$

Using Eqns. (3.25), (3.35) (3.40) and (3.47) in Eq.(3.59) we get

$$\begin{aligned} A_{vp}(F \longrightarrow VP) &= 2Gm_V f_P A_0^{FV}(m_P^2)\epsilon^*.K, \\ A_{pv}(F \longrightarrow PV) &= 2Gm_V f_V F_1^{FP}(m_V^2)\epsilon^*.K. \end{aligned} \tag{3.60}$$

The decay rates are given by

$$\begin{aligned} \Gamma(F \longrightarrow VP) &= \frac{|\mathbf{k}|}{8m_F^2\pi}|A_{vp}|^2, \\ \Gamma(F \longrightarrow PV) &= \frac{|\mathbf{k}|}{8m_F^2\pi}|A_{pv}|^2, \end{aligned} \tag{3.61}$$

From Appendix B we have the following polarization vectors ϵ of the vector meson

$$\begin{aligned} \epsilon^\mu(\pm) &= \frac{1}{\sqrt{2}}(0, \mp 1, -i, 0), \\ \epsilon^\mu(0) &= \frac{1}{m_V}(|\mathbf{k}|, 0, 0, E). \end{aligned} \tag{3.62}$$

In the rest frame of the decaying heavy flavor F we have

$$\begin{aligned} \epsilon(\pm).K &= 0, \\ \epsilon(0).K &= \frac{m_F}{m_V}|\mathbf{k}|. \end{aligned} \tag{3.63}$$

Substituting Eq. (3.63) in Eq. (3.60) we obtain

$$\begin{aligned} A_{vp}(F \longrightarrow VP) &= 2Gm_F f_P A_0^{FV}(m_P^2)|\mathbf{k}|, \\ A_{pv}(F \longrightarrow PV) &= 2Gm_F f_V F_1^{FP}(m_V^2)|\mathbf{k}|. \end{aligned} \tag{3.64}$$

The decay rates then become,

$$\begin{aligned} \Gamma(D \longrightarrow VP) &= \frac{G^2 f_P^2}{2\pi}\left(A_0^{FV}(m_P^2)\right)^2|\mathbf{k}|^3, \\ \Gamma(D \longrightarrow PV) &= \frac{G^2 f_V^2}{2\pi}\left(F_1^{FP}(m_V^2)\right)^2|\mathbf{k}|^3. \end{aligned} \tag{3.65}$$

3.4.3 $P(K) \longrightarrow V_1(k_1)V_2(k_2)$

These decays are of the type

$$0^- \longrightarrow 1^-1^-. \tag{3.66}$$

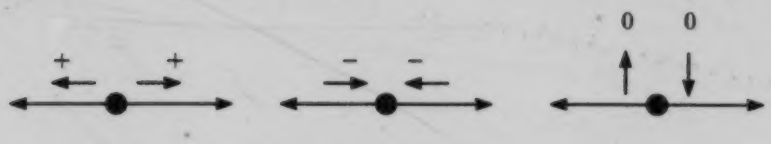

Figure 3.4: Helicities of the the particles V_1V_2 in the parent rest frame

Assuming factorization the amplitude for this process is given by

$$A_{vv}(F \longrightarrow PV) = G\langle V_1(k_1)|J_\mu|0\rangle\langle V_2(k_2)|J'\mu|F(K)\rangle \tag{3.67}$$

Using Eqns. (3.40), (3.42) and (3.47) with the condition

$$\epsilon_1.q = \epsilon_1.k_1 = 0, \tag{3.68}$$

we get for the decay amplitude:

$$\begin{aligned} A_{vv}(F \longrightarrow V_1V_2) \;=\; & G\left\{\frac{2m_{V_1}f_{V_1}}{m_F+m_{V_2}}\varepsilon_{\mu\nu\rho\sigma}\epsilon_1^{*\mu}\epsilon_2^{*\nu}K^\rho k_2^\sigma V(q^2)\right. \\ & +im_{V_1}f_{V_1}[\epsilon_1^*.\epsilon_2^*(m_F+m_{V_2})A_1(q^2) \\ & \left.-\frac{\epsilon_2^*.(K-k_2)}{m_F+m_{V_2}}\epsilon_1^*.(K+k_2)A_2(q^2)]\right\}. \end{aligned} \tag{3.69}$$

Conservation of angular momentum (see Appendix B) requires the particles in the final state to be in S, P and D partial waves, and the helicities, λ and λ', of the two final-state vector particles to be the same (Fig. 3.4).

3.4.4 Calculation of the Helicity Amplitudes A_{00} and $A_{\pm\pm}$

By $A_{\lambda\lambda'}$ we denote the helicity amplitude.

1. **Longitudinal amplitude A_{00}**

   We need to evaluate each of the three terms in Eq. (3.69). In the rest frame of the parent (decaying) particle we have

   $$\mathbf{K} = \mathbf{k}_1 + \mathbf{k}_2 = 0, \tag{3.70}$$

we select the positive z-axis to be parallel to the direction of the momentum $\mathbf{k}_1$ of the particle V_1, thus $\mathbf{k}_1 = -\mathbf{k}_2 = \mathbf{k}$. The momenta of the particles are given by,

$$\begin{aligned} K &= (m_F, 0, 0, 0) \\ k_1 &= (E_1, 0, 0, |\mathbf{k}|) \\ k_2 &= (E_2, 0, 0, -|\mathbf{k}|). \end{aligned} \tag{3.71}$$

We have from Appendix B

$$\begin{aligned} \epsilon_1(0, \theta = 0) &= \frac{1}{m_1}(\,|\mathbf{k}|,\ \ 0,\ \ 0,\ \ E_1\,), \\ \epsilon_2(0, \theta = \pi) &= \frac{1}{m_2}(\,-|\mathbf{k}|,\ \ 0,\ \ 0,\ \ E_2\,), \end{aligned} \tag{3.72}$$

and

$$\begin{aligned} \varepsilon_{\mu\nu\rho\sigma}\epsilon_1^{*\mu}\epsilon_2^{*\nu}K^\rho k_2^\sigma V'(q^2) &= 0, \\ \epsilon_1^*(0).\epsilon_2^*(0) &= -\frac{|\mathbf{k}|^2 + E_1E_2}{m_1m_2}, \\ \frac{\epsilon_2^*.(K - k_2)}{m_F + m_2}\epsilon_1^*.(K + k_2) &= \frac{-2m_F^2|\mathbf{k}|^2}{m_1m_2(m_F + m_2)}. \end{aligned} \tag{3.73}$$

The longitudinal amplitude is then,

$$\begin{aligned} A_{00}(q^2) &= -iGm_1f_1\left(\frac{|\mathbf{k}|^2 + E_1E_2}{m_1m_2}(m_F + m_2)A_1(q^2)\right. \\ &\quad \left. -\frac{2m_F^2|\mathbf{k}|^2}{m_1m_2(m_F + m_2)}A_2(q^2)\right). \end{aligned} \tag{3.74}$$

In addition, we have the following kinematic relations,

$$\begin{aligned} E_1E_2 + |\mathbf{k}|^2 &= \frac{m_F^2 - m_1^2 - m_2^2}{2}, \\ |\mathbf{k}|^2 &= \frac{1}{4m_F^2}\left[\left(m_F^2 - (m_1 + m_2)^2\right)\left(m_F^2 - (m_1 - m_2)^2\right)\right]. \end{aligned} \tag{3.75}$$

we define

$$t = \frac{m_1}{m_F}, \quad \text{and} \quad r = \frac{m_2}{m_F}, \tag{3.76}$$

Eq. (3.74) can be recast in the following form

$$A_{00}(q^2) = -iGm_1 f_1(m_F + m_2)\left(\frac{1-r^2-t^2}{2rt}A_1(q^2) - \frac{2|\mathbf{k}|^2/m_F^2}{rt(1+r)^2}A_2(q^2)\right). \tag{3.77}$$

2. **Transverse amplitudes $A_{\pm\pm}$**

The polarization vectors are

$$\begin{aligned}
\epsilon_1(\pm 1, \theta = 0) &= \frac{1}{\sqrt{2}}(0, \mp 1, -i, 0), \\
\epsilon_2(\pm 1, \theta = \pi) &= \frac{1}{\sqrt{2}}(0, \pm 1, -i, 0).
\end{aligned} \tag{3.78}$$

As with the case of A_{00}, we have from Appendix B:

$$\varepsilon_{\mu\nu\rho\sigma}\epsilon_1^{*\mu}(\pm)\epsilon_2^{*\nu}(\pm)K^\rho k_2^\sigma V(q^2) = \mp i m_F|\mathbf{k}|V(q^2), \tag{3.79}$$

$$\begin{aligned}
\epsilon_1^*(\pm).\epsilon_2^*(\pm) &= 1, \\
\epsilon_2^*(\pm).(K - k_2) &= 0, \\
\epsilon_1^*(\pm).(K + k_2) &= 0
\end{aligned} \tag{3.80}$$

The transverse amplitudes are then given by,

$$\begin{aligned}
A_{\pm\pm}(q^2) &= G\left\{\frac{2m_1 f_1}{m_F + m_2}(\mp i m_F|\mathbf{k}|)V(q^2) + i m_1 f_1(m_F + m_2)A_1(q^2)\right\} \\
&= iGm_1 f_1(m_F + m_2)\left(A_1(q^2) \mp 2\frac{|\mathbf{k}|/m_F}{(1+r)^2}V(q^2)\right).
\end{aligned} \tag{3.81}$$

The helicity and partial wave amplitudes are related by (see Appendix B);

$$\begin{aligned}
A_{00} &= -\frac{1}{\sqrt{3}}S + \sqrt{\frac{2}{3}}D, \\
A_{++} &= \frac{1}{\sqrt{3}}S + \frac{1}{\sqrt{2}}P + \frac{1}{\sqrt{6}}D \\
A_{--} &= \frac{1}{\sqrt{3}}S - \frac{1}{\sqrt{2}}P + \frac{1}{\sqrt{6}}D
\end{aligned} \tag{3.82}$$

Solving for S, P and D,

$$\begin{aligned} S &= \frac{1}{\sqrt{3}}(A_{++} + A_{--} - A_{00}), \\ P &= \frac{1}{\sqrt{2}}(A_{++} - A_{--}), \\ D &= \frac{1}{\sqrt{6}}(A_{++} + A_{--} + 2A_{00}). \end{aligned} \tag{3.83}$$

For completeness, we introduce here the transversity basis [12], A_0, $A_\parallel$ and $A_\perp$, through

$$\begin{aligned} A_0 &= A_{00} \\ &= -\sqrt{\frac{1}{3}}S + \sqrt{\frac{2}{3}}D \\ A_\parallel &= \sqrt{\frac{1}{2}}(A_{++} + A_{--}) \\ &= \sqrt{\frac{2}{3}}S + \sqrt{\frac{1}{3}}D \\ A_\perp &= \sqrt{\frac{1}{2}}(A_{++} - A_{--}) \\ &= P. \end{aligned} \tag{3.84}$$

Each of the three bases form a complete set, and could be used in the analysis. The partial wave amplitudes are in general complex and can be expressed as follows,

$$\begin{aligned} S &= |S| \exp i\delta_S, \\ P &= |P| \exp i\delta_P, \\ D &= |D| \exp i\delta_D, \end{aligned} \tag{3.85}$$

where δ_X is the phase shift associated with the corresponding partial wave.

S, P and D amplitudes were calculated first by using the amplitudes in Eqns. (3.77) and (3.81) in (3.83) and feeding in the phases by hand as shown in Eq. (3.85). One gets,

$$|S| = G\left|\frac{im_1 f_1(m_F + m_2)}{2\sqrt{3}rt}\left[(1 - r^2 + 4rt - t^2)A_1 - \frac{4|\mathbf{k}|^2/m_F^2}{(1+r)^2}A_2\right]\right|,$$

$$
\begin{aligned}
|P| &= G\left|im_1 f_1(m_F+m_2)\sqrt{2}\frac{2|\mathbf{k}|/m_F}{(1+r)^2}V(q^2)\right|, \\
|D| &= G\left|\frac{im_1 f_1(m_F+m_2)}{\sqrt{6}rt}\left[((t+r)^2-1)A_1+\frac{4|\mathbf{k}|^2/m_F^2}{(1+r)^2}A_2\right]\right|. \qquad (3.86)
\end{aligned}
$$

In terms of the helicity, the partial-wave and the transversity amplitudes, the decay rate is given by

$$
\begin{aligned}
\Gamma(F\longrightarrow V_1V_2) &= \frac{|\mathbf{k}|}{8m_F^2\pi}\left\{|\,A_{++}\,|^2+|\,A_{--}\,|^2+|\,A_{00}\,|^2\right\} \\
&= \frac{|\mathbf{k}|}{8m_F^2\pi}\left\{|\,S\,|^2+|\,P\,|^2+|\,D\,|^2\right\}, \\
&= \frac{|\mathbf{k}|}{8m_F^2\pi}\left\{|\,A_0\,|^2+|\,A_{\|}\,|^2+|\,A_{\perp}\,|^2\right\} \qquad (3.87)
\end{aligned}
$$

and is independent of the phases δ_X. The results in Eq. (3.87) follow from the fact that each basis is complete.

The longitudinal polarization is defined by the ratio of the longitudinal decay rate to the total decay rate,

$$
\begin{aligned}
P_L &= \frac{\Gamma_{00}}{\Gamma}, \\
&= \frac{|\,A_{00}\,|^2}{|\,A_{++}\,|^2+|\,A_{--}\,|^2+|\,A_{00}\,|^2}. \qquad (3.88)
\end{aligned}
$$

One can work with the helicity amplitudes or the partial-wave amplitudes. We prefer to work with the latter as the dependence of the polarization on the partial-wave phases is more obvious in that basis. Using Eq. (3.82) and (3.85)we get

$$
|\,A_{00}\,|^2 = \frac{1}{3}|\,S\,|^2+\frac{2}{3}|\,D\,|^2-\frac{2\sqrt{2}}{3}|\,S\,||\,D\,|\cos(\delta_S-\delta_D). \qquad (3.89)
$$

The polarization is then

$$
P_L=\frac{1}{3}\frac{|\,S\,|^2+2|\,D\,|^2-2\sqrt{2}|\,S\,||\,D\,|\cos\delta_{SD}}{|\,S\,|^2+|\,P\,|^2+|\,D\,|^2}. \qquad (3.90)
$$

In contrast to the decay rate Eq. (3.87), the polarization depends on the phase difference $\delta_{SD}=\delta_S-\delta_D$ arising from the interference between S and D waves.

The decay rate, Eq. (3.87), is given by the sum of square of partial waves amplitude (no interference term,), consequently small amplitudes (D waves) are masked by larger one (S waves). In the other hand, the polarization, Eq. (3.90), involves an interference term where the small D-amplitude is multiplied by the large S-amplitude and by a factor $2\sqrt{2} \sim 3$, hence a large enhancement of the contribution from D-wave, which could have large effect on the polarization.

We observe that if we use Eq. (3.86) in (3.87) the decay rate exhibits a dependence on $|\mathbf{k}|$, $|\mathbf{k}|^3$, $|\mathbf{k}|^5$ which reflect the threshold behavior expected of S, P and D waves respectively.

Bibliography

[1] S. L. Adler and R. Dashen, Current Algebras and Applications to Particle physics (Benjamin, New York, 1968); R. E. Marshak, Riazuddin, C. P. Ryan, Theory of Weak Interactions in Particle Physics, (Wiley-Interscience, 1969).

[2] Thomas G. Rizzo and Ling-Lie Chau Wang, BNL - 27950 (1980); D. Zeppenfeld, Z. Phys. C 8, 77 (1981); L. L. Chau Wang and F. Wilczek, Phys. Rev. Lett. 43, 816 (1979).

[3] Ling-Lie Chau, Phys. Rep. 95 (1983); Ling-Lie Chau and Hai-Yang Cheng, Phys. Rev. D36, 137 (1987); *ibd*, Phys. Rev. D39, 2788 (1989). P. Żenczykowski, Acta. Phys. Pol. B 28, 1605 (1997).

[4] M. Bauer, B. Stech, M. Wirbel, Z. Phys. C 34, 103 (1987); M. Wirbel, B. Stech, M. Bauer, Z. Phys. C 29, 637 (1985); M. Bauer, M. Wirbel, Z. Phys. C 42, 671 (1989).

[5] L. L. Chau, H. Y. Cheng and T. Huang, Z. Phys. C 53, 413 (1992).

[6] L. L. Chau, H. Y. Cheng, W. K. Sze, H. Yao, B. Tseng, Phys. Rev. D 43, 2176 (1991); M. Gronau, O. F. Hernandez, D. London, Jonathan L. Rosner, Phys. Rev. D 50, 4529 (1994).

[7] F. Buccella, M. Lusignoli, G. Miele, A. Pugliese, and P. Santorelli, Phys. Rev. D 51, 3478 (1995).

[8] M. Neubert, Phys. Lett. B424, 152 (1998). See also Gronau et al. in Ref. [6]. Ch. Smith, Eur. Phys. J. C 10, 639 (1999).

[9] J. F. Donoghue, Phys. Rev. D 33, 1516 (1986).

[10] M. Gell - Mann and F. Zachariasen, Phys. Rev. 124, 953 (1961); N. Kroll, T. D. Lee, and B. Zumino, Phys. Rev. Lett. 18, 1029 (1967); J. F. Donoghue, Phys. Rev. D 13, 2064 (1976).

[11] N. Isgur and B. Wise, Phys. Rev. D 42, 2388 (1990).

[12] A. S. Dighe, I. Dunietz, H. J. Lipkin and J. L. Rosner, Phys. Lett. B 369, 144 (1996).

Chapter 4

$D_s^+ \to \phi\rho^+$ Decay

4.1 Introduction

The branching ratio and the longitudinal polarization in $D_s^+ \to \phi\rho^+$ have now been measured

$$\begin{aligned} B(D_s^+ \to \phi\rho^+) &= (6.7 \pm 2.3)\% \ [1] \\ P_L(D_s^+ \to \phi\rho^+) &= \Gamma_L/\Gamma \\ &= (0.370 \pm 0.035 \pm 0.038) \ [2]. \end{aligned} \tag{4.1}$$

Theoretically, Gourdin et al. [3] studied the ratio

$$\begin{aligned} R_h &= B(D_s^+ \to \phi\rho^+)/B(D_s^+ \to \phi\pi^+) \\ &= 1.86 \pm 0.26 \pm {}^{0.29}_{0.40}. \ [4] \end{aligned} \tag{4.2}$$

Within the context of the factorization scheme, which the authors of [3] adopt, this ratio is independent of the normalization of the form factor $A_1^{D_s\phi}(0)$. It depends on the ratios $x^{D_s\phi}(0)$ and $y^{D_s\phi}(0)$ defined by:

$$\begin{aligned} x^{D_s\phi}(q^2) &\equiv \frac{A_2^{D_s\phi}(q^2)}{A_1^{D_s\phi}(q^2)}, \\ y^{D_s\phi}(q^2) &\equiv \frac{V^{D_s\phi}(q^2)}{A_1^{D_s\phi}(q^2)}, \end{aligned} \tag{4.3}$$

and on the q^2 dependence of the form factors. For the definitions of the form factors, see Bauer, Stech and Wirbel [5]. No particular model for the form factors was assumed in [3] . Instead, R_h was studied as a function of $x^{D_s\phi}(0)$ and $y^{D_s\phi}(0)$ in three different scenarios for the q^2 dependence of the form factors. The result of [3] was that the $(x^{D_s\phi}(0), y^{D_s\phi}(0))$ domain allowed by R_h was inconsistent with the measurement of $x^{D_s\phi}(0)$ and $y^{D_s\phi}(0)$ from the semileptonic data, $D_s \longrightarrow \phi l^+ \nu_l$, in Ref. [6], and just barely consistent with that of Ref. [7] . The allowed domain of $x^{D_s\phi}(0)$ and $y^{D_s\phi}(0)$ was also inconsistent with the theoretical prediction of [5]. Ref. [3] also concluded that within the factorization scheme, the allowed range of $x^{D_s\phi}(0)$ and $y^{D_s\phi}(0)$ implied the following limits on the longitudinal polarization:

$$\begin{aligned} &\text{Monopole form factors with pole-mass 2.53 GeV:} && 0.43 \leq P_L \leq 0.55, \\ &\text{Monopole form factors with pole-mass 3.50 GeV:} && 0.33 \leq P_L \leq 0.55, \\ &\text{Flat form factors:} && 0.36 \leq P_L \leq 0.55. \end{aligned} \quad (4.4)$$

Subsequently, the authors of [8] incorporated nonfactorized contributions in the decay matrix elements, and using the average of $x^{D_s\phi}(0)$ and $y^{D_s\phi}(0)$ from data [6, 7, 9], showed that R_h of Eq. (4.2) and

$$\begin{aligned} R_{sl} &\equiv B(D_s^+ \to \phi l^+ \nu_l)/B(D_s^+ \to \phi\pi^+) \\ &= 0.54 \pm 0.10, \ [10] \end{aligned} \quad (4.5)$$

could be understood within a scenario where the form factors have a monopole dependence as in [5]. However, there had to be significant nonfactorization contribution to $D_s^+ \to \phi\pi^+$, though factorization need not be violated in $D_s^+ \to \phi\rho^+$. The authors of ref. [8] did not study longitudinal polarization.

An important point to be made is that there are three partial waves in $P \to VV'$ decays, S, P and D, and though the decay rate, Eq. (4.24), does not depend on their phases, the longitudinal polarization, Eq. (4.25), does depend on the phase difference

$$\delta_{SD} = \delta_S - \delta_D. \quad (4.6)$$

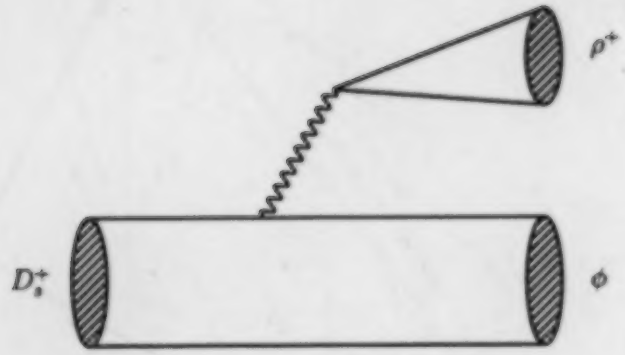

Figure 4.1: External W-emission diagram contributing to the Cabibbo favored $D_s^+ \longrightarrow \rho^+\phi$ decay

The authors of ref. [3] did not consider the effect of partial wave amplitude phases on the longitudinal polarization.

In this chapter [11] we have studied the data given in Eq. (4.1) within the context of factorization invoking several form factor models, details of which are given in the next section, and allowing for nonzero S, P and D wave phases.

4.2 Details of the Calculations

The decay $D_s^+ \longrightarrow \rho^+\phi$ is Cabibbo-favored and is induced by the effective weak Hamiltonian given by Eq. (3.15)

$$\begin{aligned} \mathcal{H} &= \frac{G_F}{\sqrt{2}}\cos^2\theta_c[a_1(\bar{u}d)(\bar{s}c) + C_2O_8], \\ &= G'_F[a_1(\bar{u}d)(\bar{s}c) + C_2O_8], \end{aligned} \tag{4.7}$$

where

$$G'_F = \frac{G_F}{\sqrt{2}}\cos^2\theta_c, \tag{4.8}$$

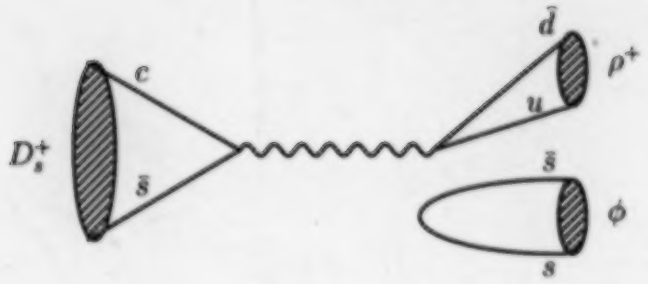

Figure 4.2: Hair-pin quark diagram for $D_s^+ \longrightarrow \rho^+\phi$ decay. The singlet meson ϕ is created from the vacuum.

and the parameter a_1 is defined to be [8]

$$\begin{aligned} a_1 &= C_1 + \frac{C_2}{3} \\ &= 1.09 \pm 0.04. \end{aligned} \tag{4.9}$$

In the factorization approximation one neglects the contribution from the octet current part, O_8, and the matrix element of the first term is written as a product of two current matrix elements. The quark diagram which contributes to $D_s^+ \longrightarrow \rho^+\phi$ decay is shown in (Fig. 4.1). It should be pointed out that there are no W-annihilation or W-exchange terms in $D_s^+ \rightarrow \rho^+\phi$ decay (see (Fig. 3.1)). However, hair-pin graphs (Fig. 4.2) are allowed, but as we discussed in Chapter 2 they have negligible contribution. We neglect them in what follows. In the factorization approximation, the decay amplitude takes the following form:

$$A(D_s^+ \longrightarrow \rho^+\phi) = G_F' a_1 \langle \phi \mid \bar{s}c \mid D_s^+ \rangle \langle \rho^+ \mid \bar{u}d \mid 0 \rangle, \tag{4.10}$$

Each of the current matrix elements can be expressed in terms of meson decay constants and invariant form factors. According to Eqns. (3.40), (3.42) and (3.43) we have

$$\langle \rho^+ \mid \bar{u}d \mid 0 \rangle = m_\rho f_\rho \epsilon^*_{\rho_\nu} \tag{4.11}$$

$$\langle \phi \mid \bar{s}c \mid D_s \rangle = \frac{2}{m_{D_s}+m_\phi}\varepsilon_{\mu\nu\rho\sigma}\epsilon_\phi^{*\nu}k_{D_s}^\rho k_\phi^\sigma V(q^2) + i\{\epsilon_{\phi\mu}^*(m_{D_s}+m_\phi)A_1(q^2) - \frac{\epsilon_\phi^*.q}{m_{D_s}+m_\phi}(k_\phi+k_{D_s})_\mu A_2(q^2) - \frac{\epsilon_\phi^*.q}{q^2}2m_\phi q_\mu A_3(q^2) + \frac{\epsilon_\phi^*.q}{q_2}2m_\phi q_\mu A_0(q^2)\}, \quad (4.12)$$

where

$$q = k_{D_s} - k_\phi, \quad (4.13)$$

is the momentum transfer, f_ρ (for which we use 212.0 MeV) is the decay constant of the ρ meson and ϵ_ϕ, ϵ_ρ are the polarization vectors of the vector mesons ϕ and ρ respectively, $A_i(q^2)$, $(i = 1, 2, 3)$ and $V(q^2)$ are the invariant weak transition $D_s^+ \longrightarrow \phi$ form factors defined in [5].

The longitudinal and transverse helicity amplitudes A_{00}, A_{++} and A_{--} for $D_s^+ \longrightarrow \rho^+\phi$ are given by equations (3.77) and (3.81)

$$A_{00}(D_s^+ \longrightarrow \rho^+\phi) = -iG_F' m_\rho f_\rho (m_{D_s}+m_\phi) a_1 \left\{\alpha A_1^{D_s\phi}(m_\rho^2) - \beta A_2^{D_s\phi}(m_\rho^2)\right\} \quad (4.14)$$

where the parameter α and β are defined as follows,

$$\alpha = \frac{1-r^2-t^2}{2rt}, \qquad \beta = \frac{\mathcal{K}^2}{2rt(1+r)^2}, \quad (4.15)$$

and the function $\mathcal{K}(r,t)$ is given by

$$\mathcal{K}^2 = \frac{4|\mathbf{k}|^2}{m_{D_s}^2}, \qquad \mathcal{K}^2 = (1+r^4+t^4-2r^2-2t^2-2r^2t^2) \quad (4.16)$$

with

$$r = \frac{m_\phi}{m_{D_s}}, \qquad t = \frac{m_\rho}{m_{D_s}}. \quad (4.17)$$

The other two helicity amplitudes are:

$$A_{\pm\pm}(D_s^+ \longrightarrow \rho^+\phi) = iG_F' m_\rho f_\rho (m_{D_s}+m_\phi) a_1 \left\{A_1^{D_s\phi}(m_\rho^2) \mp \gamma V^{D_s\phi}(m_\rho^2)\right\}, \quad (4.18)$$

where the parameter γ is given by

$$\gamma = \frac{\mathcal{K}}{(1+r)^2}. \tag{4.19}$$

The partial waves amplitudes, S, P and D, were calculated first by using the helicity amplitudes shown in Eqns. (4.14) and (4.18) in Eq. (3.83) we obtain the following results (see Eq. (3.86))

$$\begin{aligned}
S &= i G'_F a_1 m_\rho f_\rho (m_{D_s} + m_\phi) \frac{1}{\sqrt{3}} \left[\frac{(1 - r^2 + 4rt - t^2)}{2rt} A_1^{D_s\phi}(m_\rho^2) \right. \\
&\quad \left. - \frac{4|\mathbf{k}|^2/m_{D_s}^2}{2rt(1+r)^2} A_2^{D_s\phi}(m_\rho^2) \right], \\
P &= -i G'_F a_1 m_\rho f_\rho (m_{D_s} + m_\phi) \sqrt{2} \frac{2|\mathbf{k}|/m_{D_s}}{(1+r)^2} V^{D_s\phi}(m_\rho^2), \\
D &= i G'_F a_1 m_\rho f_\rho (m_{D_s} + m_\phi) \sqrt{\frac{2}{3}} \left[\frac{(t+r)^2 - 1)}{2rt} A_1^{D_s\phi}(m_\rho^2) \right. \\
&\quad \left. + \frac{4|\mathbf{k}|^2/m_{D_s}^2}{2rt(1+r)^2} A_2^{D_s\phi}(m_\rho^2) \right],
\end{aligned} \tag{4.20}$$

then feeding in the phases by hand as shown in Eq. (3.85).

In the following calculation we are mainly interested in the ratio of partial wave amplitudes, therefore we drop a common factor of

$$\mathcal{F} = i G'_F a_1 m_\rho f_\rho (m_{D_s} + m_\phi), \tag{4.21}$$

from the equation (4.20) which reduces to the following simple form

$$\begin{aligned}
S &= \frac{1}{\sqrt{3}} \left\{ (2+\alpha) A_1^{D_s\phi}(m_\rho^2) - \beta A_2^{D_s\phi}(m_\rho^2) \right\}, \\
P &= -\sqrt{2} \gamma V^{D_s\phi}(m_\rho^2), \\
D &= \sqrt{\frac{2}{3}} \left\{ (1-\alpha) A_1^{D_s\phi}(m_\rho^2) + \beta A_2^{D_s\phi}(m_\rho^2) \right\}.
\end{aligned} \tag{4.22}$$

Let us define the ratios r_{SP} and r_{SD} as follows:

$$\begin{aligned}
r_{SP} &= \frac{|S|}{|P|}, \\
&= \frac{1}{\sqrt{6}} \frac{| (2+\alpha) A_1^{D_s\phi}(m_\rho^2) - \beta A_2^{D_s\phi}(m_\rho^2) |}{| \gamma V^{D_s\phi}(m_\rho^2) |},
\end{aligned}$$

$$
\begin{aligned}
&= \frac{1}{\sqrt{6}} \frac{|\,(2+\alpha) - \beta\, x^{D_s\phi}(m_\rho^2)\,|}{|\,\gamma\, y^{D_s\phi}(m_\rho^2)\,|}, \\
r_{SD} &= \frac{|S|}{|D|}, \\
&= \frac{1}{\sqrt{2}} \frac{|\,(2+\alpha)\, A_1^{D_s\phi}(m_\rho^2) - \beta\, A_2^{D_s\phi}(m_\rho^2)\,|}{|\,(1-\alpha)\, A_1^{D_s\phi}(m_\rho^2) + \beta\, A_2^{D_s\phi}(m_\rho^2)\,|}, \\
&= \frac{1}{\sqrt{2}} \frac{|\,(2+\alpha) - \beta\, x^{D_s\phi}(m_\rho^2)\,|}{|\,(1-\alpha) + \beta\, x^{D_s\phi}(m_\rho^2)\,|}.
\end{aligned} \tag{4.23}
$$

The decay rate is expressed as follows

$$
\begin{aligned}
\Gamma(D_s^+ \longrightarrow \rho^+\phi) &= |\mathcal{F}|^2 \frac{|\mathbf{k}|}{8m_{D_s}^2\pi} \left\{|S|^2 + |P|^2 + |D|^2\right\}, \\
&= |\mathcal{F}|^2 \frac{|\mathbf{k}|}{8m_{D_s}^2\pi} |S|^2 \left\{1 + r_{SP}^{-2} + r_{SD}^{-2}\right\}
\end{aligned} \tag{4.24}
$$

In the same manner the longitudinal polarization is given by Eq. (3.90)

$$
\begin{aligned}
P_L &= \frac{1}{3} \frac{|\,S\,|^2 + 2\,|\,D\,|^2 - 2\sqrt{2}\,|\,S\,||\,D\,|\cos\delta_{SD}}{|\,S\,|^2 + |\,P\,|^2 + |\,D\,|^2}, \\
&= \frac{1}{3} \frac{1 + 2r_{SD}^{-2} - 2\sqrt{2}\, r_{SD}^{-1}\cos\delta_{SD}}{1 + r_{SP}^{-2} + r_{SD}^{-2}}.
\end{aligned} \tag{4.25}
$$

For $D_s^+ \longrightarrow \rho^+\phi$ decay the values of the parameters r, t, $\mathcal{K}$, α, β and γ are:

$$
\begin{aligned}
r &= 0.518, \quad t = 0.390, \quad \mathcal{K} = 0.415, \\
\alpha &= 1.433, \quad \beta = 0.185, \quad \gamma = 0.180,
\end{aligned} \tag{4.26}
$$

then, the partial waves amplitudes S, P, D are

$$
\begin{aligned}
S &= \frac{1}{\sqrt{3}} \left\{3.433\, A_1^{D_s\phi}(m_\rho^2) - 0.185\, A_2^{D_s\phi}(m_\rho^2)\right\}, \\
P &= -0.180\sqrt{2}\, V^{D_s\phi}(m_\rho^2), \\
D &= \sqrt{\frac{2}{3}} \left\{-0.433\, A_1^{D_s\phi}(m_\rho^2) + 0.185\, A_2^{D_s\phi}(m_\rho^2)\right\},
\end{aligned} \tag{4.27}
$$

and the ratios r_{SP} and r_{SD}

$$
r_{SP} = \frac{1}{\sqrt{6}} \frac{|\,3.433\, A_1^{D_s\phi}(m_\rho^2) - 0.185\, A_2^{D_s\phi}(m_\rho^2)\,|}{|\,0.180\, V^{D_s\phi}(m_\rho^2)\,|},
$$

$$
\begin{aligned}
&= \frac{1}{\sqrt{6}} \frac{|\, 3.433 - 0.185\, x^{D_s\phi}(m_\rho^2)\,|}{|\, 0.180\, y^{D_s\phi}(m_\rho^2)\,|}, \\
r_{SD} &= \frac{1}{\sqrt{2}} \frac{|\, 3.433\, A_1^{D_s\phi}(m_\rho^2) - 0.185\, A_2^{D_s\phi}(m_\rho^2)\,|}{|\, -0.433\, A_1^{D_s\phi}(m_\rho^2) + 0.185\, A_2^{D_s\phi}(m_\rho^2)\,|}, \\
&= \frac{1}{\sqrt{2}} \frac{|\, 3.433 - 0.185\, x^{D_s\phi}(m_\rho^2)\,|}{|\, -0.433 + 0.185\, x^{D_s\phi}(m_\rho^2)\,|}.
\end{aligned} \tag{4.28}
$$

To continue with the numerical analysis of the decay rate $\Gamma(D_s \longrightarrow \rho\phi)$ the ratios r_{SP}, r_{SD} and the longitudinal polarization P_L, we have used form factors from six different sources:

1. Bauer, Stech and Wirbel (BSW*I*) [5], where an infinite momentum frame is used to calculate the form factors at $q^2 = 0$, and a monopole form (pole masses are as in [5]) for q^2 dependence is assumed to extrapolate all the form factors to the desired value of q^2.

2. BSW*II* is a modification of BSW*I*, where while $F_0(q^2)$ and $A_1(q^2)$ are the same as in BSW*I*, a dipole q^2 dependence is assumed for $A_2(q^2)$ and $V(q^2)$.

3. Altomari and Wolfenstein (AW) model [12], where the form factors are evaluated in the limit of zero recoil, and a monopole form is used to extrapolate to the desired value of q^2.

4. CDDGFN model [13], where the form factors are evaluated at $q^2 = 0$ in an effective Lagrangian satisfying heavy quark spin-flavor symmetry in which light vector particles are introduced as gauge particles in a broken chiral symmetry. A monopole form is used for the q^2 dependence. We mention here that we have updated this model by using more recent experimental results of the form factors [1], and the decay constant f_{D_s} [14]:

$$
\begin{aligned}
A_1^{DK^*}(0) &= 0.55 \pm 0.03, \\
A_2^{DK^*}(0) &= 0.40 \pm 0.08, \\
V^{DK^*}(0) &= 1.0 \pm 0.2,
\end{aligned}
$$

$$f_{D_s} = 241 \pm 37\ MeV, \tag{4.29}$$

in calculating the weak couplings constant, of the model, at $q^2 = 0$ [13] , which are subsequently used in evaluating the required form factors.

5. Isgur, Scora, Grinstein and Wise (ISGW) model [15], where a non-relativistic quark model is used to calculate the form factors at zero recoil and an exponential q^2 dependence is used to extrapolate them to the desired q^2.

6. The experimental values [1] of the form factors at $q^2 = 0$ and extrapolating them using monopole forms.

4.3 Results and Discussion

In Table 4.1 we present the predicted values of ratios $x^{D_s\phi}(q^2)$, $y^{D_s\phi}(q^2)$ and the form factors at $q^2 = 0$ and $q^2 = m_\rho^2$ in different models as well as their experimental values at $q^2 = 0$:

$$\begin{aligned} A_1^{D_s\phi}(0) &= 0.62 \pm 0.06, \\ A_2^{D_s\phi}(0) &= 1.0 \pm 0.3, \\ V^{D_s\phi}(0) &= 0.9 \pm 0.3, \\ x^{D_s\phi}(0) &= 1.6 \pm 0.4, \\ y^{D_s\phi}(0) &= 1.5 \pm 0.5, \end{aligned} \tag{4.30}$$

determined from semileptonic decays, $D_s^+ \longrightarrow \phi l^+ \nu_l$ [1], and extrapolated them with monopole forms to $q^2 = m_\rho^2$.

The results for the decay rate $\Gamma(D_s^+ \longrightarrow \rho\phi)$, the phase difference δ_{SD} and the ratios r_{SP}, r_{SD} are summarized in Table 4.2. For the entries in the last column of Table 4.2 we have used the experimental values Eq. (4.30) of the form factors.

First, we note from the Table 4.2 that all models, except the CDDGFN and the one where experimentally measured form factors are used, overestimate the decay

rate. This fact arises from an overestimate of the form factor A_1. Reference [16] has noted this fact and attributes it to the imposing of chiral symmetry. Further, as Ref. [17] has argued, more theoretical as well as experimental studies are needed for a better understanding of the q^2 dependence of form factors. Second, we observe that all the six sources of form factors allow a range for the longitudinal polarization which overlaps with experiment with a phase difference $\delta_{SD} \neq 0$. Note that the polarization is independent of the normalization of A_1. It is also found that most of the final state in the decay $D_s^+ \to \rho^+ \phi$ is in the S wave. If we consider the final state to get contribution only from S wave the decay rates would only be reduced by (5 to 12) %, while the polarization would be

$$P_L(S) = \frac{1}{3}. \tag{4.31}$$

It is also seen from the Table 4.2 that the hierarchy of the sizes of the partial wave amplitudes is :

$$| S | > | P | > | D |, \tag{4.32}$$

which is in accordance with intuitive expectations based on threshold arguments.

Calculations in Table 4.2 show that

$$\begin{aligned} r_{SP} &\simeq 4 \quad \longrightarrow \quad r_{SP}^{-1} \simeq 0.25, \\ r_{SD} &\simeq 10 \quad \longrightarrow \quad r_{SD}^{-1} \simeq 0.1. \end{aligned} \tag{4.33}$$

the decay rate is then Eq. (4.24)

$$\Gamma \equiv |S|^2 \{1 + 0.063 + 0.01\}. \tag{4.34}$$

Eq. (4.34) shows that contributions from P and D waves to the decay rate is about 7% which is in agreement with a dominantly S wave final state. However, for the polarization Eq. (4.25), we have

$$\begin{aligned} P_L &= \frac{1}{3} \frac{1 + 0.02 - 0.2\sqrt{2} \cos \delta_{SD}}{1 + 0.063 + 0.01}, \\ &= \frac{1}{3} \{0.951 - 0.264 \cos \delta_{SD}\}, \end{aligned} \tag{4.35}$$

taking the ratio of P_L in Eq. (4.35) with $P_L(S)$ of pure S wave final state, in Eq. (4.31) we obtain

$$\begin{aligned} \tau_P &= \frac{P_L}{P_L(S)}, \\ &= 0.951 - 0.264 \cos \delta_{SD}. \end{aligned} \tag{4.36}$$

The allowed range of τ_P is Eq. (4.36)

$$0.69 \leq \tau_P \leq 1.22. \tag{4.37}$$

Equation (4.37) shows that a small D wave component of one order of magnitude smaller than S could have a large effect, up to 30%, on the longitudinal polarization.

We observe from Table 4.2 that the errors in the phase difference δ_{SD} are large despite the fact that the errors in the polarization P_L are small. It is the S-wave dominance which makes an accurate determination of δ_{SD} difficult. As the polarization is sensitive to D waves, a more precise measurements of P_L is required for an accurate determination of phase difference δ_{SD}.

Table 4.1: Model predictions of $A_1^{D_s\phi}(0)$, $A_2^{D_s\phi}(0)$, $V^{D_s\phi}(0)$, $A_1^{D_s\phi}(m_\rho^2)$, $A_2^{D_s\phi}(m_\rho^2)$, and $V^{D_s\phi}(m_\rho^2)$ form factors and the ratios $x^{D_s\phi}(0)$, $y^{D_s\phi}(0)$, $x^{D_s\phi}(m_\rho^2)$, $y^{D_s\phi}(m_\rho^2)$ for the processes $D_s^+ \longrightarrow \rho^+\phi$. In the last column we use the experimentally measured form factors from the semi leptonic decays $D_s^+ \longrightarrow \phi l^+\nu_l$.

	BSWI	*BSWII*	*AW*	*CDDGFN*	*ISGW*	*Expt.FF*[1]
$A_1^{D_s\phi}(0)$	0.820	0.820	0.815	0.517	0.788	0.62 ± 0.06
$A_2^{D_s\phi}(0)$	1.076	1.076	0.506	0.419	0.696	1.0 ± 0.3
$V^{D_s\phi}(0)$	1.319	1.319	1.559	1.076	1.068	0.9 ± 0.3
$A_1^{D_s\phi}(m_\rho^2)$	0.903	0.903	0.898	0.570	0.951	0.68 ± 0.07
$A_2^{D_s\phi}(m_\rho^2)$	1.185	1.306	0.557	0.462	0.841	1.10 ± 0.33
$V^{D_s\phi}(m_\rho^2)$	1.521	1.753	1.798	1.495	1.290	1.04 ± 0.35
$x^{D_s\phi}(0)$	1.312	1.312	0.621	0.810	0.883	1.60 ± 0.24[18]
$y^{D_s\phi}(0)$	1.608	1.608	1.913	2.081	1.356	1.92 ± 0.32[18]
$x^{D_s\phi}(m_\rho^2)$	1.312	1.446	0.620	0.811	0.884	1.61 ± 0.51
$y^{D_s\phi}(m_\rho^2)$	1.684	1.941	2.002	2.623	1.356	1.52 ± 0.53

Table 4.2: Decay rate, Γ, phase difference $\delta_{SD} = \delta_S - \delta_D$ and the ratios $r_{SP} = \frac{|S|}{|P|}$, $r_{SD} = \frac{|S|}{|D|}$ for $D_s^+ \longrightarrow \rho^+\phi$ decay. The values of Γ must be multiplied by $10^{12}s^{-1}$. δ_{SD} is the value needed to get agreement with the experimental values, to one standard deviation, of the longitudinal polarization $P_L = 0.370 \pm 0.052$. The last column uses experimentally measured form factors (see Table 4.1). 'Expt.FF' stands for 'Experimental form factors'.

	BSWI	*BSWII*	*AW*	*CDDGFN*	*ISGW*	*Expt.FF*
Γ	0.32	0.32	0.35	0.15	0.37	0.18 ± 0.04[1]
δ°_{SD}	135 ± 45	138 ± 43	122 ± 32	140 ± 40	120 ± 35	134 ± 46
$\frac{\|S\|}{\|P\|}$	4.3	3.7	3.8	2.8	5.5	4.7
$\frac{\|S\|}{\|D\|}$	11.9	13.5	7.4	8.2	8.6	16.5

Experimental value of decay rate	$\Gamma = 0.14 \pm 0.05$ [1]
Experimental value of polarization	$P_L = 0.370 \pm 0.052$ [2]

Bibliography

[1] Particle Data Group, R. M. Barnett *et al.*, Phys. Rev. **D 54**, 1 (1996).

[2] CLEO collaboration, V. Balic (private comunication).

[3] M. Gourdin, A. N. Kamal, Y. Y. Keum, and X. Y. Pham, Phys. Lett. **B 339**, 173 (1994).

[4] CLEO Collaboration, P. Avery *et al.*, Phys. Rev. Lett. **68**, 1279 (1992).

[5] M. Bauer, B. Stech, and M. Wirbel, Z. Phys. **C 34**, 103, (1987); M. Wirbel, B. Stech, and M. Bauer, Z. Phys. **C 29**, 637 (1985); M. Buer and M. Wirbel, Z. Phys. **C 42**, 671 (1989).

[6] E-653 Collaboration, K.Kodama *et al.*, Phys. Lett. **B 309**, 483 (1993).

[7] E-687 Collaboration, P. L. Frabetti *et al.*, Phys. Lett. **B 328**, 187 (1994).

[8] A. N. Kamal and A. B. Santra, Z. Phys. **C 71**, 101 (1996).

[9] CLEO Collaboration, P. Avery *et al.*, Phys. Lett. **B 337**, 405 (1994).

[10] M.S.Witherell, in *Lepton Photon Interaction*, Proceeding of the XVI International Symposium, Ithaca, N.Y. 1993; edited by P. Drell and D. Rubin, AIP Conf. Proc. No. 302, (AIP, New York, 1994), p. 198.

[11] El hassan El aaoud, Phys. Rev. **D 58**, 037502 (1998).

[12] T. Altomari and L. Wolfenstein, Phys. Rev. **D 37**, 681 (1988).

[13] R. Casalbuoni, A. Deandrea, N. Di Bartolomeo, R. Gatto, F. Feruglio, and G. Nardulli, Phys. Lett. **B 299**, 139 (1993).

[14] J. D. Richman, in *ICHEP'96* Proceedings of the 28th International Conference on High Energy Physics, Warsaw, Poland, edited by Z. Ajduk and A. Wroblewski (World Scientefic, Singapore, 1997), hep-exp/9701014.

[15] N. Isgur, D. Scora, B. Grinstein, and M. Wise, Phys. Rev. **D 39**, 799 (1989).

[16] F. Buccella, M. Lusignoli, G. Miele, A. Pugliese, and P. Santorelli, Phys. Rev. **D 51**, 3478 (1995).

[17] R. Casalbuoni, A. Deandrea, N. Di Bartolomeo, R. Gatto, F. Feruglio, and G. Nardulli, Phys. Rep. **281**, 145 (1997), hep-ph/9605342.

[18] Particle Data Group, D. E. Groom *et al.*, Eur. Phys. J.**C 15**, 1 (2000).

Chapter 5

Helicity and partial wave amplitude analysis of $D \to K^*\rho$ decay

5.1 Introduction

The weak hadronic decay of the charm D meson to two resonant vector particles is difficult to analyze experimentally, as well as to understand theoretically. At the theoretical level much of the effort in the past was devoted to understanding mainly the decay rate $\Gamma(D \to V_1V_2)$ (V stands for vector meson). Studies based on the factorization model were carried out by Bauer *el al.* [1] and Kamal *et al.* [2]. Approaches based on flavor $SU(3)$ symmetry and broken $SU(3)$ symmetry were pursued also by Kamal *et al.* [2] and by Hinchliffe and Kaeding [3]. Bedaque *et al.* [4] have carried out a pole-dominance model calculation .

One peculiarity of a pseudoscalar meson, P, decaying into two vector mesons is that the final-state particles are produced in different correlated polarization states. The hadronic matrix element

$$A = \langle V_1V_2 \mid \mathcal{H} \mid P \rangle , \tag{5.1}$$

involves three invariant amplitudes which can be expressed in terms of three different, but equivalent, bases;

- the helicity basis $|++\rangle, |--\rangle, |00\rangle$,
- the partial-wave basis (or the LS-basis) $|S\rangle, |P\rangle, |D\rangle$
- the transversity basis $|0\rangle, |\,\|\rangle, |\,\perp\rangle$.

The interrelations between the amplitudes in these bases are presented in chapter 2 and Appendix B. The data [5] for $D \to K^*\rho$ decay are quoted either in terms of the helicity branching ratios or the partial-wave branching ratios. Hence our study of the process $D \to K^*\rho$ is carried out in these two bases. We have undertaken a theoretical analysis for the particular decay, $D \to K^*\rho$, assuming factorization approximation and using a variety of models for the form factors [6]. Such a study has not been undertaken in the past.

The experimental analysis of $D \to K^*\rho$, measurement of the branching ratio, partial-wave branching ratios, polarization etc. is done by considering the resonant substructure of the four-body decays $D \to K\pi\pi\pi$ [7, 8]. There are several two-body decay modes[1], for example:

$$\begin{aligned} D &\longrightarrow K^*\rho \longrightarrow K\pi\pi\pi, \\ D &\longrightarrow K_1(1270)\pi \longrightarrow K\pi\pi\pi, \\ D &\longrightarrow Ka_1(1260) \longrightarrow K\pi\pi\pi, \end{aligned} \tag{5.2}$$

which contribute to the final states in $D^0 \to \bar{K}^0\pi^-\pi^+\pi^0, D^+ \to K^-\pi^+\pi^+\pi^0, D^0 \to K^-\pi^+\pi^+\pi^-$. Following standard practice, Refs. [7, 8] took the signal terms of the probability density function to be a coherent sum of complex amplitudes for each decay chain leading to the four-body decays of D. Hence, the different contributing amplitudes can interfere among themselves. In general, the interference terms do not

[1] three-body modes can also contribute see Refs. [7, 8, 10]

integrate to zero (see [9] for more details about the three-body decay $D \to K\pi\pi$). Consequently, the sum of the fractions f_i does not add up to unity: $\sum f_i \neq 1$ (see Refs. [7, 9, 10]). The branching fractions into two-body channels are then determined by maximizing the likelihood function. The branching fraction into any particular two-body channel, such as $D \to K^*\rho$, can be analyzed in terms of the helicity amplitudes (A_{++}, A_{--}, A_{00}), or the partial-wave amplitudes (S, P, D), or the transversity amplitudes (A_0, $A_\parallel$, $A_\perp$). As a result of the completeness of each one of these bases, the decay rate $\Gamma(D \to K^*\rho)$ is expressed as an incoherent sum of the helicity, or the partial-wave, the transversity amplitudes [11, 12, 13]

$$\begin{aligned}
\Gamma(D \longrightarrow K^*\rho) &= \frac{|\mathbf{k}|}{8\pi m_D^2}\{|S|^2 + |P|^2 + |D|^2\}, \\
&= \frac{|\mathbf{k}|}{8\pi m_D^2}\{|A_{00}|^2 + |A_{++}|^2 + |A_{--}|^2\}, \\
&= \frac{|\mathbf{k}|}{8\pi m_D^2}\{|A_0|^2 + |A_\parallel|^2 + |A_\perp|^2\}. \qquad (5.3)
\end{aligned}$$

This imposes some constraints on the helicity and the partial-wave branching fractions, B, as they should add up to the total branching fraction for the mode $D \to K^*\rho$ as follows:

$$\begin{aligned}
B_{K^*\rho} &= \frac{\Gamma(D \longrightarrow K^*\rho)}{\Gamma(D \longrightarrow all)}, \\
&= B_S + B_P + B_D, \\
&= B_{++} + B_{--} + B_{00}, \\
&= B_0 + B_{-\parallel} + B_\perp. \qquad (5.4)
\end{aligned}$$

A similar situation occurs in $\bar{n}p$ annihilation to 3 (and 5) pions [14] where S and P waves are treated incoherently. Having said that, the data for the decay $D^0 \longrightarrow \bar{K}^{*0}\rho^0$ is [5]:

$$\begin{aligned}
B_{\bar{K}^{*0}\rho^0} &= 1.47 \pm 0.33\%, \\
B_S &= 2.8 \pm 0.6\%, \\
B_D &= 1.9 \pm 0.6\%,
\end{aligned}$$

$$B_{K^{*0}\rho^0_{\text{transverse}}} = 1.5 \pm 0.5\ \%. \tag{5.5}$$

An obvious problem with the $D^0 \to K^{*0}\rho^0$ data in Eq. (5.5) is that one of the constraints in Eq. (5.4) is violated: the sum of the branching fractions into S and D states exceeds the total branching fraction. The fact that this sum also exceeds the transverse branching fraction is, by itself, not a problem due to the interference between the S and D waves. However, the problem with the data [5] is that the transverse branching fraction saturates the total branching fraction. There is, therefore, an internal inconsistency in the data: all the data listings cannot be correct. The Particle Data Group listing of $D \to K^*\rho$ data has remained unchanged since 1992.

We believe that the source of the inconsistency in the data [5, 7, 8] has to do with the identification of the partial-wave amplitudes, S, P and D, with the Lorentz structures in the decay amplitude (see Table II and, especially, Eqns. (32) - (34) of [7]). The decay amplitude A for the process $P \to V_1V_2$ is expressed in terms of three independent Lorentz structures and their coefficients, represented in the notation of [15, 16] by a, b, c, and in the notation of [17] by the form factors $A_1(q^2), A_2(q^2)$ and $V(q^2)$. We discuss this point in detail in the next section, but suffice it to say here that in [7] the P-wave amplitude is identified with c of [15, 16] (or $V(q^2)$ of [17]), which is correct; however, they identify the S-wave amplitude with a of [15, 16] (or $A_1(q^2)$ of [17]) and D-wave amplitude with b of [15, 16] (or $A_2(q^2)$ of [17]), which is incorrect. We discuss this point in some detail in sections 5.3 and 5.4.

Part of the problem could also be that the transverse amplitudes A_{++}, A_{--} and the longitudinal amplitude A_{00} were fitted independently in [7]. Their argument for doing so was the large measured polarization of K^* in the semileptonic decay $D \longrightarrow K^*l\nu_l$ [18]. However, later measurements [19] of the polarization of K^* being much smaller vitiate this procedure.

5.2 Method

The decay $D \to K^*\rho$ is Cabibbo-favored and is induced by the effective weak Hamiltonian which can be reduced to the following color-favored (CF) and color-suppressed (CS) forms Eqns. (3.15), (4.8):

$$\mathcal{H}_{CF} = G'_F [a_1(\bar{u}d)(\bar{s}c) + C_2 O_8], \tag{5.6}$$

$$\mathcal{H}_{CS} = G'_F [a_2(\bar{u}c)(\bar{s}d) + C_1 \tilde{O}_8], \tag{5.7}$$

we use the following values for the parameters a_1 and a_2 [20]:

$$\begin{aligned} a_1 &= 1.26 \pm 0.04, \\ a_2 &= -0.51 \pm 0.05. \end{aligned} \tag{5.8}$$

In general a_1 and a_2 are related to the Wilson coefficients C_1 and C_2 by Eq. (3.13)

$$a_1 = C_1 + \frac{C_2}{N}, \qquad a_2 = C_2 + \frac{C_1}{N}, \tag{5.9}$$

where N is an effective number of colors, and $C_1 = 1.26$, $C_2 = -0.51$ [21]. Using a value of N different from 3 is a way to parameterize nonfactorization effects. Our parameterization amounts to setting $N \to \infty$. This particular decay, $D \to K^*\rho$, has also been studied by Kamal *et al.* [20] and by Cheng [22] from the viewpoint of explicit (rather than implicit as is done here) nonfactorization.

In the factorization approximation one neglects the contribution from O_8 and $\tilde{O}_8$, and the matrix element of the first term is written as a product of two current matrix elements. Since we are effectively working with $N \neq 3$, one could argue that the nonfactorization arising from O_8 and $\tilde{O}_8$ is being included. We consider the following three decays:

1. $D^0 \longrightarrow K^{-*}\rho^+$, a color-favored decay which gets contribution from external W-exchange, known as a class I process (Fig. 5.1.a).

2. $D^0 \to \bar{K}^{0*}\rho^0$, a color-suppressed process which gets contribution from internal W - exchange, known as a class II process (Fig. 5.1.b).

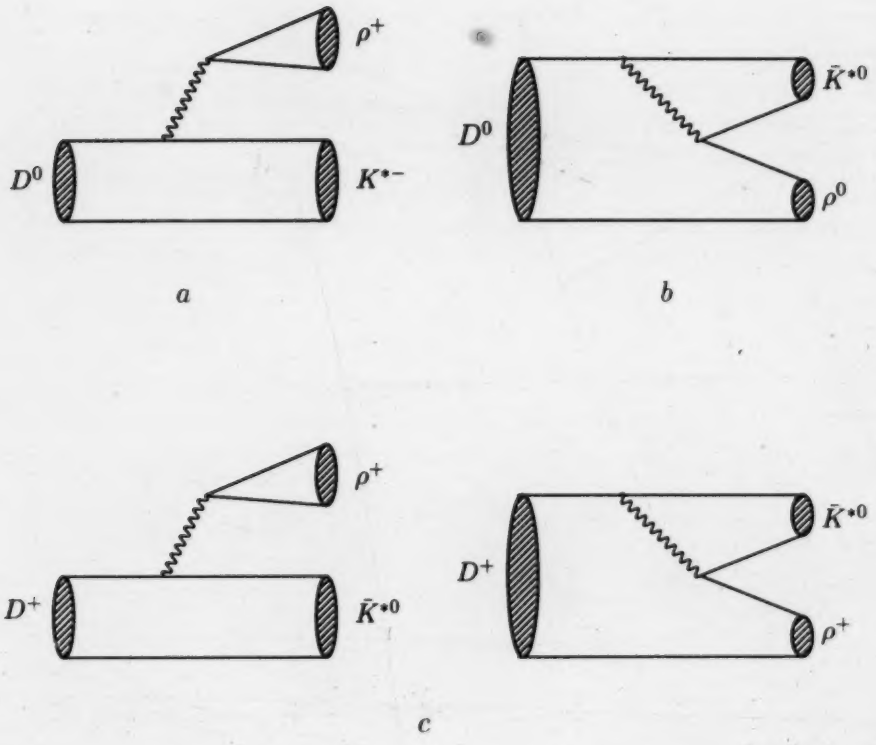

Figure 5.1: Quark diagrams contributing to $D \to K^*\rho$: a) class I or color favored tree diagram contributing to $D^0 \longrightarrow K^{-*}\rho^+$, b) class II or color suppressed tree diagram contributing to $D^0 \to \bar{K}^{0*}\rho^0$, c) class III diagram contributing to $D^+ \to \bar{K}^{0*}\rho^+$.

3. $D^+ \to \bar{K}^{0*}\rho^+$, a class III process which gets contribution from external as well as internal W-exchange mechanisms (Fig. 5.1.c).

In the factorization approximation the decay amplitudes are given by

$$\begin{aligned}
A(D^0 \to K^{-*}\rho^+) &= G'_F a_1 \langle \rho^+ \mid \bar{u}d \mid 0\rangle \langle K^{-*} \mid \bar{s}c \mid D^0\rangle. \\
A(D^0 \to \bar{K}^{0*}\rho^0) &= G'_F \frac{a_2}{\sqrt{2}} \langle \bar{K}^{0*} \mid \bar{s}d \mid 0\rangle \langle \rho^0 \mid \bar{u}c \mid D^0\rangle. \\
A(D^+ \to \bar{K}^{0*}\rho^+) &= G'_F \Big\{ a_1 \langle \rho \mid \bar{u}d \mid 0\rangle \langle \bar{K}^{*0} \mid \bar{s}c \mid D^+\rangle \\
&\quad + a_2 \langle \bar{K}^{0*} \mid \bar{s}d \mid 0\rangle \langle \rho^+ \mid \bar{u}c \mid D^+\rangle \Big\}, \\
&= A(D^0 \to K^{-*}\rho^+) + \sqrt{2} A(D^0 \to \bar{K}^{0*}\rho^0). \qquad (5.10)
\end{aligned}$$

The extra $\sqrt{2}$ in Eq. (5.10) comes from the flavor part of the wave function of ρ^0. Each of the current matrix elements can be expressed in terms of meson decay constants and invariant form factors as explained below.

The decay rate given by an incoherent sum of decay amplitudes Eq. (5.3), is independent of the partial-wave phases. However, the polarization does depend on the phase difference, $\delta_{SD} = \delta_S - \delta_D$, arising from the interference between S- and D-waves,

$$P_L = \frac{1}{3} \frac{\mid S \mid^2 + 2 \mid D \mid^2 - 2\sqrt{2} \mid S \mid\mid D \mid \cos\delta_{SD}}{\mid S \mid^2 + \mid P \mid^2 + \mid D \mid^2}. \qquad (5.11)$$

5.2.1 $D^0 \longrightarrow K^{*-}\rho^+$

To calculate the amplitude $A(D^0 \to K^{-*}\rho^+)$ given in Eq. (5.10) we use the following results from Eqns. (3.40), (3.42) and (3.43):

$$\begin{aligned}
\langle \rho^+ \mid \bar{u}d \mid 0\rangle &= m_\rho f_\rho \varepsilon^*_\mu \\
\langle K^{*-} \mid \bar{s}c \mid D\rangle &= \frac{2}{m_D + m_{K^*}} \epsilon_{\mu\nu\rho\sigma} \varepsilon^{*\nu}_{K^*} k_D^\rho k_{K^*}^\sigma V(q^2) + i\{\varepsilon^*_{K^*\mu}(m_D + m_{K^*}) A_1(q^2) \\
&\quad - \frac{\varepsilon^*_{K^*}\cdot q}{m_D + m_{K^*}} (k_{K^*} + k_D)_\mu A_2(q^2) - \frac{\varepsilon^*_{K^*}\cdot q}{q^2} 2\, m_{K^*} q_\mu A_3(q^2) \\
&\quad + \frac{\varepsilon^*_{K^*}\cdot q}{q^2} 2\, m_{K^*} q_\mu A_0(q^2)\},
\end{aligned} \qquad (5.12)$$

where

$$q = k_D - k_{K^*} \tag{5.13}$$

is the momentum transfer, f_ρ is the decay constant of the vector meson ρ, ε_{K^*} and ε_ρ are polarization vector, $A_i(q^2), (i = 1, 2, 3)$ and $V(q^2)$ are invariant weak transition $D \longrightarrow K^*$ form factors defined in [17].

The longitudinal, A_{00}, and the two transverse, A_{++}, A_{--}, helicity amplitudes are given by Eqns. (3.77) and (3.81):

$$\begin{aligned} A_{00}(D^0 \to K^{-*}\rho^+) &= -i\,G'_F\, m_\rho\, f_\rho\, (m_D + m_{K^{-*}})a_1 \left\{\alpha_1\, A_1^{DK^*}(m_\rho^2)\right. \\ &\quad \left. - \beta_1\, A_2^{DK^*}(m_\rho^2)\right\} \qquad (5.14) \\ A_{\pm\pm}(D^0 \to K^{*-}\rho^+) &= i\,G'_F\, m_\rho\, f_\rho\, (m_D + m_{K^{*-}})a_1 \left\{A_1^{DK^*}(m_\rho^2)\right. \\ &\quad \left. \mp \gamma_1\, V^{DK^*}(m_\rho^2)\right\}, \qquad (5.15) \end{aligned}$$

where α_1, β_1, γ_1 and $\mathcal{K}_1$ are function of r and t and given by

$$\begin{aligned} \alpha_1 &= \frac{1 - r^2 - t^2}{2rt}, \\ \beta_1 &= \frac{\mathcal{K}_1^2}{2rt(1+r)^2}, \\ \gamma_1 &= \frac{\mathcal{K}_1}{(1+r)^2}, \\ \mathcal{K}_1^2 &= (1 + r^4 + t^4 - 2r^2 - 2t^2 - 2r^2t^2), \qquad (5.16) \end{aligned}$$

with

$$r = \frac{m_{K^*}}{m_D}, \quad t = \frac{m_\rho}{m_D}. \tag{5.17}$$

Equivalently one can work with the partial wave amplitudes which are related to the helicity amplitudes by Eq. (3.82). Using Eqns. (5.14), (5.15) in Eq. (3.83) we obtain the partial wave amplitudes S_1, P_1, and D_1 for the decay $D^0 \to K^{-*}\rho^+$ in term of form factors

$$S_1 = i\,G'_F\, a_1\, m_\rho\, f_\rho (m_D + m_{K^*}) \frac{1}{\sqrt{3}} \left[\frac{(1 - r^2 + 4rt - t^2)}{2rt}\, A_1^{DK^*}(m_\rho^2)\right.$$

$$
\begin{aligned}
& - \frac{4|\mathbf{k}|^2/m_D^2}{2rt(1+r)^2} A_2^{DK^*}(m_\rho^2)\Big], \\
P_1 &= -i\,G_F'\,a_1\,m_\rho\,f_\rho\,(m_D + m_{K^*})\,\sqrt{2}\,\frac{2|\mathbf{k}|/m_D}{(1+r)^2}\,V^{DK^*}(m_\rho^2), \\
D_1 &= i\,G_F'\,a_1\,m_\rho\,f_\rho\,(m_D + m_{K^*})\sqrt{\frac{2}{3}}\Big[\frac{(t+r)^2-1)}{2rt} A_1^{DK^*}(m_\rho^2) \\
& + \frac{4|\mathbf{k}|^2/m_D^2}{2rt(1+r)^2} A_2^{DK^*}(m_\rho^2)\Big], \qquad (5.18)
\end{aligned}
$$

In the following we drop a common factor of

$$
\begin{aligned}
\mathcal{F}_1 &= iG_F' m_\rho f_\rho (m_D + m_{K^{-*}}) a_1, \\
&= i\,G_F'\,\mathcal{F}_\rho\,a_1, \qquad (5.19)
\end{aligned}
$$

the partial wave amplitude are then

$$
\begin{aligned}
S_1 &= \frac{1}{\sqrt{3}}\Big\{(2+\alpha_1)A_1^{DK^*}(m_\rho^2) - \beta_1 A_2^{DK^*}(m_\rho^2)\Big\}, \\
P_1 &= -\sqrt{2}\,\gamma_1\,V^{DK^*}(m_\rho^2), \\
D_1 &= \sqrt{\frac{2}{3}}\Big\{(1-\alpha_1)A_1^{DK^*}(m_\rho^2) + \beta_1 A_2^{DK^*}(m_\rho^2)\Big\} \qquad (5.20)
\end{aligned}
$$

These real amplitudes are assumed to be the magnitudes of the partial wave amplitudes. The phases are then fed in by hand. For $D \to K^{*-}\rho^+$ the values of the parameters α_1, β_1 and γ_1 are

$$
\begin{aligned}
t &= 0.411, \quad r = 0.479, \quad \mathcal{K}_1 = 0.454, \\
\alpha_1 &= 1.525, \quad \beta_1 = 0.239, \quad \gamma_1 = 0.207. \qquad (5.21)
\end{aligned}
$$

Then, the partial waves amplitudes S_1, P_1, D_1 are

$$
\begin{aligned}
S_1 &= \frac{1}{\sqrt{3}}\Big\{3.525\,A_1^{DK^*}(m_\rho^2) - 0.239\,A_2^{DK^*}(m_\rho^2)\Big\}, \\
P_1 &= -0.207\,\sqrt{2}\,V^{DK^*}(m_\rho^2), \\
D_1 &= \sqrt{\frac{2}{3}}\Big\{-0.525\,A_1^{DK^*}(m_\rho^2) + 0.239\,A_2^{DK^*}(m_\rho^2)\Big\}, \qquad (5.22)
\end{aligned}
$$

and the ratios r_{SP} and r_{SD}

$$\begin{aligned} r_{SP} &= \frac{1}{\sqrt{6}} \frac{|\, 3.525\, A_1^{DK^*}(m_\rho^2) - 0.239\, A_2^{DK^*}(m_\rho^2)\,|}{|\, 0.207\, V^{DK^*}(m_\rho^2)\,|}, \\ &= \frac{1}{\sqrt{6}} \frac{|\, 3.525\, - 0.239\, x^{DK^*}(m_\rho^2)\,|}{|\, 0.207\, y^{DK^*}(m_\rho^2)\,|}, \\ r_{SD} &= \frac{1}{\sqrt{2}} \frac{|\, 3.525\, A_1^{DK^*}(m_\rho^2) - 0.239\, A_2^{DK^*}(m_\rho^2)\,|}{|\, -0.525\, A_1^{DK^*}(m_\rho^2) + 0.239\, A_2^{DK^*}(m_\rho^2)\,|}, \\ &= \frac{1}{\sqrt{2}} \frac{|\, 3.525\, - 0.239\, x^{DK^*}(m_\rho^2)\,|}{|\, -0.525\, + 0.239\, x^{DK^*}(m_\rho^2)\,|}. \end{aligned} \tag{5.23}$$

5.2.2 $D^0 \longrightarrow \bar{K}^{*0}\rho^0$

The amplitude for this decay is given by Eq. (5.10), the matrix element needed are

$$\langle K^* \mid \bar{u}d \mid 0\rangle = m_{K^*} f_{K^*} \varepsilon_\mu^* \tag{5.24}$$

$$\begin{aligned} \langle \rho^0 \mid \bar{s}c \mid D\rangle &= \frac{2}{m_D + m_\rho} \epsilon_{\mu\nu\rho\sigma} \varepsilon_\rho^{*\nu} k_D^\rho k_\rho^\sigma V^{D\rho}(q^2) + i\{\varepsilon_{\rho\mu}^*(m_D + m_\rho) A_1^{D\rho}(q^2) \\ &\quad - \frac{\varepsilon_\rho^* . q}{m_D + m_\rho}(k_\rho + k_D)_\mu A_2^{D\rho}(q^2) - \frac{\varepsilon_\rho^* . q}{q^2} 2\, m_\rho q_\mu A_3^{D\rho}(q^2) \\ &\quad + \frac{\varepsilon_\rho^* . q}{q^2} 2\, m_\rho q_\mu A_0^{D\rho}(q^2)\}, \end{aligned} \tag{5.25}$$

The calculation is the same as in the previous decay with the following changes: the parameter a_1 is replaced by a_2 and the the vector mesons ρ and K^* are interchanged. Hence the partial wave amplitudes are.

$$\begin{aligned} S_2 &= i G_F' \frac{a_2}{\sqrt{2}} m_{K^*} f_{K^*} (m_D + m_\rho) \frac{1}{\sqrt{3}} \left[\frac{(1 - r^2 + 4rt - t^2)}{2rt} A_1^{D\rho}(m_{K^*}^2) \right. \\ &\quad \left. - \frac{4|\mathbf{k}|^2/m_D^2}{2rt(1+r)^2} A_2^{D\rho}(m_{K^*}^2) \right], \\ P_2 &= -i G_F' \frac{a_2}{\sqrt{2}} m_{K^*} f_{K^*} (m_D + m_\rho) \sqrt{2} \frac{2|\mathbf{k}|/m_D}{(1+r)^2} V^{D\rho}(m_\rho^2), \\ D_2 &= i G_F' \frac{a_2}{\sqrt{2}} m_{K^*} f_{K^*} (m_D + m_\rho) \sqrt{\frac{2}{3}} \left[\frac{(t+r)^2 - 1)}{2rt} A_1^{D\rho}(m_{K^*}^2) \right. \\ &\quad \left. + \frac{4|\mathbf{k}|^2/m_D^2}{2rt(1+r)^2} A_2^{D\rho}(m_{K^*}^2) \right], \end{aligned} \tag{5.26}$$

In the following we drop a common factor of

$$\begin{aligned} \mathcal{F}_2 &= iG'_F m_{K^*} f_{K^*}(m_D + m_\rho)\frac{a_2}{\sqrt{2}}, \\ &= i\,G'_F\,\mathcal{F}_{K^*}\,\frac{a_2}{\sqrt{2}} \end{aligned} \tag{5.27}$$

$$\begin{aligned} S_2 &= \frac{1}{\sqrt{3}}\left\{(2+\alpha_2)A_1^{D\rho}(m_{K^*}^2) - \beta_2 A_2^{D\rho}(m_{K^*}^2)\right\}, \\ P_2 &= -\sqrt{2}\,\gamma_2\,V^{D\rho}(m_{K^*}^2), \\ D_2 &= \sqrt{\frac{2}{3}}\left\{(1-\alpha_2)A_1^{D\rho}(m_{K^*}^2) + \beta_2 A_2^{D\rho}(m_{K^*}^2)\right\} \end{aligned} \tag{5.28}$$

For $D \to \bar{K}^{*0}\rho^0$ the values of the parameters α_2, β_2 and γ_2 are

$$\begin{aligned} t &= 0.479, \quad r = 0.411, \quad \mathcal{K}_2 = 0.454, \\ \alpha_2 &= 1.525, \quad \beta_2 = 0.263, \quad \gamma_2 = 0.228. \end{aligned} \tag{5.29}$$

then, the partial waves amplitudes S_2, P_2, D_2 are

$$\begin{aligned} S_2 &= \frac{1}{\sqrt{3}}\left\{3.525\,A_1^{D\rho}(m_{K^*}^2) - 0.263\,A_2^{D\rho}(m_{K^*}^2)\right\}, \\ P_2 &= -0.228\sqrt{2}\,V^{D\rho}(m_{K^*}^2), \\ D_2 &= \sqrt{\frac{2}{3}}\left\{-0.525\,A_1^{D\rho}(m_{K^*}^2) + 0.263\,A_2^{D\rho}(m_{K^*}^2)\right\}, \end{aligned} \tag{5.30}$$

and the ratios r_{SP} and r_{SD}

$$\begin{aligned} r_{SP} &= \frac{1}{\sqrt{6}}\frac{|\,3.525\,A_1^{D\rho}(m_{K^*}^2) - 0.263\,A_2^{D\rho}(m_{K^*}^2)\,|}{|\,0.228\,V^{D\rho}(m_{K^*}^2)\,|}, \\ &= \frac{1}{\sqrt{6}}\frac{|\,3.525 - 0.263\,x^{D\rho}(m_{K^*}^2)\,|}{|\,0.228\,y^{D\rho}(m_{K^*}^2)\,|}, \\ r_{SD} &= \frac{1}{\sqrt{2}}\frac{|\,3.525\,A_1^{D\rho}(m_{K^*}^2) - 0.263\,A_2^{D\rho}(m_{K^*}^2)\,|}{|\,-0.525\,A_1^{D\rho}(m_{K^*}^2) + 0.263\,A_2^{D\rho}(m_{K^*}^2)\,|}, \\ &= \frac{1}{\sqrt{2}}\frac{|\,3.525 - 0.263\,x^{D\rho}(m_{K^*}^2)\,|}{|\,-0.525 + 0.263\,x^{D\rho}(m_{K^*}^2)\,|}. \end{aligned} \tag{5.31}$$

5.2.3 $D^+ \longrightarrow \bar{K}^{*0}\rho^+$

Using equation (5.10) with equations (5.18), (5.26) we obtain for the partial wave amplitudes for the decay $D^+ \longrightarrow \bar{K}^{*0}\rho^+$

$$\begin{aligned}
S_3 &= S_1 + \sqrt{2}S_2, \\
&= i\frac{G'_F}{\sqrt{3}}\left[\mathcal{F}_\rho a_1\{(2+\alpha_1)A_1^{DK^*} - \beta_1 A_2^{DK^*}\}\right. \\
&\quad \left. + \mathcal{F}_{K^*} a_2\{(2+\alpha_2)A_1^{D\rho} - \beta_2 A_2^{D\rho}\}\right], \\
P_3 &= P_1 + \sqrt{2}P_2, \\
&= -i G'_F \sqrt{2}\left[\mathcal{F}_\rho a_1 \gamma_1 V^{DK^*} + \mathcal{F}_{K^*} a_2 \gamma_2 V^{D\rho}\right], \\
D_3 &= D_1 + \sqrt{2}D_2, \\
&= i G'_F \sqrt{\frac{2}{3}}\left[\mathcal{F}_\rho a_1\{(1-\alpha_1)A_1^{DK^*} + \beta_1 A_2^{DK^*}\}\right. \\
&\quad \left. + \mathcal{F}_{K^*} a_2\{(1-\alpha_2)A_1^{D\rho} + \beta_2 A_2^{D\rho}\}\right]. \qquad (5.32)
\end{aligned}$$

The knowledge of the different form factors is required to proceed further with the numerical estimate of the decay rate, Γ, and the longitudinal polarization P_L. Since it is not yet possible to obtain the q^2 dependence of these form factors from experimental data, and a rigorous theoretical calculation is still lacking, we have relied on several theoretical models for the form factors in our analysis. They are the following: i) Bauer, Stech, and Wirbel (BSWI) [17], where an infinite momentum frame is used to calculate the form factors at $q^2 = 0$, and a monopole form (pole masses are as in [17]) for q^2 dependence is assumed to extrapolate all the form factors to the desired value of q^2, ii) BSWII [21] is a modification of BSWI, where while $F_0(q^2)$ and $A_1(q^2)$ are the same as in BSWI, a dipole q^2 dependence is assumed for $A_2(q^2)$ and $V(q^2)$, iii) Altomari and Wolfenstein (AW) model [24], where the form factors are evaluated in the limit of zero recoil, and a monopole form is used to extrapolate to the desired value of q^2, iv) Casalbuoni, Deandrea, Di Bartolomeo, Feruglio, Gatto, and Nardulli (CDDGFN) model [25], where the form factors are evaluated at $q^2 = 0$ in an effective Lagrangian satisfying heavy quark spin-flavor symmetry in which light vector particles

are introduced as gauge particles in a broken chiral symmetry. A monopole form is used for the q^2 dependence. The experimental inputs for this model are from the semileptonic decay $D \to K^* l\nu$, and we have used the recent experimental values [26] of the form factors and the decay constant f_D [27]

$$\begin{aligned} A_1^{DK^*}(0) &= 0.55 \pm 0.03, \\ A_2^{DK^*}(0) &= 0.40 \pm 0.08, \\ V^{DK^*}(0) &= 1.0 \pm 0.2, \\ f_D &= 194^{+14}_{-10} \pm 10 MeV, \end{aligned} \tag{5.33}$$

in calculating the weak coupling constants of the model at $q^2 = 0$ [25], which are subsequently used in evaluating the required form factors. v) Isgur, Scora, Grinstein, and Wise (ISGW) model [28], where a non-relativistic quark model is used to calculate the form factors at zero recoil and an exponential q^2 dependence, based on a potential-model calculation of the meson wave function, is used to extrapolate them to the desired q^2. vi) Bajc, Fajfer and Oakes (BFO) model [29], where the form factors $A_1(q^2)$ and $A_2(q^2)$ are assumed to be flat, and a monopole behavior is assumed for $V(q^2)$; and finally (vii), a parameterization that uses experimental values (Exp.F) [26] of the form factors at $q^2 = 0$ and extrapolates them using monopole forms.

5.3 Results

5.3.1 Parameters

For the numerical calculations we use the following values for the CKM matrix elements and meson decay constants:

$$\begin{aligned} \cos\theta_c &\simeq V_{cs} \simeq V_{ud} = 0.975, \\ f_\rho &= 0.212 \text{ GeV}, \qquad f_{K^*} = 0.221 \text{ GeV} \end{aligned} \tag{5.34}$$

In Table 5.1 we present the predicted values of the form factors in the different models as well as their experimental values [30]. One observes that while the model predictions for the form factors $A_1(q^2)$ and $V(q^2)$ are in the range $(0.6 - 1)$ and $(0.8 - 1.6)$, respectively, the model-dependence of $A_2(q^2)$ shows a spread over a larger range: $(0.4 - 3.7)$. A striking feature of the BFO model [29] is the large value of the form factor A_2, which is incompatible with its experimental determination.

5.3.2 $D^0 \to K^{*-}\rho^+$

We calculate the experimental value of polarization from the listing of Ref. [5]:

$$\begin{aligned} P_L &= \frac{\Gamma(D^0 \longrightarrow \rho^+ \bar{K}^{*-}_{longitudinal})}{\Gamma(D^0 \longrightarrow \rho^+ \bar{K}^{*-})} \\ &= \frac{2.9 \pm 1.2}{6.1 \pm 2.4} \\ &= 0.475 \pm 0.271. \end{aligned} \tag{5.35}$$

In Table 5.2 we have summarized the results for the decay rates Γ, longitudinal polarization P_L, and partial-wave ratios $\frac{|S|}{|P|}$ and $\frac{|S|}{|D|}$ in different models.

We note from Table 5.2 that the models CDDGFN, BFO, and the scheme that uses experimentally measured form factors, predict a decay rate within a standard deviation of the central measured value. All other models overestimate the rate by several standard deviations. As for the longitudinal polarization, given the freedom of the unknown $\cos\delta_{SD}$, all models are able to fit the data. In particular, all models except BFO are able to predict the polarization correctly for $\delta_{SD} = 0$; in the BFO model for $\delta_{SD} = 0$, $D^0 \to K^{*-}\rho^+$ becomes totally transversely polarized. This circumstance arises from the fact that BFO model predicts a large D-wave contribution, $\frac{|S|}{|D|} \approx \sqrt{2}$. It then becomes evident from Eq. (3.82) that A_{00} vanishes. All models except BFO also display the partial-wave-amplitude hierarchy: $\mid S \mid > \mid P \mid > \mid D \mid$; BFO model on the other hand predicts $\mid S \mid > \mid D \mid > \mid P \mid$, which we believe is less likely. The reasoning goes as follows: For decays close to threshold, one anticipates the L^{th} partial-wave amplitude to behave like $(\mid \mathbf{k} \mid /\Lambda)^L$, where $\mid \mathbf{k} \mid$ is the center of

Table 5.1: Model and experimental predictions for the form factors: $A_1^{DK^*}(q^2)$, $A_2^{DK^*}(q^2), V^{DK^*}(q^2), A_1^{D\rho}(q^2), A_2^{D\rho}(q^2), V^{D\rho}(q^2)$ and the ratios $x^{DK^*}(q^2)$, $y^{DK^*}(q^2)$, $x^{D\rho}(q^2)$, $y^{D\rho}(q^2)$ at $q^2 = m_{K^*}^2, m_\rho^2, 0$ for the process $D \longrightarrow K^*\rho$

	BSWI	*BSWII*	*AW*	*CDDGF*	*ISGW*	BFO	Exp.F [30]
$A_1^{DK^*}(0)$	0.880	0.880	0.805	0.550	0.799	0.578	0.55 ± 0.03
$A_2^{DK^*}(0)$	1.147	1.147	0.642	0.40	0.816	3.747	0.40 ± 0.08
$V^{DK^*}(0)$	1.226	1.226	1.390	1.0	1.1	0.669	1.0 ± 0.2
$x^{DK^*}(0)$	1.30	1.30	0.80	0.73	1.02	6.5	0.73 [32]
$y^{DK^*}(0)$	1.39	1.39	1.73	1.82	1.38	1.16	1.87 [32]
$A_1^{DK^*}(m_\rho^2)$	0.969	0.969	0.887	0.606	0.909	0.578	0.606
$A_2^{DK^*}(m_\rho^2)$	1.264	1.392	0.707	0.441	0.929	3.747	0.441
$V^{DK^*}(m_\rho^2)$	1.414	1.630	1.602	1.153	1.25	0.773	1.153
$x^{DK^*}(m_\rho^2)$	1.30	1.44	0.80	0.73	1.02	6.5	0.73
$y^{DK^*}(m_\rho^2)$	1.45	1.68	1.81	1.90	1.38	1.34	1.90
$A_1^{D\rho}(0)$	0.775	0.775	0.721	0.631	0.595	0.605	0.55 ± 0.03
$A_2^{D\rho}(0)$	0.923	0.923	0.730	0.420	0.744	3.574	0.40 ± 0.08
$V^{D\rho}(0)$	1.225	1.225	1.076	1.063	1.1	0.588	1.0 ± 0.2
$A_1^{D\rho}(m_{K^*}^2)$	0.898	0.898	0.835	0.732	0.766	0.605	0.637
$A_2^{D\rho}(m_{K^*}^2)$	1.070	1.240	0.846	0.487	0.958	3.574	0.464
$V^{D\rho}(m_{K^*}^2)$	1.529	1.908	1.343	1.326	1.41	0.713	1.248

mass momentum and Λ a mass scale. For $|\mathbf{k}| \sim 0.4$ GeV and $\Lambda \sim m_D$, one expects the hierarchy $|S| > |P| > |D|$.

5.3.3 $D^+ \to \bar{K}^{*0}\rho^+$

In contrast to the decay mode $D^0 \to \bar{K}^{*-}\rho^+$, here the data listing [5] is at best confusing. First, since the longitudinal and/or transverse branching ratios are not listed, it is not possible to calculate the longitudinal polarization. Second, though in Refs. [7, 10] the identification of the transversity amplitudes (A_T, A_L and $A_{l=1}$ in the notation of Ref. [7]) in terms of the partial-wave amplitudes is correct (see Eqns. (20) - (26) of Ref. [7]), their identification of the partial-wave amplitudes S and D in terms of the Lorentz structure of the decay amplitude is incorrect. In Table II, and more succinctly in Eqns. (32) and (34) of Ref. [7], the S-wave amplitude is identified with the Lorentz structure that goes with the form factor A_1, and the D-wave amplitude with that of A_2. In fact, the correct identification of the S- and D-wave amplitudes given in Eqns. (5.20), (5.28) shows that they are both linear superpositions of A_1 and A_2.

With the caveat that the identification of the partial waves in Refs. [7, 10] is incorrect (note also that the listing of Ref. [5] uses these references only), we take the S-, P-, and D-wave branching ratios at their face value and calculate the 'experimental' ratios $\frac{|S|}{|P|}$ and $\frac{|S|}{|D|}$.

In Table 5.3, we have shown the calculated decay rate, the longitudinal polarization and the ratios of the partial-wave amplitudes in different models and compared them with the data. The BFO [29] model is the only one that reproduces the total rate correctly. This model also generates a large D-wave amplitude, with the partial-wave hierarchy $|S| > |D| > |P|$. This feature of the BFO model is due to the exceptionally large value of the form factor A_2, which is in contradiction with the experimental determination of the form factor as shown in Table 5.1.

5.3.4 $D^0 \to \bar{K}^{*0}\rho^0$

Reference [5] lists the branching ratio, and the transverse branching ratio. This enables us to calculate the longitudinal polarization from

$$\begin{aligned} P_L &= 1 - P_T, \\ &= 1 - \frac{B(D^0 \to \bar{K}^{*0}\rho^0_{transverse})}{B(D^0 \to \bar{K}^{*0}\rho^0)} \\ &= 0.0 \pm \begin{smallmatrix} 0.4 \\ 0.0 \end{smallmatrix} \end{aligned} \tag{5.36}$$

Reference [5] also lists the S- and D-wave branching ratios. However, our criticism of these numbers in the previous subsection applies also to $D^0 \to \bar{K}^{*0}\rho^0$ decay. With this caution, we have taken their [5] numbers at face value and calculated the experimental and theoretical ratios of the partial wave amplitudes and listed them in Table 5.4.

We note from Table 5.4 that the rate in the BFO model is too low by three standard deviations; the rates predicted in BSWI and BSWII models are 1.5 standard deviations too high, while all other models fit the rate within one standard deviation. As for the longitudinal polarization, all models predict a value consistent with the data. All models also satisfy the $\frac{|S|}{|P|}$ bound, but only the BFO model fits the $\frac{|S|}{|D|}$ ratio. This is because the BFO model generates a large D-wave amplitude.

A final comment: The inconsistency of the data is evident in the listing [5] of the total branching ratio and the individual partial-wave branching ratios. We know that the total branching ratio is an incoherent sum of the individual branching ratios in S, P, and D waves. Yet, in the Particle Data Group listing [5], the sum of S- and D-wave branching ratios exceeds the total. This by itself should cast doubt on the veracity of the data.

5.4 S-wave and $A_1(q^2)$ dominance

Since S-wave and D-wave amplitudes are linear superpositions of the form factors A_1 and A_2, see Eqns. (5.20), (5.28), the concept of S wave dominance is different from

that of A_1 dominance. All the models we have discussed, with the exception of the BFO model [29], predict that S-wave amplitude is the dominant amplitude. Further, since Ref. [7] identifies $S \sim A_1$ and $D \sim A_2$, we need to look at what is meant by S wave dominance and contrast it with A_1 dominance.

Consider first the concept of S-wave dominance. We see from Eqns. (5.3), (3.82) that in this approximation,

$$\Gamma \propto | S |^2, \tag{5.37}$$

and

$$\begin{aligned} | A_{00} | &= | A_{++} | \\ &= | A_{--} | \\ &= \frac{| S |}{\sqrt{3}}. \end{aligned} \tag{5.38}$$

In practice, most of the models predict the S-wave amplitude to be roughly an order of magnitude larger than the D-wave amplitude. Consequently, D wave would contribute only 1% to the rate relative to the S wave. However, it could influence the longitudinal polarization considerably through its interference with the S wave. Depending on the value of δ_{SD} the interference term could amount to a 30% correction to P_L Sec. 4.3 (see also Ref. [31]). However, regardless of the exact size of the D-wave amplitude, S-wave dominance would lead to:

$$P_L \rightarrow \frac{1}{3}, \quad \text{for} \quad \delta_{SD} = \frac{\pi}{2}. \tag{5.39}$$

Consider now the concept of A_1 dominance. From Eqns. (5.14) and (5.15), we see that:

$$\begin{aligned} A_{00} &\propto \alpha A_1, \text{ and} \\ A_{++} &= A_{--}, \\ &\propto A_1. \end{aligned} \tag{5.40}$$

With $\alpha = 1.52$, the longitudinal helicity amplitude is the largest, and the longitudinal polarization becomes

$$P_L = \frac{\alpha^2}{2+\alpha^2} = 0.54, \tag{5.41}$$

in contrast to a value 1/3 (with an error from $S-D$ interference) for S-wave dominance. Further, from Eqns. (5.20), (5.28), we note that in A_1 dominance,

$$\begin{aligned} S &\propto \frac{2+\alpha}{\sqrt{3}} A_1(q^2), \\ D &\propto \sqrt{\frac{2}{3}}(1-\alpha) A_1(q^2), \end{aligned} \tag{5.42}$$

which makes the S-wave amplitude five times larger than the D-wave amplitude — not quite what one would term "S-wave dominance."

5.5 Conclusion

We have carried out an analysis of the process $D \to K^*\rho$ in terms of the helicity, and partial-wave amplitudes. We used several models for the form factors, as well as their experimental values, when available, from semileptonic decays. A general feature of our calculation is that all the models, with the exception of the BFO model [29], are consistent with the expected threshold behavior $|S| > |P| > |D|$. The *BFO* model, on the other hand, gives $|S| > |D| > |P|$. Even though in most models the D-wave amplitude is almost an order of magnitude smaller than the S-wave amplitude, it could affect the polarization prediction significantly through $S-D$ interference.

As we see from Table 5.2, models BSWI, BSWII, AW, and ISGW grossly overestimate the rate for $D^0 \to K^{*-}\rho^+$, while models CDD, BFO, and the model that uses experimental form factor input, more or less agree with the measured rate. For this decay mode, we trust the measurement of the longitudinal branching ratio as the identification of the transversity amplitudes in Ref. [7] is correct. Due to the large error in P_L, and the uncertainty arising from the $S-D$ interference, all models are consistent with the polarization measurement.

For the decay mode $D^+ \to \bar{K}^{*0}\rho^+$, all the models, with the exception of the BFO model [29], grossly overestimate the rate. Before one gets the impression that the BFO model does well, we would like to point out that its prediction for the form factor A_2 is in sharp disagreement with the measurements from the semileptonic decays. There are no direct measurements of the longitudinal (or transverse) polarization for this mode. The predicted values of the polarization in every model are almost the same as for the mode $D^0 \to K^{*-}\rho^+$.

For the decay mode $D^0 \to \bar{K}^{*0}\rho^0$, BSWI and BSWII models predict a rate which is within 1.5 standard deviations from observed values. The remaining models, with the exception of the BFO model, predict a rate in agreement with data within one standard deviation. The BFO model underestimates the rate by three standard deviations. The transverse rate has been measured [5], from which we have calculated the longitudinal polarization. The measured value of P_L has large errors, but it is consistent with the longitudinal polarization in $D^0 \to K^{*-}\rho^+$. Given the freedom of the S–D interference, all models are consistent with the measured polarization. The predicted longitudinal polarization is almost decay-mode independent.

A final comment: Because of the misidentification of the S- and D-waves with the Lorentz structures in [7, 10], we do not trust the partial-wave branching ratios listed in [5]. For this reason the listings of $\frac{|S|}{|P|}$ and $\frac{|S|}{|D|}$ ratios in the last column of Tables 5.2, 5.3, 5.4 have to be read with this caveat.

Table 5.2: Decay rates for $D^0 \longrightarrow \bar{K}^{*-}\rho^+$. The values of Γ must be multiplied by $10^{11}s^{-1}$. The experimental values of P_L are listed only if measurements of longitudinal or transverse branching ratios are available [5].

model	Γ	P_L	$\frac{\lvert S\rvert}{\lvert P\rvert}$	$\frac{\lvert S\rvert}{\lvert D\rvert}$
BSWI	4.99	$0.319 - 0.084\cos\delta_{SD}$	4.3	10.6
BSWII	4.96	$0.313 - 0.071\cos\delta_{SD}$	3.7	12.3
AW	4.63	$0.316 - 0.122\cos\delta_{SD}$	3.6	7.0
CDDGFN	2.20	$0.315 - 0.127\cos\delta_{SD}$	3.5	6.7
ISGW	4.56	$0.324 - 0.108\cos\delta_{SD}$	4.7	8.3
BFO	1.03	$0.418 - 0.417\cos\delta_{SD}$	2.9	1.4
Exp.F[30]	2.20	$0.315 - 0.127\cos\delta_{SD}$	3.5	6.7
Expt.	1.47 ± 0.58	0.475 ± 0.271	—	—

Table 5.3: Decay rates for $D^+ \longrightarrow \bar{K}^{*0}\rho^+$. The values of Γ must be multiplied by $10^{11}s^{-1}$. The experimental values of P_L are listed only if measurements of longitudinal or transverse branching ratios are available [5].

model	Γ	P_L	$\frac{\lvert S\rvert}{\lvert P\rvert}$	$\frac{\lvert S\rvert}{\lvert D\rvert}$
BSWI	1.56	$0.326 - 0.086\cos\delta_{SD}$	5.5	10.6
BSWII	1.54	$0.325 - 0.079\cos\delta_{SD}$	5.3	11.5
AW	1.50	$0.319 - 0.141\cos\delta_{SD}$	3.6	6.1
CDDGFN	0.409	$0.318 - 0.128\cos\delta_{SD}$	3.7	6.7
ISGW	1.69	$0.333 - 0.129\cos\delta_{SD}$	6.9	7.0
BFO	0.268	$0.416 - 0.416\cos\delta_{SD}$	2.8	1.4
Exp.F[30]	0.559	$0.321 - 0.134\cos\delta_{SD}$	4.0	6.5
Expt.	0.20 ± 0.12	—	> 2 [33]	1.3 ± 0.8 [33]

Table 5.4: Decay rates for $D^0 \longrightarrow \bar{K}^{*0}\rho^0$. The values of Γ must be multiplied by $10^{11}s^{-1}$. The experimental values of P_L are listed only if measurements of longitudinal or transverse branching ratios are available [5].

model	Γ	P_L	$\frac{\lvert S\rvert}{\lvert P\rvert}$	$\frac{\lvert S\rvert}{\lvert D\rvert}$
BSWI	0.481	$0.309 - 0.080\cos\delta_{SD}$	3.4	10.7
BSWII	0.488	$0.249 - 0.060\cos\delta_{SD}$	2.7	13.7
AW	0.426	$0.314 - 0.097\cos\delta_{SD}$	3.6	8.9
CDDGFN	0.353	$0.313 - 0.125\cos\delta_{SD}$	3.3	6.8
ISGW	0.351	$0.379 - 0.074\cos\delta_{SD}$	3.1	11.5
BFO	0.124	$0.420 - 0.419\cos\delta_{SD}$	3.0	1.4
Exp.F[30]	0.267	$0.307 - 0.119\cos\delta_{SD}$	3.0	7.1
Expt.	0.354 ± 0.080	$0.0^{+0.4}_{-0}$	> 2.8 [33]	1.21 ± 0.23 [33]

Bibliography

[1] M. Bauer, B. Stech, M. Wirbel, Z. Phys. C **34**, 103 (1987).

[2] A. N. Kamal, R. C. Verma, N. Sinha, Phys. Rev. D **43**, 843 (1991).

[3] I. Hinchliffe and T. A. Kaeding, Phys. Rev. D **54**, 914 (1996).

[4] P. Bedaque, A. Das, and V. S. Mathur, Phys. Rev. D **49**, 269 (1994).

[5] Particle Data Group, C. Caso *et al.* Eur. Phys. J. C **3**, 1 (1998).

[6] El hassan El aaoud and A. N. Kamal, Phys. Rev. **D 59**, 114013 (1999).

[7] MARK III Collaboration, D. Coffman *et al.*, Phys. Rev. D **45**, 2196 (1992).

[8] E-691 Collaboration, J. C. Anjos *et al.* Phys. Rev. D **46**, 1941 (1992).

[9] MARK III Collaboration, J. Adler *et al.* Phys. Lett. B **196**, 107 (1987).

[10] D. F. DeJongh, Ph.D. thesis, California Institute of Thechnology, 1991.

[11] A. Ali, J. G. Körner, and G. Kramer, Z. Phys. C **1**, 269 (1979).

[12] A. S. Dighe, I.Dunietz, H. J. Lipkin, and J. L. Rosner, Phys. Lett. B **369**, 144 (1996).

[13] M. Gourdin, A. N. Kamal, Y. Y. Keum, and X. Y. Pham, Phys. Let. B **339**, 173 (1994); El hassan El aaoud, Phys. Rev. D **58**, 037502 (1998).

[14] OBELIX Collaboration, A. Amado *et al.*, Nucl. Phys. A **558**, 13c (1993).

[15] G. Valencia, Phys. Rev. D **39**, 3339 (1989).

[16] G. Kramer and W. F. Palmer, Phys. Rev. D **45**, 193 (1992); *ibid.* Phys. Rev. D **46**, 2969 (1992); G. Kramer, T. Mannel, and W. F. Palmer, Z. Phys. C **55**, 497 (1992).

[17] M. Wirbel, B. Stech and M. Bauer, Z. Phys. C **29**, 637 (1985); M. Bauer and M. Wirbel, Z. Phys. C **42**, 671 (1989).

[18] E-691 Collaboration, J. C. Anjos et al. Phys. Rev. Lett. **62**, 722 (1989).

[19] Particle Data Group, L. Montanet *et al.*, Phys. Rev. D **50**, 1173 (1994); S. Stone, in *Heavy Flavours*, edited by A. J. Buras and M. Lindner (World Scientific, Singapore, 1992), p. 334.

[20] A. N. Kamal, A. B. Santra, and T. Uppal, R. C. Verma, Phys. Rev. D **53**, 2506 (1996).

[21] M. Neubert, V. Rieckert, B. Stech, and Q. P. Xu, in *Heavy Flavours*, edited by A. J. Buras and M. Lindner (World Scientific, Singapore, 1992), p. 286.

[22] Hai-Yang Cheng, Z. Phys. C **69**, 647 (1996); Phys. Lett. B **335**, 428 (1994).

[23] Nita Sinha, Ph.D thesis, University of Alberta, (1989).

[24] T. Altomari and L. Wolfenstein, Phys. Rev. D **37**, 681 (1988).

[25] R. Casalbuoni, A. Deandrea, N. Di Bartolomeo, R. Gatto, F. Feruglio, and G. Nardulli, Phys. Lett. B **299**, 139 (1993).

[26] Particle Data Group, R. M. Bartnett *et al.* Phys. Rev. D **54**, 1 (1996).

[27] A. X. El-Khadra, A. S. Kronfeld, P. B. Mackenzie, S. M. Ryan, and J. N. Simone, Phys. Rev. D **58**, 014506 (1998).

[28] N. Isgur, D. Scora, B. Grinstein, and M. B. Wise, Phys. Rev. D **39**, 799 (1989).

[29] B. Bajc, S. Fajfer, and R. J. Oakes, Phys. Rev. D **53**, 4957 (1996); B. Bajc, S. Fajfer, R. J. Oakes, and S. Prelovšek, Phys. Rev. D **56**, 7207 (1997).

[30] The value of experimental form factors (Exp. F) are caculated using the nearest pole approximation: $F^{DK^*}(m^2) = \frac{F^{DK^*}(0)}{1-\frac{m^2}{\Lambda^2}}$ where the values of $F^{DK^*}(0)$ are taken from [26] and the pole masse Λ are from [17]. In calculating $F^{D\rho^+}(m^2_{K^*})$ we have used the approximation $F^{D\rho^+}(0) \approx F^{DK^*}(0)$.

[31] H. Arenhövel, W. Leidemann, and E. L. Tomusiak, Nucl. Phys. **A 641**, 517 (1998).

[32] E791 Collaboration, E. M. Aitala *et al.*, Phys. lett. **B** 440, 435 (1998), hep-ex/9809026.

[33] These values represent numbers extracted from [5]. See, however, our criticism of data.

Chapter 6

Resonant final-state interactions in $D^0 \to \bar{K}^0\eta, \bar{K}^0\eta'$ Decays

6.1 Introduction

A common method of evaluating the matrix elements of two-body hadronic decays of heavy mesons, B and D, is based on the factorization approximation [1] which utilizes model form factors. However, this approximation has had only limited success in describing two-body hadronic decays of the D meson [2, 3, 4, 5, 6]. In particular, the factorization approximation not only underestimates the decay rates for $D^0 \to \bar{K}^0\eta$ and $D^0 \to \bar{K}^0\eta'$, it generates $\Gamma(D^0 \to \bar{K}^0\eta) > \Gamma(D^0 \to \bar{K}^0\eta')$ in contradiction with the experiment [7]. In an attempt to remedy this discrepancy, Ref. [5] studied the above decays in the factorization approximation but included the annihilation term. They found that unlikely large form factors for $K \to \eta$ and $K \to \eta'$ transitions were required in order to bridge the gap between theory and experiment. Ref. [6] on the other hand introduced nonfactorized contributions and used a flavor-$SU(3)$ parameterization for the nonfactorized matrix elements to fit the data. Their conclusions imply a large value for the hair-pin amplitude.

Hadronic decays of mesons are complicated by the presence of final-state strong

interactions (FSI) between hadrons in the final state. The importance of FSI in hadronic decays of D meson has been known for a long time; its role was emphasized by several authors [8] almost twenty years ago. The long-range FSI generates phases in the decay amplitudes [9] and the most dramatic effect of FSI is induced by the interference between different isospin amplitudes which depends on the phase difference [1, 8, 10] between different isospin amplitudes. In decays with a single isospin final state, as in $D^0 \to \bar{K}^0\eta$ and $D^0 \to \bar{K}^0\eta'$, isospin interference effects are absent. However, FSI also leads to a change in the magnitude of the decay amplitude, and not simply a rotation in the complex amplitude plane. Hence we expect FSI to affect the decay rates in single-isospin channel decays too.

In this chapter [11] we have considered the FSI effect of $\bar{K}_0^*(1950)$ resonance on $D^0 \to \bar{K}^0\eta$ and $D^0 \to \bar{K}^0\eta'$ decays. The mechanism we are proposing for resonant FSI is as follows: $D^0 \to \bar{K}^0\eta$ and $D^0 \to \bar{K}^0\eta'$ are color-suppressed decays in the factorization approximation, see (Fig. 6.1). The resonance $\bar{K}_0^*(1950)$ has a substantial branching ratio ($\sim 50\%$) to $K\pi$ mode, leaving room for its coupling to $K\eta$ and $K\eta'$ channels. We propose that the effect of $\bar{K}_0^*(1950)$ on $D^0 \to \bar{K}^0\eta$ and $D^0 \to \bar{K}^0\eta'$ could be estimated via the Feynman diagram shown in (Fig. 6.2) where in the loop we include both $K^-\pi^+$ (color-favored decay) and $\bar{K}^0\pi^0$ (color-suppressed decay) states. Such mechanism has been invoked in Ref. [12] in $D^0 \to \bar{K}^0K^0$ decay. However, in contrast to Ref. [12], where only the on-shell loop contribution is retained, we evaluate both on- and off-shell loop contributions in (Fig. 6.2).

Recently, Gronau [13] has also discussed the role of resonant FSI on D decays. We relegate a discussion of these works [12, 13], and their relationship to ours, to the last section of this chapter.

6.2 Method of calculation

6.2.1 Calculation without final-state interactions

The decays $D^0 \to \bar{K}^0\eta$ and $D^0 \to \bar{K}^0\eta'$ are Cabibbo-favored and are induced by the effective weak Hamiltonian Eq. (3.15):

$$\begin{aligned} \mathcal{H}_{CF} &= G'_F[a_1(\bar{u}d)(\bar{s}c) + C_2 O_8], \\ \mathcal{H}_{CS} &= G'_F[a_2(\bar{u}c)(\bar{s}d) + C_1 \tilde{O}_8], \end{aligned} \tag{6.1}$$

The quark diagram which contributes to $D^0 \to \bar{K}^0\eta$ and $D^0 \to \bar{K}^0\eta'$ decays is shown in (Fig. 6.1). The physical particles η and η' are mixtures of the flavor-singlet η_0 and the flavor-octet η_8 given by (Appendix C):

$$\begin{aligned} \eta_0 &= \frac{1}{\sqrt{3}} \mid u\bar{u} + d\bar{d} + s\bar{s}\rangle, \\ \eta_8 &= \frac{1}{\sqrt{6}} \mid u\bar{u} + d\bar{d} - 2s\bar{s}\rangle, \end{aligned} \tag{6.2}$$

with a mixing angle $\theta_p = -20^\circ$ [14]:

$$\eta = \eta_8 \cos\theta_p - \eta_0 \sin\theta_p \tag{6.3}$$

$$\eta' = \eta_8 \sin\theta_p + \eta_0 \cos\theta_p. \tag{6.4}$$

The factorized amplitude for the decay $D^0 \to \bar{K}^0\eta, \bar{K}^0\eta'$ is given by (superscript f refers to 'factorized')

$$\begin{aligned} A^f(D^0 \to \bar{K}^0\eta) &= G'_F a_2 \langle \bar{K}^0 \mid \bar{s}d \mid 0\rangle\langle\eta \mid \bar{u}c \mid D^0\rangle, \\ A^f(D^0 \to \bar{K}^0\eta') &= G'_F a_2 \langle \bar{K}^0 \mid \bar{s}d \mid 0\rangle\langle\eta' \mid \bar{u}c \mid D^0\rangle. \end{aligned} \tag{6.5}$$

In calculating the decay amplitude in Eq. (6.5), we use the following results,

$$\langle K(p) \mid (\bar{s}d)_\mu \mid 0\rangle = -if_K p_\mu \tag{6.6}$$

$$\begin{aligned} \langle \eta(p_\eta) \mid (\bar{u}c)_\mu \mid D(p_D)\rangle &= \left(p_D + p_\eta - \frac{m_D^2 - m_\eta^2}{q^2} q\right)_\mu F_1^{D\eta}(q^2) \\ &\quad + \frac{m_D^2 - m_\eta^2}{q^2} q_\mu F_0^{D\eta}(q^2), \end{aligned} \tag{6.7}$$

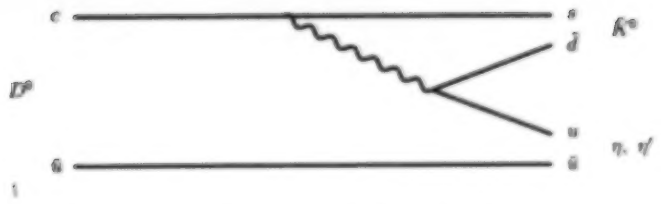

Figure 6.1: Quark diagram contributing to the factorized amplitude A^f for $D^0 \to \bar{K}^0\eta$ and $D^0 \to \bar{K}^0\eta'$.

where

$$q = p_D - p_\eta, \tag{6.8}$$

is the momentum transfer, f_K is the decay constant of the K meson, $F_i^{D\eta}(q^2), (i = 0, 1)$ are invariant form factors defined in [15]. The factorized amplitudes for $D^0 \to \bar{K}^0\eta$ and $D^0 \to \bar{K}^0\eta'$ are

$$\begin{aligned} A^f(D^0 \to \bar{K}^0\eta) &= -iG'_F \frac{a_2}{\sqrt{2}} f_K \sin\theta'(m_D^2 - m_\eta^2) F_0^{D\eta}(m_K^2), \\ A^f(D^0 \to \bar{K}^0\eta') &= -iG'_F \frac{a_2}{\sqrt{2}} f_K \cos\theta'(m_D^2 - m_{\eta'}^2) F_0^{D\eta'}(m_K^2), \end{aligned} \tag{6.9}$$

where θ' is given by (see Appendix C)

$$\begin{aligned} \sin\theta' &= \frac{1}{\sqrt{3}}\cos\theta_P - \sqrt{\frac{2}{3}}\sin\theta_P \\ \cos\theta' &= \sqrt{\frac{2}{3}}\cos\theta_P + \sqrt{\frac{1}{3}}\sin\theta_P. \end{aligned} \tag{6.10}$$

The corresponding decay rates are given by

$$\begin{aligned} \Gamma^f(D^0 \to \bar{K}^0\eta) &= |\, A^f(D^0 \to \bar{K}^0\eta)\,|^2 \frac{|\,\mathbf{p}\,|}{8\pi m_D^2}, \\ \Gamma^f(D^0 \to \bar{K}^0\eta') &= |\, A^f(D^0 \to \bar{K}^0\eta')\,|^2 \frac{|\,\mathbf{p}'\,|}{8\pi m_D^2}, \end{aligned} \tag{6.11}$$

where $\mathbf{p}$, $\mathbf{p}'$ are the center of mass momentum of the final state particle in the decay $D^0 \to \bar{K}^0\eta$ and $D^0 \to \bar{K}^0\eta'$ respectively; m_D is the mass of the decaying D meson.

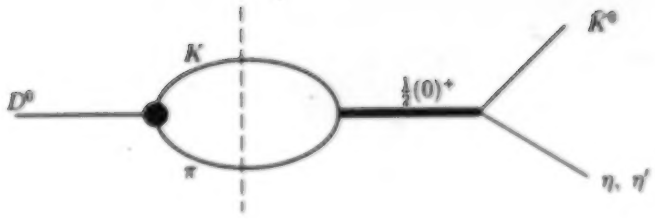

Figure 6.2: Resonant contribution to $D^0 \to \bar{K}^0\eta$ and $D^0 \to \bar{K}^0\eta'$. The vertical dashed line represents the cut when the particles, $K\pi$, in the loop are on-shell. The thick line represents the resonance $K_0^*(1950)$, and the shaded circle represents the weak vertex $\mathcal{V}(k^2)$.

6.2.2 Calculation with resonant final-state interactions

The resonances contributing to $D^0 \to \bar{K}^0\eta, \bar{K}^0\eta'$ must have isospin and spin-parity assignment $I(J^P) = \frac{1}{2}(0^+)$. $I = 1/2$, because this resonance eventually decays through strong interaction into $(K\eta)$ system which has $I = 1/2$; $J^P = 0^+$, because it couples to D^0 which has spin 0 and decays via strong interactions into two pseudoscalar particles forming an S-state. There are two particles, $\bar{K}_0^*(1950)$ and $\bar{K}_0^*(1430)$, with such properties [7]:

$$\begin{aligned} m_1 &= m_{\bar{K}_0^*} = 1945 \pm 10 \pm 20\ MeV, \quad \Gamma_1 = 201 \pm 34 \pm 79\ MeV, \\ m_2 &= m_{\bar{K}_0^*} = 1429 \pm 4 \pm 5\ MeV, \quad \Gamma_2 = 287 \pm 10 \pm 21\ MeV. \end{aligned} \tag{6.12}$$

Although $m_2 + \frac{\Gamma_2}{2}$ is much smaller than m_D and $\bar{K}_0^*(1430)$ decays almost exclusively to πK channel, we cannot prejudice its effect to be insignificant in $D^0 \to \bar{K}^0\eta, \bar{K}^0\eta'$ [16]. However, in this chapter we consider the contribution from $\bar{K}_0^*(1950)$ only.

The contribution of $\bar{K}_0^*(1950)$ to $D^0 \to \bar{K}^0\eta$ and $D^0 \to \bar{K}^0\eta'$ is represented by Feynman diagram shown in (Fig. 6.2), where in the loop we consider both the color-favored state $K^-\pi^+$ and the color-suppressed state $\bar{K}^0\pi^0$. Evaluation of the diagram in (Fig. 6.2) gives the following amplitudes (superscript r and subscript $-+$, 00 refer

to 'resonant' and $K^-\pi^+$, $\bar{K}^0\pi^0$ intermediate state, respectively)

$$A^r_{-+} = \frac{i}{(2\pi)^4}\int d^4k \frac{\mathcal{V}^{(1/2)}_{-+}(k^2)}{(k^2-m_\pi^2)((w-k)^2-m_K^2)} \times A^{strong}_{-+} \equiv I_{-+} \times A^{strong}_{-+}, \quad (6.13)$$

with

$$A^{strong}_{-+} = g_{-+}\frac{1}{(m_D^2-m_R^2)+i\Gamma m_R} f, \quad (6.14)$$

and

$$A^r_{00} = \frac{i}{(2\pi)^4}\int d^4k \frac{\mathcal{V}^{(1/2)}_{00}(k^2)}{(k^2-m_\pi^2)((w-k)^2-m_K^2)} \times A^{strong}_{00} \equiv I_{00} \times A^{strong}_{00}, \quad (6.15)$$

with

$$A^{strong}_{00} = g_{00}\frac{1}{(m_D^2-m_R^2)+i\Gamma m_R} f, \quad (6.16)$$

where g_{-+} and g_{00} are the couplings of $K^-\pi^+$ and $\bar{K}^0\pi^0$ states to $\bar{K}^*_0(1950)$ and f is the coupling of $\bar{K}^0\eta, \bar{K}^0\eta'$ state to $\bar{K}^*_0(1950)$, m_R is the resonance mass, Γ its width, w is the four momentum of the decaying particle ($w = (m_D, 0)$ in the C.M.) and k is the loop momentum to be integrated over; $\mathcal{V}^{(1/2)}_{-+}(k^2)$ and $\mathcal{V}^{(1/2)}_{00}(k^2)$ are the vertex functions in isospin 1/2 state. They are related to the amplitudes $A(D^0 \to K^-\pi^+)$ and $A(D^0 \to \bar{K}^0\pi^0)$ and are evaluated in the following.

Although A^r_{-+} and A^r_{00} get contributions from color-favored and color-suppressed intermediate states respectively, they are not independent but are related by isospin and $SU(3)$ symmetry as the following analysis elucidates.

Isospin Symmetry

As the resonance $\bar{K}^*_0(1950)$ has isospin 1/2 and as strong interactions conserve isospin, only the isospin component $A^{(1/2)}(D \to \bar{K}\pi)$ in the following will contribute to $\mathcal{V}^{(1/2)}_{-+}(k^2)$ and $\mathcal{V}^{(1/2)}_{00}(k^2)$. The isospin decomposition of the decay amplitudes,

$$A(D^0 \to K^-\pi^+) = \sqrt{\frac{1}{3}}A^{(3/2)} + \sqrt{\frac{2}{3}}A^{(1/2)}$$

$$A(D^0 \to \bar{K}^0\pi^0) \;=\; \sqrt{\frac{2}{3}}A^{(3/2)} - \sqrt{\frac{1}{3}}A^{(1/2)}, \tag{6.17}$$

allows us to calculate $A^{(1/2)}$ which is needed as the input. For the color-favored intermediate state $K^-\pi^+$ we get from Eq. (6.17)

$$\begin{aligned}\mathcal{V}_{-+}^{(1/2)}(k^2) &= \sqrt{\frac{2}{3}}A^{(1/2)} \\ &= \sqrt{\frac{2}{3}}\left\{\sqrt{\frac{2}{3}}A(D^0 \to K^-\pi^+) - \sqrt{\frac{1}{3}}A(D^0 \to K^0\pi^0)\right\},\end{aligned} \tag{6.18}$$

while for the color-suppressed intermediate state, we get

$$\begin{aligned}\mathcal{V}_{00}^{(1/2)}(k^2) &= -\sqrt{\frac{1}{3}}A^{(1/2)} \\ &= -\sqrt{\frac{1}{3}}\left\{\sqrt{\frac{2}{3}}A(D^0 \to K^-\pi^+) - \sqrt{\frac{1}{3}}A(D^0 \to K^0\pi^0)\right\}.\end{aligned} \tag{6.19}$$

Therefore, isospin symmetry offers the following relation between the two vertex functions $\mathcal{V}_{-+}^{(1/2)}(k^2)$ and $\mathcal{V}_{00}^{(1/2)}(k^2)$

$$\mathcal{V}_{-+}^{(1/2)}(k^2) = -\sqrt{2}\mathcal{V}_{00}^{(1/2)}(k^2). \tag{6.20}$$

Let us now turn to the strong decay of $\bar{K}_0^*(1950)$ to two pseudoscalar mesons.

SU(3) Symmetry and Strong Decay of $\bar{K}_0^*(1950)$

Consider the strong decay of scalar octet particle S to two pseudoscalars octet particles P_1 and P_2

$$S \longrightarrow P_1 \;\; P_2 \tag{6.21}$$

where the pseudoscalar octet particles are given by

$$P = \begin{pmatrix} \frac{\pi^0}{\sqrt{2}} + \frac{\eta_8}{\sqrt{6}} & \pi^+ & K^+ \\ \pi^- & -\frac{\pi^0}{\sqrt{2}} + \frac{\eta_8}{\sqrt{6}} & K^0 \\ K^- & \bar{K}^0 & -\frac{2}{\sqrt{6}}\eta_8 \end{pmatrix}. \tag{6.22}$$

The scalar octet S has the same form as the octet P with pseudoscalar parti cles replaced by the equivalent scalar particles. The strong Hamiltonian for the coupling in Eq. (6.21) is,

$$\mathcal{H}_{str} = g_{ijk} P_j P_k S_i, \tag{6.23}$$

where $g_{ijk}, i, j, k = 1, 2, ..., 8$ is real constant and P_j, P_k and S_i are the meson fields. We need to choose g_{ijk} such that the coupling in Eq. (6.23) is invariant under $SU(3)$. The $SU(3)$ group has two types of structure constants: d_{ijk} are symmetric, and f_{ijk} are antisymmetric (see Appendix A). Thus, we have two types of couplings:

$$\mathcal{H}_{str} = \begin{cases} \frac{g}{\sqrt{2}} f_{ijk} P_j P_k S_i & \text{F-type} \\ \frac{g}{\sqrt{2}} d_{ijk} P_j P_k S_i & \text{D-type} \end{cases}, \tag{6.24}$$

where g is the strong coupling constant of two pseudoscalar octets to a scalar octet. The $1/\sqrt{2}$ in Eq. (6.24) was introduced for latter convenience. Since the coupling must be symmetric under the exchange of the two pseudoscalar particles $P_i \leftrightarrow P_j$ the coupling must be of D-type. Using

$$d_{ijk} = \frac{1}{4} Tr(\{\lambda_j, \lambda_k\}\lambda_i), \tag{6.25}$$

the pseudoscalar and scalar octet are given by

$$\begin{aligned} P &= \frac{1}{\sqrt{2}} \sum_{i=1}^{8} \lambda_i P_i, \\ S &= \frac{1}{\sqrt{2}} \sum_{i=1}^{8} \lambda_i S_i, \end{aligned} \tag{6.26}$$

λ_i, i =1, 2, ..., 8 are Gell-Mann matrices given in Appendix A. The $SU(3)$-invariant strong Hamiltonian which couples a scalar octet S to two pseudoscalars octets P reduce to the following form

$$\begin{aligned} \mathcal{H}_{str} &= \frac{g}{2} Tr(\{P^T, P^T\}S), \\ &= g Tr(P^T P^T S). \end{aligned} \tag{6.27}$$

From Eq. (6.27) we obtain the following relation for the strong coupling constants

$$\begin{aligned} g &= g_{K_0^* K^- \pi^+} = g_{-+}, \\ &= -\sqrt{2}\, g_{K_0^* K^0 \pi^0} = -\sqrt{2}\, g_{00}, \\ &= -\sqrt{6}\, g_{K_0^* K^0 \eta_8} = -\sqrt{6} g_8. \end{aligned} \tag{6.28}$$

From equations (6.14), (6.16) and (6.28), $SU(3)$ symmetry gives the following relation between the strong amplitudes A_{-+}^{strong} and A_{00}^{strong}:

$$A_{-+}^{strong} = -\sqrt{2} A_{00}^{strong}. \tag{6.29}$$

Hence, using equations (6.13), (6.15), (6.20) and (6.29) the resonant amplitudes A_{-+}^r and A_{00}^r are related by

$$A_{-+}^r = 2A_{00}^r, \tag{6.30}$$

and the total resonant amplitude A^r is

$$\begin{aligned} A^r &= A_{-+}^r + A_{00}^r \\ &= \frac{3}{2} A_{-+}^r. \end{aligned} \tag{6.31}$$

Because of Eq. (6.31), the calculation of the resonant amplitude A^r reduces to that of $A_{-+}^r = I_{-+} A_{-+}^{strong}$ given in Eq. (6.13). The amplitude A_{-+}^r have two parts, a strong part given by A_{-+}^{strong} in Eq. (6.14) and a weak part given by

$$I_{-+} = \frac{i}{(2\pi)^4} \int d^4k \frac{\mathcal{V}_{-+}^{(1/2)}(k^2)}{(k^2 - m_\pi^2)((w-k)^2 - m_K^2)}. \tag{6.32}$$

Calculation of A_{-+}^{strong}

The resonant amplitude A_{-+}^{strong} depends on the strengths and the signs of strong coupling constants f and g which we determine as follows. The decay rate of a scalar particle, of mass m_S, decaying into two pseudoscalars is given by

$$\Gamma(S \to PP) = \frac{|\,\mathbf{p}\,|\, g_{SPP}^2}{8\pi m_S^2}. \tag{6.33}$$

For $\bar{K}_0^*(1950)$, we have the following measured branching ratio [7]

$$s \equiv Br(\bar{K}_0^* \to K\pi) = 52 \pm 14\%. \tag{6.34}$$

Using Eqs. (6.28), (6.33) and the central value of s in Eq. (6.34), we get

$$g = \pm 2.707\ GeV. \tag{6.35}$$

Since the determination of the strong couplings

$$f \equiv \begin{cases} g_{\bar{K}_0^* K^0 \eta} & = g_\eta \\ g_{\bar{K}_0^* K^0 \eta'} & = g_{\eta'} \end{cases}, \tag{6.36}$$

is complicated by $\eta - \eta'$ mixing and the fact that no measurements are available for the branching ratios $Br(\bar{K}_0^* \to K\eta)$ and $Br(\bar{K}_0^* \to K\eta')$, we provide some details of how we calculate g_η and $g_{\eta'}$. We include $\eta - \eta'$ mixing in the strong decay of the resonance as follows,

$$\begin{aligned} g_\eta &= g_8 \cos\theta_p - g_0 \sin\theta_p \\ g_{\eta'} &= g_8 \sin\theta_p + g_0 \cos\theta_p, \end{aligned} \tag{6.37}$$

where the octet coupling g_8 is determined from Eq (6.28) to be

$$g_8 \equiv g_{\bar{K}_0^* K^0 \eta_8} = -g/\sqrt{6}, \tag{6.38}$$

and the unknown singlet coupling is $g_0 \equiv g_{\bar{K}_0^* K^0 \eta_0}$. We treat the following unmeasured branching ratio sum as a variable,

$$\begin{aligned} r &= Br(\bar{K}_0^*(1950) \to K\eta) + Br(\bar{K}_0^*(1950) \to K\eta') \\ &= \frac{1}{\Gamma_1 8\pi m_1^2}(|\mathbf{p}|g_\eta^2 + |\mathbf{p}'|g_{\eta'}^2), \end{aligned} \tag{6.39}$$

where $\mathbf{p}$ and $\mathbf{p}'$ are center of mass momenta of the final state particle in the decays $\bar{K}_0^* \to K\eta$ and $\bar{K}_0^* \to K\eta'$, respectively. Since g_8 is known[1] from flavor-$SU(3)$ symmetry, we use Eqs. (6.37) and (6.39) to solve for the singlet coupling $g_0(r)$ in terms of

[1]The results of this chapter were obtained using the positive value $g = 2.707\ GeV$. We learn nothing new if the negative value of g is used. See Discussion.

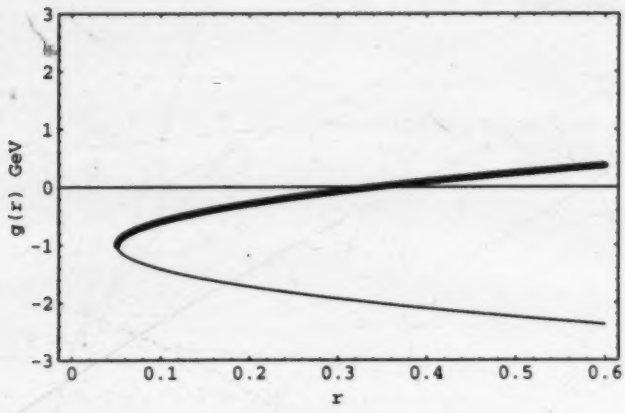

Figure 6.3: Plot for the two sets of solutions, $g_\eta^i(r), i = 1, 2$, as a function of the branching ratio sum $r = Br(K_0^*(1950) \to K^0\eta) + Br(K_0^*(1950) \to \bar{K}^0\eta')$. The thick and light parts of the curve correspond to $g_\eta^1(r)$ and $g_\eta^2(r)$, respectively.

r. We obtain two solutions for g_0, denoted by $g_0^i(r), i = 1, 2$; we then substitute $g_0^i(r)$ in Eq. (6.37) and get two sets of solutions $(g_\eta^i(r), g_{\eta'}^i(r)), i = 1, 2$. Their dependence on r is shown in (Fig. 6.3) and (Fig. 6.4). In order for the strong coupling constants $g_\eta(r), g_{\eta'}(r)$ to be real we find that we must have $r > 5\%$. We also, have the constraint $r + s \leq 100\%$, which restricts the allowed range for r to: $(5\% \leq r \leq 52\%)$. Using Eqs. (6.14) and (6.28) with $g = 2.707GeV$, the amplitudes A_{-+}^{strong} are found to be

$$\begin{aligned} A_{-+}^{strong}(\bar{K}^0\eta) &= -5.45 g_\eta^i(r) exp(i52^\circ), \\ A_{-+}^{strong}(\bar{K}^0\eta') &= -5.45 g_{\eta'}^i(r) exp(i52^\circ). \end{aligned} \tag{6.40}$$

Calculation of I_{-+}

For an explicit calculation of the weak amplitude $I{-}+$ in Eq. (6.32) we require the momentum dependence of the vertex function $\mathcal{V}_{-+}^{(1/2)}(k^2)$. Hence, we rely on models and approximations. We assume the form dictated by the factorization assumption but with both π and K not necessarily on their mass-shells (see Ref. [17]),

$$A^f(D^0 \to K^-(p)\pi^+(k)) = -iG_F' a_1 f_\pi (m_D^2 - p^2) F_0^{DK}(k^2)$$

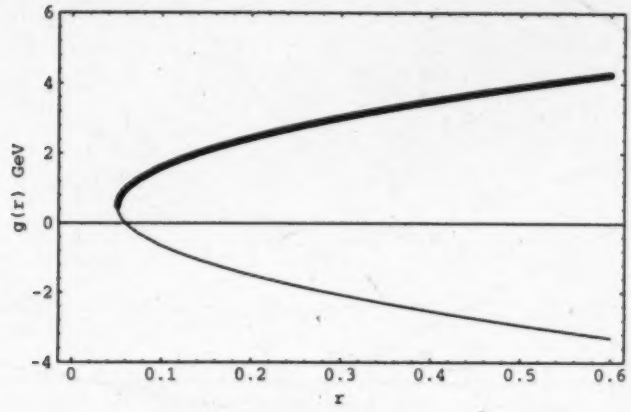

Figure 6.4: Plot for the two sets of solutions, $g^i_{\eta'}(r), i = 1, 2$, as a function of the branching ratio sum $r = Br(K_0^*(1950) \to K^0\eta) + Br(K_0^*(1950) \to \bar{K}^0\eta')$. The thick and light parts of the curve correspond to $g^1_{\eta'}(r)$ and $g^2_{\eta'}(r)$, respectively.

$$A^f(D^0 \to \bar{K}^0(p)\pi^0(k)) \;=\; -iG'_F\frac{a_2}{\sqrt{2}}f_K(m_D^2 - k^2)F_0^{D\pi}(p^2). \tag{6.41}$$

From Eqs. (6.18) and (6.41) we then obtain

$$\begin{aligned}\mathcal{V}^{(1/2)}_{-+}(k^2) \;&=\; -iG'_F\sqrt{\frac{2}{3}}\left\{\sqrt{\frac{2}{3}}a_1 f_\pi(m_D^2 - (w-k)^2)F_0^{DK}(k^2)\right.\\ &\left.-\frac{a_2}{\sqrt{6}}f_K(m_D^2 - k^2)F_0^{D\pi}((w-k)^2)\right\},\end{aligned} \tag{6.42}$$

where p and k are four-momenta of K and π mesons in the loop, respectively. They are related by momentum conservation at the vertex, $w = p + k$. Since in our calculation, the intermediate particles (K, π) are allowed to be off-shell, we have to assume a behavior of the form factors in the vertex function, Eq. (6.42), as the particles go off-shell. Form factors with a dipole dependence: $F(k_X^2) = \left(\frac{\lambda^2 - m_X^2}{\lambda^2 - k_X^2}\right)^2$ (where λ is fixed by experiment) have been used in the past [18] to describe off-shellness of intermediate state particles. In this work we have used the following phenomenological form factor

$$F_0^{DX}(k^2) = \frac{F_0^{DX}(0)}{(1 - \frac{k^2}{\Lambda^2})(1 - \frac{(w-k)^2 - m_X^2}{\Lambda^2})}. \tag{6.43}$$

In principle, one could use two different mass scales, Λ_1 and Λ_2. We chose to work with a single mass scale for simplicity[2]. Beside having a dipole dependence, this form factor satisfies the following limit: As K goes on-shell i.e.

$$p^2 = (w-k)^2 \longrightarrow m_X^2 = m_K^2, \tag{6.44}$$

the form factor in Eq. (6.43) reduces to the usual monopole form,

$$F_0^{DK}(k^2) = \frac{F_0^{DK}(0)}{1-\frac{k^2}{\Lambda^2}}, \tag{6.45}$$

with the pole mass Λ given in Ref. [15].

Furthermore, as the pseudoscalar particles in the loop go off-shell, the decay constants f_π and f_K would also change. For large off-shell masses one knows from heavy quark effective theory that $f_\pi \sim \frac{1}{\sqrt{q^2}}$ where q^2 is the virtual mass squared of the pseudoscalar particle. However, the integration is over a range where the particles are not always far off-shell. Hence, we have chosen to use constant values for f_π and f_K.

Using the vertex function given in Eq. (6.42) in Eq. (6.32) we get the following integral, (to make the factorized amplitude real we drop a common factor of i from the amplitudes in Eqs. (6.9) and (6.41))

$$\begin{aligned} I_{-+} &= \frac{-iG'_F}{(2\pi)^4}\sqrt{\frac{2}{3}}\int \frac{d^4k}{(k^2-m_\pi^2)((w-k)^2-m_K^2)} \times \\ &\quad \left\{\sqrt{\frac{2}{3}}a_1 f_\pi (m_D^2-(w-k)^2)F_0^{DK}(k^2)\right. \\ &\quad \left. -\frac{a_2}{\sqrt{6}}f_K(m_D^2-k^2)F_0^{D\pi}((w-k)^2)\right\}, \end{aligned} \tag{6.46}$$

where $d^4k = dk_0 d^3\mathbf{k}$, $k^2 = k_0^2 - |\mathbf{k}|^2$, and $w = (m_D, 0)$. Using form factors as explained in the text, the integral I_{-+} reduces to the following form,

$$\begin{aligned} I_{-+} &= \frac{-G'_F}{(2\pi)^4}\sqrt{\frac{2}{3}}\left\{a_1\sqrt{\frac{2}{3}}\Lambda^4 f_\pi F_0^{DK}(0)\left[(m_D^2-m_K^2)I_1^{DK}-I_2^{DK}\right]\right. \\ &\quad \left. -a_2\frac{f_K}{\sqrt{6}}\Lambda^4 F_0^{D\pi}(0)\left[(m_D^2-m_\pi^2)I_1^{D\pi}-I_3^{D\pi}\right]\right\}, \end{aligned} \tag{6.47}$$

[2]The mass scale Λ in the factor F_0^{DK} is different from the Λ in the form factor $F_0^{D\pi}$.

where the integrals I_i are given by

$$I_1 = \frac{1}{(\Lambda^2 - m_\pi^2)(\Lambda^2 - m_K^2)} (I_{\Lambda\Lambda} - I_{\Lambda K} - I_{\pi\Lambda} + I_{\pi K}), \tag{6.48}$$

$$I_2 = \frac{-1}{(\Lambda^2 - m_\pi^2)} I_{\pi\Lambda} + \frac{1}{(\Lambda^2 - m_\pi^2)} I_{\Lambda\Lambda}, \tag{6.49}$$

$$I_3 = \frac{-1}{(\Lambda^2 - m_k^2)} I_{\Lambda K} + \frac{1}{(\Lambda^2 - m_k^2)} I_{\Lambda\Lambda}. \tag{6.50}$$

The integrals $I_i \equiv I_i^{DK(\pi)}$ with Λ having the appropriate mass given in Eq. (6.53). The integral I_{XY} has the generic form

$$I_{XY} = i \int \frac{dk_0 d^3\mathbf{k}}{(k^2 - m_X^2)((w-k)^2 - m_Y^2)}. \tag{6.51}$$

First we integrate over dk_0 in the complex plane with a contour closed in the lower half plane. We have used a mass scale Eq. (6.53) $\Lambda > m_{D^0} + m_K$, therefore the integration over $d^3\mathbf{k}$ is well defined for all the integrals except $I_{\pi K}$ which has a pole contributing to the imaginary part of I_{-+}.

For numerical calculations we used the following parameters,

$$\begin{aligned} V_{cs} &= 0.974, \quad V_{ud} = 0.975, \\ f_\pi &= 0.131\ GeV, \quad f_K = 0.160\ GeV, \end{aligned} \tag{6.52}$$

and the pole mass Λ,

$$m(sc(0^+)) = 2.6\ GeV, \quad m(dc(0^+)) = 2.47\ GeV. \tag{6.53}$$

The above calculation leads to the following result,

$$\begin{aligned} I_{-+} &= 10^{-3} G'_F \sqrt{\frac{2}{3}} \left\{ 8.735 F_0^{DK}(0) + 1.769 F_0^{D\pi}(0) \right. \\ &\quad \left. + i(8.328 F_0^{DK}(0) + 2.211 F_0^{D\pi}(0)) \right\}\ GeV, \\ &= 10^{-3} G'_F \sqrt{\frac{2}{3}} F_0^{DK}(0) \left\{ 8.735 + 1.769 \frac{F_0^{D\pi}(0)}{F_0^{DK}(0)} + i(8.328 + 2.211 \frac{F_0^{D\pi}(0)}{F_0^{DK}(0)}) \right\}, \\ &= |I_{-+}| exp(i\delta_I)\ GeV. \end{aligned} \tag{6.54}$$

The integral I_{-+} is obviously complex, the real part arising from the region where both π and K are off-shell and the imaginary part coming from the region where both π and K are on-shell.

Now, model predictions [19] as well as experiments [20] give a ratio

$$\frac{F_0^{D\pi}(0)}{F_0^{DK}(0)} \sim 1. \tag{6.55}$$

Consequently the phase $\delta_I \approx 45°$ and it is insensitive to form factor-models. The magnitude of I_{-+} depends on $F_0^{DK}(0)$. We use the value $F_0^{DK}(0) = 0.76$ [19, 20] to obtain

$$I_{-+} = 0.723 \times 10^{-7} exp(i45°)\ \ GeV. \tag{6.56}$$

Finally the total resonant amplitude A^r is (in the following calculation all the amplitudes are scaled by a factor of 10^{-7}),

$$\begin{aligned} A^r_{-+}(D^0 \to \bar{K}^0\eta) &= I_{-+} \times A^{strong}_{-+}(\bar{K}^0\eta), \\ &= -3.94 g^i_\eta(r) exp(i97°)\ \ GeV, \\ A^r_{-+}(D^0 \to \bar{K}^0\eta') &= I_{-+} \times A^{strong}_{-+}(\bar{K}^0\eta') \\ &= -3.94 g^i_{\eta'}(r) exp(i97°)\ \ GeV, \end{aligned} \tag{6.57}$$

and the total resonant amplitude A^r,

$$\begin{aligned} A^r &= \frac{3}{2} A^r_{-+}, \\ &= -5.91 g^i_{\eta(\eta')}(r) exp(i97°)\ \ GeV. \end{aligned} \tag{6.58}$$

Note that the amplitude A^{strong} defined in Eq. (6.14) is complex; however, the phase of A^r is not the phase of A^{strong}. The total amplitude for $D^0 \to \bar{K}^0\eta(\eta')$ is the coherent sum

$$A = A^f + A^r. \tag{6.59}$$

6.3 Results

6.3.1 Factorized Amplitude

For the purpose of comparison with experiment we have calculated the factorized amplitude $A^f(D^0 \to K\eta(\eta'))$ using the following models for the form factors: i) Bauer, Stech and Wirbel (BSW) model [15], where an infinite momentum frame is used to calculate the form factors at $q^2 = 0$, and a monopole form for q^2 dependence is assumed to extrapolate all the form factors to the desired value of q^2; ii) Casalbuoni, Deandrea, Di Bartolomeo, Feruglio, Gatto and Nardulli (CDDGFN) model [21], where the form factors are evaluated at $q^2 = 0$ in an effective Lagrangian satisfying heavy quark spin-flavor symmetry in which light vector particles are introduced as gauge particles in a broken chiral symmetry. A monopole form is used for the q^2 dependence. The experimental inputs for this model are from the semileptonic decay $D \to \pi l\nu$, and we have used the value of the form factors [22]

$$\begin{aligned} F_1^{D\pi}(0) &= F_0^{D\pi}(0), \\ &= 0.83 \pm 0.08, \end{aligned} \tag{6.60}$$

extracted from data, and decay constants [23],

$$\begin{aligned} f_{D_s} &= 213^{+14}_{-11} \pm 11, \\ f_D &= 194^{+14}_{-10} \pm 10\ MeV \end{aligned} \tag{6.61}$$

in calculating the weak coupling constants of the model at $q^2 = 0$ [21] , which are subsequently used in evaluating the required form factors ; vi) Isgur, Scora, Grinstein and Wise (ISGW) model [24], where a non-relativistic quark model is used to calculate the form factors at zero recoil and an exponential q^2 dependence, based on a potential-model calculation of the meson wave function, is use to extrapolate them to the desired q^2; iv) Lubicz, Martinelli, McCarthy and Sachrajda (LMMS) model [25], where the form factors are obtained from lattice calculation of D meson semileptonic decays. The values of the form factors are presented in Table 6.1.

Table 6.1: Model predictions for the form factors : $F_0^{D\eta(\eta')}(m_K^2)$, $F_0^{DK(\pi)}(0)$ and the ratio $\frac{F_0^{D\pi}(0)}{F_0^{DK}(0)}$ for the processes $D^0 \longrightarrow \bar{K}^0\eta, \bar{K}^0\eta', K\pi$.

	BSWI	*CDDFGN*	*ISGW*	*LMMS*
$F_0^{D\eta}(m_K^2)$	0.710	0.313	0.638	0.344
$F_0^{D\eta'}(m_K^2)$	0.683	-	0.937	0.240
$F_0^{DK}(0)$	0.762	0.699	0.769	0.63
$F_0^{D\pi}(0)$	0.692	0.83	0.510	0.58
$\frac{F_0^{D\pi}(0)}{F_0^{DK}(0)}$	0.91	1.19	0.66	0.92

Table 6.2: Model predictions for the factorized amplitude A^f for the process $D^0 \longrightarrow \bar{K}^0\eta$ and $D^0 \longrightarrow \bar{K}^0\eta'$ These values must be multiplied by a factor of $10^{-7}GeV$.

	BSWI	*CDDFGN*	*ISGW*	*LMM*	*Expt.*[7]
$A^f(D^0 \longrightarrow \bar{K}^0\eta)$	8.37	3.70	7.53	4.06	11.3 ± 0.8
$A^f(D^0 \longrightarrow \bar{K}^0\eta')$	4.50	-	6.18	1.58	20.54 ± 1.54

The factorized amplitudes with model form factors and the experimentally determined amplitudes are presented in Table 6.2. The prediction for $D^0 \to K\eta$ amplitude is too low in every case; an enhancement of a factor of 1.5 to 3, depending on the model, is needed to match the experimental amplitude. For $D^0 \to K\eta'$, the situation is worse.

6.3.2 Resonant Amplitude

In the following we list the amplitude represented by the diagram of (Fig. 6.2) separately for the cases where the loop particles are on-shell and off-shell.

6.3.3 On-shell contribution

The contribution to the resonant amplitude A^r from on-shell loop particles is obtained by taking the imaginary part of the integral I_{-+}. We get from eq. (6.31), (6.56) and (6.40),

$$\begin{aligned} A^r(on\text{-}shell) &= \frac{3}{2} iIm(I_{-+}) \times A_{-+}^{strong} \\ &= -4.18 g^i_{\eta(\eta')}(r) exp(i142^\circ)\ GeV. \end{aligned} \tag{6.62}$$

6.3.4 Off-shell contribution

For the loop particles off-shell the resonant amplitude A^r is obtained by taking the real part of the integral I_{-+}. We get,

$$\begin{aligned} A^r(off\text{-}shell) &= \frac{3}{2} Real(I_{-+}) \times A_{-+}^{strong} \\ &= -4.18 g^i_{\eta(\eta')}(r) exp(i52^\circ)\ GeV. \end{aligned} \tag{6.63}$$

Note that the on-shell contribution, Eq. (6.62), is of the same size as the off-shell, Eq. (6.63), but advanced by a phase of 90° which comes from the factor i. The on-shell and off-shell, amplitudes have the same magnitude but different phases, therefore including off-shell effect will modify both the amplitude and the phase of the resonant amplitude. The total resonant amplitude A^r is given by,

$$A^r = A^r(on\text{-}shell) + A^r(off\text{-}shell). \tag{6.64}$$

Finally, the total decay amplitude is obtained by adding the factorized amplitude A^f to the resonant amplitude A^r,

$$A = A^f - 5.91 g^i_{\eta(\eta')}(r) exp(i97^\circ)\ GeV. \tag{6.65}$$

Plots of the magnitude $|A| = |A^f + A^r|$ as a function of r are given in (Fig. 6.5) and (Fig. 6.6) for the decays $D \to \bar{K}^0\eta$ and $D \to \bar{K}^0\eta'$, respectively. In these figures we

Table 6.3: Phases of the total resonant and on-shell amplitudes defined in Eqs. (6.58) and (6.62), respectively, as functions of r for the processes $D^0 \longrightarrow \bar{K}^0\eta(\eta')$. δ_r is the phase of A^r (Eq. (6.58)) and $\delta_{on\text{-}shell}$ is the phase of $A^r(on\text{-}shell)$ (Eq. (6.62)).

Solution	Decay	r	δ_r	$\delta_{on\text{-}shell}$
$i=1$	$D^0 \longrightarrow \bar{K}^0\eta$	$(5 \leq r \leq 35)\%$	$97°$	$142°$
		$(35 \leq r \leq 48)\%$	$(97 \pm 180)°$	$(142 \pm 180)°$
	$D^0 \longrightarrow \bar{K}^0\eta'$	$(5 \leq r \leq 48)\%$	$(97 \pm 180)°$	$(142 \pm 180)°$
$i=2$	$D^0 \longrightarrow \bar{K}^0\eta$	$(5 \leq r \leq 48)\%$	$97°$	$142°$
	$D^0 \longrightarrow \bar{K}^0\eta'$	$(5 < r \leq 48)\%$	$97°$	$142°$

have used

$$\begin{aligned} A^f(D^0 \to \bar{K}^0\eta) &= 8.37\ GeV, \\ A^f(D^0 \to \bar{K}^0\eta') &= 4.5\ GeV, \end{aligned} \tag{6.66}$$

as predicted in BSW model only. We discuss the results in the next section.

6.3.5 Strong phases

The phase of the total resonant amplitude and the on-shell amplitude can be determined from Eqs. (6.58) and (6.62), respectively. The sign of the coupling constant, g^i_η and $g^i_{\eta'}$ is important; a change in sign introduces a phase difference of 180° which leads to a different pattern of interference (constructive or destructive) between the factorized amplitude A^f and the resonant amplitude A^r. We use the graphs of (Fig. 6.3) and (Fig. 6.4) to read the signs of $g_\eta(r)$ and $g_{\eta'}(r)$ and then determine the strong phase of the resonant amplitudes. The phases are summarized in Table 6.3.

6.4 Discussion

The factorization prediction for the amplitude $A(D^0 \to \bar{K}^0\eta)$ is too low compared to the experimental data and the situation is even worse for $A(D^0 \to \bar{K}^0\eta')$ (see Table 6.2).

Amplitudes with the inclusion of resonant FSI (Eq. (6.65)) are plotted in (Fig. 6.5) and (Fig. 6.6) for $A(D^0 \to \bar{K}^0\eta)$ and $A(D^0 \to \bar{K}^0\eta')$, respectively. From (Fig. 6.5) we notice that for solution $i = 1$, $A(D^0 \to \bar{K}^0\eta) \sim A^f(D^0 \to \bar{K}^0\eta)$ over most of the range of r, except where r is low, $r \leq 14\%$, when $A^f(D^0 \to \bar{K}^0\eta)$ gets a small enhancement over its factorized value, but stays below the experimental value. On the other hand, Fig. 6.6 shows that for solution $i = 1$, $A(D^0 \to \bar{K}^0\eta')$ rises with r and fits the experiment in the range $30\% \leq r \leq 42\%$. Although, for lower values of r $A(D^0 \to \bar{K}^0\eta')$ is underestimated, it still gets large enhancement over its factorized value. Solution $i = 1$ does not accommodate a simultaneous fit to $A(D^0 \to \bar{K}^0\eta)$ and $A(D^0 \to \bar{K}^0\eta')$.

As for solution $i = 2$, we notice from (Fig. 6.5) and (Fig. 6.6) that both $A(D^0 \to \bar{K}^0\eta)$ and $A(D^0 \to \bar{K}^0\eta')$ rise with r. In particular, a fit to $A(D^0 \to \bar{K}^0\eta)$ is secured for $6\% \leq r \leq 20\%$. Despite the fact that in this range of r $A(D^0 \to \bar{K}^0\eta')$ could be raised by almost 100% over its factorized value, it still remains well below its measured value. Again a simultaneous fit to $A(D^0 \to \bar{K}^0\eta)$ and $A(D^0 \to \bar{K}^0\eta')$ is eluded.

Recently Dai et al. [12] have used the same mechanism, but kept only the on-shell loop contribution to estimate the effect of resonant FSI in the decay $D^0 \to K^0\bar{K}^0$. Hence, contrary to our case, the strong phase is solely determined by the resonant propagator.

In a recent paper Gronau [13] has calculated the contribution of $K_0^*(1430)$ in the direct channel (annihilation topology, as in our case) to $D^0 \to K^-\pi^+$ decay in a model-independent way and found it to be a substantial fraction ($\sim 20\%$) of the total amplitude (which is largely isospin 1/2). He argues that the effect of $\bar{K}_0^*(1950)$ on

$D^0 \to K^-\pi^+$ decay could even be larger. The difference between his approach and ours (apart from the fact that we are dealing with different D^0 decay modes) is that we have used the factorized input for the weak transition $D^0 \to \bar{K}_0^*(1950)$ through a πK loop, while Ref. [13] uses current algebra, with smoothness assumption, to relate $D^0 \to \bar{K}_0^*(1430)$ vertex to $D^+ \to \bar{K}_0^*(1430)\pi^+$ measured rate. Thus while the $D^0 \to \bar{K}_0^*(1950)$ vertex of Ref. [13] is assumed to be real, ours is complex. If our resonant contribution is equated to the W-exchange amplitude of Ref. [13], then clearly the resonant contribution has a phase around 90° (modulo π) relative to the tree amplitude (see Eq. (6.65)).

In summary we find that the resonant FSI due to $K_0^*(1950)$ in the direct channel affects $A(D \to \bar{K}^0\eta)$ and $A(D \to \bar{K}^0\eta')$ significantly. However, a simultaneous fit to both decay amplitudes is not possible.

A final comment: We tried the same calculation with a negative sign for g, $g = -2.707\ GeV$. Apart from leading to a phase shift of 180° in the strong phase δ_r, it did not change our conclusions. It was still impossible to fit both $A(D \to \bar{K}^0\eta)$ and $A(D \to \bar{K}^0\eta')$ simultaneously.

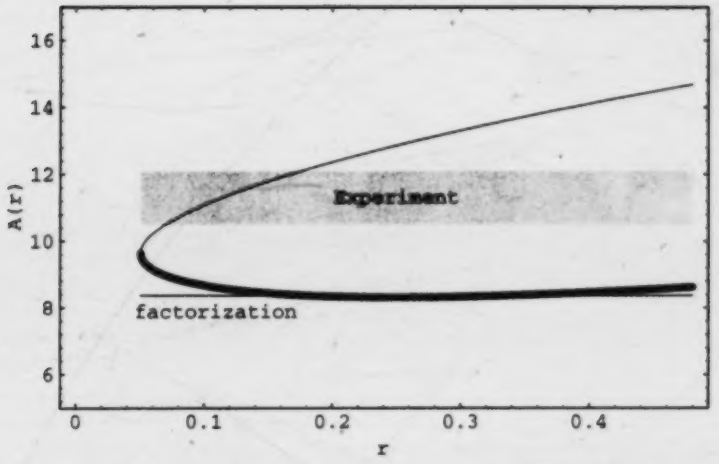

Figure 6.5: Plot of the magnitude of the total amplitude $|A| = |A^I + A^r|$ in Eq. (6.65) for $D^0 \to \bar{K}^0\eta$ as a function of the branching ratio sum $r = Br(\bar{K}_0^*(1950) \to \bar{K}^0\eta) + Br(\bar{K}_0^*(1950) \to \bar{K}^0\eta')$. The thick and light parts of the curve correspond to the solution g_η^1 and g_η^2, respectively. The shaded region represents the experimental value of the amplitude, the horizontal line represents the factorized amplitude A^I. The values on the y-axis must be multiplied by a factor of 10^{-7} GeV to get the absolute magnitude of the decay amplitude.

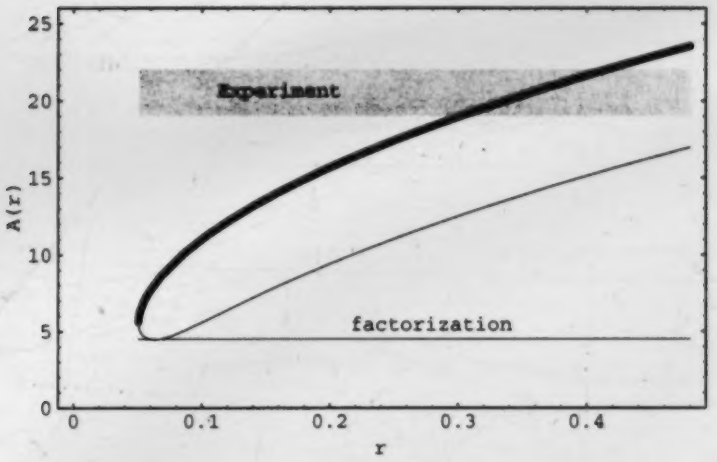

Figure 6.6: Plot of the magnitude of the total amplitude $|A| = |A^I + A^r|$ in Eq. (6.65) for $D^0 \to \bar{K}^0\eta'$ as a function of the branching ratio sum $r = Br(\bar{K}_0^*(1950) \to \bar{K}^0\eta) + Br(\bar{K}_0^*(1950) \to \bar{K}^0\eta')$. The thick and light parts of the curve correspond to the solution $g_{\eta'}^1$ and $g_{\eta'}^2$, respectively. The shaded region represents the experimental value of the amplitude, the horizontal line represents the factorized amplitude A^I. The values on the y-axis must be multiplied by a factor of 10^{-7} GeV to get the absolute magnitude of the decay amplitude.

Bibliography

[1] M. Bauer, B. Stech, and M. Wirbel, Z. Phys. C **34**, 103 (1987).

[2] A. N. Kamal, Q. P. Xu, and A. Czarnecki, Phys. Rev. D **49**, 1330 (1994); H. Y. Cheng, Z. Phys. C **69**, 647 (1996); *ibid.* Phys. Lett. B **335**, 428 (1994); K. Terasaki, Phys. Rev. D **59**, 114001 (1999); A. N. Kamal and T. N. Pham, Phys. Rev. D **50**, 6849 (1994); *ibid*, **50**, R1832 (1994); S. Stone, *in Heavy Flavours*, edited by A. J. Buras and M. Lindner (World Scientefic, Singapore, 1992) p. 334; A. C. Katoch and K. K. Sharma, Z. Phys. C **75**, 651 (1997). K. K. Sharma, A. C. Katoch, and R. C. Verma, Z. Phys. C **75**, 253 (1997); A. N. Kamal and A. B. Santra. Z. Phys. C **71**, 101 (1996).

[3] A. N. Kamal, A. B. Santra, T. Uppal, and R. C. Verma, Phys. Rev. D **53**, 2506 (1996).

[4] F. Buccella, M. Lusignoli, A. Pugliese, Phys. Lett. B **379**, 249 (1996); F. Buccella, M. Lusignoli, G. Miele, A. Pugliese, and P. Santorelli, Phys. Rev. D **51**, 3478 (1995).

[5] R. C. Verma, A. N. Kamal, and M. P. Khanna, Z. Phys. C **65**, 255 (1995)

[6] R. C. Verma, Phys. Lett. B **365**, 377 (1996); K. K. Sharma, A. C. Katoch, and R. C. Verma, Z. Phys. C **76**, 311 (1997).

[7] Particle Data Group, C. Caso et al., Eur. Phys. J. C **3**, 1 (1998).

[8] H. J. Lipkin, Phys. Rev. Lett. **44**, 710 (1980); A. N. Kamal and E. D. Cooper, Z. Phys. C **8**, 67 (1981); C. Sorensen, Phys. Rev. D **23**, 2618 (1981);

[9] A. N. Kamal, Int. J. Mod. Phys. A **7**, 3515 (1992).

[10] J. Wiss, Nuovo Cimento **109A**, 895 (1996).

[11] El hassan El aaoud and A. N. Kamal, Int. J. Mod. Phys. **A XX**, XXXX (2000) (accepted for publication), hep-ph/9910327.

[12] Y. S. Dai, D. S. Du, X. Q. Li, Z. T. Wei, and B. S. Zou, Phys. Rev. D **60**, 014014 (1999).

[13] M. Gronau, Phys. Rev. Lett. **83**, 4005 (1999) hep-ph/9908237.

[14] Particle Data Group, R. M. Barnett et al. Phys. Rev. D **54**, 1 (1996).

[15] M. Wirbel, B. Stech, and M. Bauer, Z. Phys. C **29**, 637 (1985); M. Bauer and M. Wirbel, Z. Phys. C **42**, 671 (1989).

[16] El hassan El aaoud and A. N. Kamal, work in progress.

[17] J. F. Donoghue, E. Golowich, W. A. Ponce, and B. R. Holstein, Phys. Rev. D **21**, 186 (1980).

[18] X. Q. Li and B. S. Zou, Phys. Lett. B **399**, 297 (1997); D. S. Du, X. Q. Lie, Z. T. Wei, and B. S. Zou, Eur. Phys. J. A **4**, 91 (1999); O. Gortchakov, M. P. Locher, V. E. Markushin, and S. von. Rotz, Z. Phys. A **353**, 447 (1996)

[19] For model prediction see Table. 6.1, see also: M. Crisafulli, G. Martinelli, V. J. Hill, and C. T. Sachrajda, Phys. Lett. B **223**, 90 (1989); C. A. Dominguez and N. Paver, Phys. Lett. B **207**, 499 (1988); M. A. Ivanov, P. Santorelli, N. Tancredi. hep-ph/9905209 (unpublished); J. M. Flynn, hep-lat/9710080 (unpublished); S. Narison, Phys. Lett. B **337**, 163 (1994); N. Barik and S. K. Tripathy, S. Kar,

and P. C. Dash, Phys Rev. D **56**, 4238 (1997); M. A. Ivanov, T. Mizutani, and Yu. M. Valit, Few-Body Systems **24**, 201 (1998).

[20] CLEO Collaboration, F. Butler et al., Phys. Rev. D **52**, 2656 (1995); CLEO Collaboration, J. Bartelt et al., Phys. Lett. B **405**, 373 (1997); Particle Data Group, L. Montanet et al., Phys. Rev. D **50**, 1173 (1994).

[21] R. Casalbuoni, A. Deandrea, N. Di Bartolomeo, R. Gatto, F. Feruglio, and G. Nardulli, Phys. Lett. B **299**, 139 (1993).

[22] A. N. Kamal and T. N. Pham in Ref. [2]; L. L. Chau and H. Y. Cheng, Phys. Lett. B **333**, 514 (1994).

[23] A. X. El-Khadra, A. S. Kronfeld, P. B. Mackenzie, S. M. Ryan, and J. N. Simone, Phys. Rev. D **58**, 014506 (1998).

[24] N. Isgur, D. Scora, B. Grinstein and M. B. Wise, Phys. Rev. D **39**, 799 (1989).

[25] V. Lubicz, G. Martinelli, M. S. McCarthy, and C. T. Sachrajda, Phys. Lett. B **274**, 415 (1992).

Chapter 7

Conclusions

We have presented a formalism for the analysis of the weak decays of charm D meson, to two vector mesons V_1 and V_2: $D \longrightarrow V_1V_2$. The analysis includes the decay rate $\Gamma(D \longrightarrow V_1V_2)$, the longitudinal polarization P_L and the partial wave ratios $\frac{|S|}{|P|}$, $\frac{|S|}{|D|}$. Since the final state particles are produced in different correlated polarization states and the final state involves three invariant amplitudes, the formalism is based on the use of the helicity and partial wave amplitudes. In particular we have performed a thorough analysis of the decays $D_s^+ \to \phi\rho^+$, $D^0 \to K^{*-}\rho^+$, $D^+ \to \bar{K}^{*0}\rho^+$, and $D^0 \to K^{*0}\rho^0$.

We first considered the leading and next to leading order effective weak Hamiltonian $\mathcal{H}$ relevant for two-body hadronic decays of D mesons. We have updated the Wilson coefficients C_1 and C_2 using more recent data on the strong decay constant α_s. We used the factorization approximation to derive the hadronic weak matrix elements, $A = \langle V_1V_2 \mid \mathcal{H} \mid D\rangle$, in terms of decay constants and Lorentz invariant form factors. Since the behavior of the form factors is not known at this stage we have relied on several theoretical models to evaluate these form factors. Finally, we have made a comparison with experiment. The analysis was carried as far as the experimental data would allow. We have made a critical evaluation of the data and point out some of its internal inconsistencies.

The results show that the final state is predominantly an S-wave and the interference between S and D waves has a large effect on the longitudinal polarization. The importance of this analysis is as follows:

1) It provides a clear presentation of the formalism: helicity, partial wave and transversity required not only for the theoretical analysis but also for the experimental analysis of the decay of a pseudoscalar meson to two vectors mesons.

2) The decays deal with charm mesons which are still of great interest to experimentalists as well as to theorists.

3) We have looked critically at the experimental data, which haven't changed for almost a decade, especially $D \to K^*\rho$, and showed their internal inconsistency as well as pointed out at least one possible source of error. This in turn might encourage the experimentalist to re-measure these decays more carefully.

4) Several models were used in the analysis; some of them agree better with experiments than others. This in turn might motivate the theorists to improve their models. In fact, we already received a communication from one of the authors suggesting how the predictability of their model can be improved by re-selecting the appropriate values for the parameters of the model.

The experimental analysis of $D \to K^*\rho$ measurement of the branching ratio, partial-wave branching ratios, polarization etc.. is done by considering the resonant substructure of the four-body decays $D \to K\pi\pi\pi$ [1, 2]. Another example of multi-body hadronic decays of the D mesons is the three-body decay $D \to K\pi\pi$. Although these decays account for a large fraction of the total hadronic width of the D meson [3], their theoretical as well as experimental understanding is still lacking [4, 5]. One of the main difficulties in the experimental studies of these decays is that, in addition to direct non-resonant amplitudes, there are several intermediate states contributing to their resonant substructure [6]. While models are used for the intermediate resonant decay amplitude in fitting the data, the direct non-resonant three-body and four-body decays amplitudes of D mesons are usually assumed to be constant.

Recently, Bediaga et al. [5] have argued that an explanation of the discrepancy observed in the fit to the experimental data for $D \to K\pi\pi$ is the incorrect parameterization of the non-resonant contribution. We have pointed out in a recent paper [4] the inconsistency of the data in $D \to K\pi\pi\pi$ especially in the channel $D \to K^*\rho \to K\pi\pi\pi$. But the non-resonant amplitude was assumed to be constant in fitting the data for the decay $D \to K\pi\pi\pi$. So far no theoretical investigation of the validity of this assumption has been carried out.

Based on this work and the work presented in Ref. [5] it is essential to investigate the non-resonant amplitude and its contribution to the decay $D \to K\pi\pi\pi$ and how that will influence contributions from other resonances. The approach for such study could be based on the factorization technique in conjunction with the quark model and chiral symmetry.

Charm meson decays are of considerable interest to both theoretical and experimental physicists. The data suffer from some internal inconsistency as pointed out in [4, 5]. We expect that further investigations will be carried out. This will help to clarify the complexity of four-body decays of the D meson and lead to careful re-measurement of the branching fraction and more precise analyses of the data on charm meson decays, especially $D \to K\pi\pi\pi$.

We have estimated the final state interaction effects of the $K_0^*(1950)$ resonance on $D^0 \to \bar{K}^0\eta$, $D^0 \to \bar{K}^0\eta'$ decays via a Feynman diagram approach using a factorized input for $D^0 \to K_0^*(1950)$ weak transition through a πK loop. Both on-shell and off-shell contributions from the loop were calculated as well as the strong phase of the resonant amplitude. Numerical calculations show that, although a simultanoues fit of both decays was not possible, the resonant final state interactions is significant in these decays.

The model we proposed for resonant final state interactions can be extended, as proposed in Ref. [7] to include additional intermediate states, in the loop, including higher excitations of kaons and pions.

Bibliography

[1] MARK III Collaboration, D. Coffman *et al.*, Phys. Rev. D **45**, 2196 (1992).

[2] E-691 Collaboration, J. C. Anjos *et al.* Phys. Rev. D **46**, 1941 (1992).

[3] Particle Data Group, C. Caso et al., Eur. Phys. J. C **3**, 1 (1998).

[4] El hassan El aaoud and A. N. Kamal, Phys. Rev. D **59**, 114013 (1999).

[5] I. Bediaga, C. Göbel, R. Méndez-Galain, Phys. Rev. Lett. **78**, 22 (1997).

[6] MARK III Collaboration, D. Coffman et al., Phys. Rev. D **45**, 2196 (1992). E-691 Collaboration, J. C. Anjos et al. Phys. Rev. D **46**, 1941 (1992). MARK III Collaboration, J. Adler et al. Phys. Lett. B **196**, 107(1987).

[7] A. Falk, Y. Nir, and A. Petrove, hep-ph/9911369.

Appendix A

$SU(3)$ Symmetry

The generators of the $SU(3)$ group consist of traceless unitary matrices of order 3 with determinant +1. The generators of the group are defined by [1]

$$F_i = \frac{\lambda_i}{2}, \tag{A.1}$$

where λ_i are the Gell-Mann matrices given by

$$\lambda_1 = \begin{pmatrix} 0 & 1 & 0 \\ 1 & 0 & 0 \\ 0 & 0 & 0 \end{pmatrix}, \quad \lambda_2 = \begin{pmatrix} 0 & -i & 0 \\ i & 0 & 0 \\ 0 & 0 & 0 \end{pmatrix}, \quad \lambda_3 = \begin{pmatrix} 1 & 0 & 0 \\ 0 & -1 & 0 \\ 0 & 0 & 0 \end{pmatrix},$$

$$\lambda_4 = \begin{pmatrix} 0 & 0 & 1 \\ 0 & 0 & 0 \\ 1 & 0 & 0 \end{pmatrix}, \quad \lambda_5 = \begin{pmatrix} 0 & 0 & -i \\ 0 & 0 & 0 \\ i & 0 & 0 \end{pmatrix}, \quad \lambda_6 = \begin{pmatrix} 0 & 0 & 0 \\ 0 & 0 & 1 \\ 0 & 1 & 0 \end{pmatrix},$$

$$\lambda_7 = \begin{pmatrix} 0 & 0 & 0 \\ 0 & 0 & -i \\ 0 & i & 0 \end{pmatrix}, \quad \lambda_8 = \frac{1}{\sqrt{3}} \begin{pmatrix} 1 & 0 & 0 \\ 0 & 1 & 0 \\ 0 & 0 & -2 \end{pmatrix}. \tag{A.2}$$

They satisfy the commutation relations,

$$[\lambda_i, \lambda_j] = 2i f_{ijk} \lambda_k, \tag{A.3}$$

[1] M. Greiner, Quantum Mechanics symmetries, second edition (Springer-Verlag 1994)

and the anticommutation relations

$$\{\lambda_i, \lambda_j\} = \frac{4}{3}\delta_{ij} + 2d_{ijk}\lambda_k, \tag{A.4}$$

where d_{ijk} and f_{ijk} are the SU(3) structure constants. They are given by

$$\begin{aligned} f_{ijk} &= \frac{1}{4i}Tr\left([\lambda_i, \lambda_j]\,\lambda_k\right), \\ d_{ijk} &= \frac{1}{4}Tr\left(\{\lambda_i, \lambda_j\}\,\lambda_k\right). \end{aligned} \tag{A.5}$$

Equations A,5 show that

$$\begin{aligned} f_{ijk} &= -f_{jik} = -f_{ikj}, \\ d_{ijk} &= d_{jik} = d_{ikj}. \end{aligned} \tag{A.6}$$

Therefore f_{ijk} are totally antisymmetric in all indices while d_{ijk} are totally symmetric. The non-vanishing f_{ijk} and d_{ijk} are given in Table A.1.

The matrices $\lambda^i, i = 1, ..., 8$ satisfy the relation

$$\lambda^i_{\alpha\beta}\lambda^i_{\gamma\delta} = -\frac{2}{3}\delta_{\alpha\beta}\delta_{\gamma\delta} + 2\delta_{\alpha\delta}\delta_{\gamma\beta}, \tag{A.7}$$

We can extend the algebra to a nonet symmetry[2] by introducing the matrix

$$\lambda_0 = \sqrt{\frac{2}{3}}\begin{pmatrix} 1 & 0 & 0 \\ 0 & 1 & 0 \\ 0 & 0 & 1 \end{pmatrix} = \sqrt{\frac{2}{3}}\,\mathbf{I}_3 \tag{A.8}$$

where $\mathbf{I}_3$ is the 3×3 unit matrix. The anticommutation relations in Eq.A.4 remain valid with

$$d_{0jk} = \sqrt{\frac{2}{3}}\delta_{jk}, \quad f_{0jk} = 0. \tag{A.9}$$

[2]D. Bailin, Weak Interactions, second edition (Adam Hilger Ltd 1982)

Table A.1: The non-vanishing symmetric and antisymmetric structure constants d_{ijk} and f_{ijk} for SU(3) group.

ijk	f_{ijk}	ijk	d_{ijk}
123	1	118	$1/\sqrt{3}$
147	1/2	146	1/2
156	-1/2	157	1/2
246	1/2	228	$1/\sqrt{3}$
257	1/2	247	-1/2
345	1/2	256	1/2
367	-1/2	338	$1/\sqrt{3}$
458	$\sqrt{3}/2$	344	1/2
678	$\sqrt{3}/2$	355	1/2
		366	-1/2
		377	-1/2
		448	$-1/(2\sqrt{3})$
		558	$-1/(2\sqrt{3})$
		668	$-1/(2\sqrt{3})$
		778	$-1/(2\sqrt{3})$
		888	$1/\sqrt{3}$

Appendix B

Helicity Formalism

B.1 Single Particle State

The state of a particle of mass m and momentum $\mathbf{k} = (|\mathbf{k}|, \theta, \varphi)$ is represented by $||\mathbf{k}|, \theta, \varphi, J, J_z\rangle$. The angular momentum J is given by

$$J = L + s, \qquad J_z = L_z + s_z, \tag{B.1}$$

where L and s are the orbital and spin angular momentum.

In the rest frame of the particle, $L = L_z = 0$, the state is $|\mathbf{k} = 0, J, s_z\rangle$. Boosting the particle along the z-axis, we obtain the state $||\mathbf{k}|, 0, 0, J, s_z\rangle$. The angular momentum along the z-axis is unchanged by the boost. In what follows we use λ to represent the angular momentum along the direction of motion, therefore

$$\lambda = \frac{\mathbf{J}.\mathbf{k}}{|\mathbf{k}|}. \tag{B.2}$$

Equation (B.2) shows that λ is invariant under rotation.

The general state $||\mathbf{k}|, \theta, \varphi, J, \lambda\rangle$ is obtained by performing a rotation of the boosted state $||\mathbf{k}|, 0, 0, J, \lambda\rangle$ as follows

$$||\mathbf{k}|, \theta, \varphi, J, \lambda\rangle = U(\varphi, \theta, 0)||\mathbf{k}|, 0, 0, J, \lambda\rangle, \tag{B.3}$$

where the unitary operator $U(\alpha, \beta, \gamma)$ is given by

$$\begin{aligned} U(\alpha,\beta,\gamma) &= \exp(-i\alpha J_z)\exp(-i\beta J_y)\exp(-i\gamma J_z) \\ &= U_z(\alpha)U_y(\beta)U_z(\gamma), \end{aligned} \tag{B.4}$$

J_y and J_z are the usual generators of the rotation group and α, β, γ are rotation angles about y and z-axis respectively. Such a state where the spin component along the direction of motion is specified is known as helicity eigenstate.

B.1.1 Spin 1 particle

A spin one particle at rest has three orthogonal states $||\mathbf{k}|, J, J_z\rangle \equiv |0,1,+1\rangle, |0,1,-1\rangle, |0,1,0\rangle$. A commonly used basis is $||\mathbf{k}|, J_z\rangle$:

$$\begin{aligned} |0,+1\rangle &\equiv \epsilon(+) = \frac{-1}{\sqrt{2}}(1,i,0), \\ |0,-1\rangle &\equiv \epsilon(-) = \frac{1}{\sqrt{2}}(1,-i,0), \\ |0,\ 0\rangle &\equiv \epsilon(0) = (0,0,1), \end{aligned} \tag{B.5}$$

where ϵ is the polarization vector. Boosting the particle along z direction, the polarization vector will develop a fourth component which is given, according to Lorentz transformation, by

$$\begin{aligned} \epsilon'_0 &= \gamma(\epsilon_0 + v\epsilon_z), \\ \epsilon'_x &= \epsilon_x, \\ \epsilon'_y &= \epsilon_y, \\ \epsilon'_z &= \gamma(\epsilon_z + v\epsilon_0) \end{aligned} \tag{B.6}$$

where

$$\begin{aligned} \gamma &= \frac{1}{\sqrt{(1-\frac{v^2}{c^2})}} = \frac{E}{m}, \\ v &= \frac{|\mathbf{k}|}{m}. \end{aligned} \tag{B.7}$$

The boosted polarization vectors are

$$\begin{aligned}\epsilon'(+) &= \frac{-1}{\sqrt{2}}(0,1,i,0),\\ \epsilon'(-) &= \frac{1}{\sqrt{2}}(0,1,-i,0),\\ \epsilon'(0) &= \frac{1}{m}(|\mathbf{k}|,0,0,E).\end{aligned} \tag{B.8}$$

B.2 Two Particles State

In the center of mass $\mathbf{k_1} = -\mathbf{k_2} = \mathbf{k}$ the two particles state is given by

$$\begin{aligned}|\mathbf{k}_1, J_1, \lambda_1\rangle|\mathbf{k}_2, J_2, \lambda_2\rangle &= |\mathbf{k}_1\mathbf{k}_2, J_1J_2, \lambda_1\lambda_2\rangle,\\ &= ||\mathbf{k}|\theta\varphi, J_1J_2, \lambda_1\lambda_2\rangle.\end{aligned} \tag{B.9}$$

Choosing $\mathbf{k}$ in z-direction, the helicity state for the two particles is represented by

$$\begin{aligned}|\mathbf{k}_1\mathbf{k}_2, J_1J_2, \lambda_1\lambda_2\rangle &= |\mathbf{k}_z, J_1J_2, \lambda_1\lambda_2\rangle\\ &\equiv |\lambda_1\lambda_2\rangle\end{aligned} \tag{B.10}$$

These states are related to the angular momentum state $|JMLs\rangle$ where $J = L + s$, $s = s_1 + s_2$ and $M = J_z$, by[1]

$$|\lambda_1\lambda_2\rangle = \sum_{L,s}\sqrt{\frac{2L+1}{2J+1}}\langle LsL_z\lambda|J\lambda\rangle\langle s_1s_2, \lambda_1, -\lambda_2|s\lambda\rangle|JMLs\rangle \tag{B.11}$$

where $L_z = 0$, $\lambda = \lambda_1 - \lambda_2$ and $\langle LsL_z\lambda|J\lambda\rangle$, $\langle s_1s_2, \lambda_1, -\lambda_2|s\lambda\rangle$ are Clebsch-Gordan coefficients.

B.2.1 Two Spin One Particles

In the center of mass frame, the four momenta of the two particles are given by

$$k_1 = (E_1, 0, 0, |\mathbf{k}|),$$

[1] A. D. Martin and T. D. Spearman, Elementary Particle Theory (north-Holland 1970).

$$
\begin{aligned}
k_2 &= (E_2, 0, 0, -|\mathbf{k}|), \\
K &= k_1 + k_2 \\
&= (m_F, 0, 0, 0)
\end{aligned} \tag{B.12}
$$

Using Eqns. (B.3) and (B.8) the corresponding polarization vectors are

$$
\begin{aligned}
\epsilon_1(+, \theta = \varphi = 0) &= \epsilon_1(+) = \frac{-1}{\sqrt{2}}(0, 1, i, 0), \\
\epsilon_1(-, \theta = \varphi = 0) &= \epsilon_1(-) = \frac{1}{\sqrt{2}}(0, 1, -i, 0), \\
\epsilon_1(0, \theta = \varphi = 0) &= \epsilon_1(0) = \frac{1}{m_1}(|\mathbf{k}|, 0, 0, E), \\
\epsilon_2(+, \theta = \pi, \varphi = 0) &= \epsilon_2(+) = \frac{-1}{\sqrt{2}}(0, -1, i, 0), \\
\epsilon_2(-, \theta = \pi, \varphi = 0) &= \epsilon_2(-) = \frac{1}{\sqrt{2}}(0, -1, -i, 0), \\
\epsilon_2(0, \theta = \pi, \varphi = 0) &= \epsilon_2(0) = \frac{1}{m_2}(-|\mathbf{k}|, 0, 0, E).
\end{aligned} \tag{B.13}
$$

Useful relations

The four dimensional antisymetric tensor is defined by:

$$
\varepsilon_{\mu\nu\rho\sigma} = -\varepsilon^{\mu\nu\rho\sigma}, \tag{B.14}
$$

and,

$$
\varepsilon^{\mu\nu\rho\sigma} = \begin{cases} 1 & \{\mu\nu\rho\sigma\} \text{ are even permutation of } \{0,1,2,3\} \\ -1 & \{\mu\nu\rho\sigma\} \text{ are odd permutation of } \{0,1,2,3\} \\ 0 & \text{otherwise.} \end{cases} \tag{B.15}
$$

Thus we have

$$
\begin{aligned}
\varepsilon_{\mu\nu\rho\sigma}\epsilon_1^{*\mu}\epsilon_2^{*\nu}K^{\rho}k_2^{\sigma} &= -\varepsilon_{\mu\nu03}\epsilon_1^{*\mu}(0)\epsilon_2^{*\nu}(0)m_F|\mathbf{k}| \\
&= -\varepsilon_{1203}\epsilon_1^{*1}(0)\epsilon_2^{*2}(0)m_F|\mathbf{k}| \\
&\quad -\varepsilon_{2103}\epsilon_1^{*2}(0)\epsilon_2^{*1}(0)m_F|\mathbf{k}| \\
&= 0,
\end{aligned} \tag{B.16}
$$

$$\epsilon_1^*(0).\epsilon_2^*(0) = -\frac{|\mathbf{k}|^2 + E_1E_2}{m_1m_2}, \tag{B.17}$$

$$\begin{aligned}\frac{\epsilon_2^*.(K-k_2)}{m_F+m_2}\epsilon_1^*.(K+k_2) &= \frac{-|\mathbf{k}|(m_F-E_2)-|\mathbf{k}|E_2}{m_2(m_F+m_2)}\left(\frac{|\mathbf{k}|}{m_1}(m_F+E_1)+\frac{|\mathbf{k}|}{m_1}E_2\right)\\ &= \frac{-2m_F^2|\mathbf{k}|^2}{m_1m_2(m_F+m_2)}.\end{aligned} \tag{B.18}$$

$$\begin{aligned}m_F^2 &= (E_1+E_2)^2 = m_1^2+|\mathbf{k}|^2+m_2^2+|\mathbf{k}|^2+2E_1E_2,\\ E_1E_2+|\mathbf{k}|^2 &= \frac{m_F^2-m_1^2-m_2^2}{2},\\ |\mathbf{k}|^2 &= \frac{1}{4m_F^2}\left[\left(m_F^2-m_1^2-m_2^2\right)^2-4m_1^2m_2^2\right],\\ &= \frac{1}{4m_F^2}\left[\left(m_F^2-(m_1+m_2)^2\right)\left(m_F^2-(m_1-m_2)^2\right)\right].\end{aligned} \tag{B.19}$$

$$\begin{aligned}\varepsilon_{\mu\nu\rho\sigma}\epsilon_1^{*\mu}(\pm)\epsilon_2^{*\nu}(\pm)K^\rho k_2^\sigma &= -\varepsilon_{\mu\nu03}\epsilon_1^{*\mu}(\pm)\epsilon_2^{*\nu}(\pm)m_F|\mathbf{k}|\\ &= -\varepsilon_{1203}\epsilon_1^{*1}(\pm)\epsilon_2^{*2}(\pm)m_F|\mathbf{k}|\\ &\quad -\varepsilon_{2103}\epsilon_1^{*2}(\pm)\epsilon_2^{*1}(\pm)m_F|\mathbf{k}|\\ &= \left[-\epsilon_1^{*1}(\pm)\epsilon_2^{*2}(\pm)+\epsilon_1^{*2}(\pm)\epsilon_2^{*1}(\pm)\right]m_F|\mathbf{k}|\\ &= \mp im_F|\mathbf{k}|,\end{aligned} \tag{B.20}$$

$$\begin{aligned}\epsilon_1^*(\pm).\epsilon_2^*(\pm) &= 1,\\ \epsilon_2^*(\pm).(K-k_2) &= 0,\\ \epsilon_1^*(\pm).(K+k_2) &= 0\end{aligned} \tag{B.21}$$

For two spin one particles there are three possible spins

$$\begin{aligned}s &= s_1 \oplus s_2\\ &= 0,1,2.\end{aligned} \tag{B.22}$$

With the constraints of angular-momentum $J = 0$ we must have

$$\begin{aligned} L &= 0,\ 1,\ 2, \\ \lambda_1 = \lambda_2 &= +1, -1, 0. \end{aligned} \tag{B.23}$$

Thus, there are three helicity states:

$$|\lambda_1 \lambda_2\rangle = |++\rangle,\ |--\rangle,\ |00\rangle, \tag{B.24}$$

and three angular momentum states:

$$\begin{aligned} |JMLs\rangle &\equiv |Ls\rangle, \\ &= |00\rangle,\ |11\rangle,\ |22\rangle, \end{aligned} \tag{B.25}$$

corresponding to S, P, and D waves. According to Eq. (B.11) we have the following relations between the helicity states of Eq. (B.24) and the angular momentum states of Eq. (B.25)

$$\begin{aligned} |++\rangle &= \frac{1}{\sqrt{3}}S + \frac{1}{\sqrt{2}}P + \frac{1}{\sqrt{6}}D, \\ |--\rangle &= \frac{1}{\sqrt{3}}S - \frac{1}{\sqrt{2}}P + \frac{1}{\sqrt{6}}D, \\ |00\rangle &= -\frac{1}{\sqrt{3}}S + \frac{2}{\sqrt{6}}D. \end{aligned} \tag{B.26}$$

Appendix C

η and η' particles

The physical states η and η' are given by [1]

$$\begin{aligned} \eta &= \eta_8 \cos\theta_P - \eta_1 \sin\theta_P, \\ \eta' &= \eta_8 \sin\theta_P + \eta_1 \cos\theta_P, \end{aligned} \tag{C.1}$$

where the flavor-singlet, η_1, and flavor-octet, η_8, states are defined as

$$\begin{aligned} \eta_1 &= \frac{1}{\sqrt{3}} |u\bar{u} + d\bar{d} + s\bar{s}\rangle \\ \eta_8 &= \frac{1}{\sqrt{6}} |u\bar{u} + d\bar{d} - 2\,s\bar{s}\rangle, \end{aligned} \tag{C.2}$$

and θ_P is the mixing angle.

Using Eqs. (C.1) and (C.2) the state η and η' can be arranged in the following form

$$\eta = \frac{1}{\sqrt{2}} |u\bar{u} + d\bar{d}\rangle \sin\theta' - |s\bar{s}\rangle \cos\theta', \tag{C.3}$$

$$\eta' = \frac{1}{\sqrt{2}} |u\bar{u} + d\bar{d}\rangle \cos\theta' + |s\bar{s}\rangle \sin\theta', \tag{C.4}$$

where

$$\sin\theta' = \frac{1}{\sqrt{3}} \cos\theta_P - \sqrt{\frac{2}{3}} \sin\theta_P,$$

[1] Particle Data Group, C. Caso et al., Eur. Phys. J. C3, 1 (1998)

$$
\begin{aligned}
&= \sin(35.26 - \theta_P), \\
\cos\theta' &= \sqrt{\frac{2}{3}}\cos\theta_P + \frac{1}{\sqrt{3}}\sin\theta_P, \\
&= \cos(35.26 - \theta_P). \qquad \text{(C.5)}
\end{aligned}
$$

with $\theta_P \approx -20°$,

$$\theta' \approx 55.26°. \qquad \text{(C.6)}$$